UNIVERSITY OF CALGARY

Measurement and Modeling of Asphaltene Association

by

Mayur Agrawala

A THESIS

SUBMITTED TO THE FACULTY OF GRADUATE STUDIES

IN PARTIAL FULFILMENT OF THE REQUIREMENTS FOR THE

DEGREE OF MASTER OF SCIENCE IN CHEMICAL ENGINEERING

DEPARTMENT OF CHEMICAL & PETROLEUM ENGINEERING

CALGARY, ALBERTA

January, 2001

Abstract

Asphaltene association was investigated by measuring the number average molar mass of asphaltenes in solution with a vapor pressure osmometer (VPO). The molar mass of Athabasca and Cold Lake asphaltenes in toluene and o-dichlorobenzene at different temperatures and asphaltene concentrations was measured using the VPO. VPO experiments were also performed with asphaltene-resin mixtures in toluene. The limiting molar mass of asphaltenes was found to decrease with increasing temperature and increasing solvent polarity.

Asphaltene self-association was modeled in a manner analogous to linear polymerization. The key concept in the model is that asphaltene molecules may contain single or multiple sites (functional groups) capable of linking with other asphaltenes. The model can also be extended to include the resins, which are known to reduce asphaltene association. The model fits the experimental data well and appears to be capable of capturing most of the chemistry involved in asphaltene self-association.

Acknowledgements

I wish to express my deep sense of gratitude to my supervisor, Dr. Harvey Yarranton for his valuable guidance and encouragement throughout this research project. I really thank him for being patient with me and for the numerous thought provoking discussions that have helped me with a better understanding of the field. Indeed this has enriched me tremendously not only on the academic front but on the professional front as well.

I am thankful to Rajesh Jakher and Olga Gafonova for teaching me SARA fractionation, asphaltene extractions and making me familiar with laboratory safety and ordering procedures.

I am grateful to Hussein Alboudwarej for teaching me to use the Vapor Pressure Osmometer and for the numerous suggestions and discussions, which has expanded my outlook on asphaltene phase behavior.

I wish to thank other members of the Asphaltene Research Group including Tielian, Chandresh, Subodh, Paul, Danuta, Kamran, James and Elaine for their cooperation and help and useful input during the course of the project.

I would like to thank Dr. Raj Mehta and Dr. Nancy Okazawa for letting me use the densitometer in their Oil Sands Laboratory. In addition, thanks are extended to the department administration staff including Amber, Sharon, Rita, Dolly and Dr. Mehrotra.

Finally, acknowledgement is due to the Department of Chemical and Petroleum Engineering, University of Calgary and NSERC for the financial support.

Table of Contents

List of Tables

List of Figures

List of Symbols

A_i	coefficients in equation of VPO response
cmc	critical micelle concentration
C_A	concentration of asphaltenes
C_2	solute concentration (w/w)
C_o	concentration of sucrose
C_s	concentration of SDS
C_{su}	concentration of sucroseoctaacetate
f_{insol}	insoluble fraction of asphaltenes
ΔH_v	enthalpy of vaporization
i	diminution parameter
K	association constant
K_0	VPO calibration factor
K_1	VPO instrument constant
m_o	mass of asphaltenes and resins
m_1	solvent molecular weight
m_2	solute molecular weight
M, $\bar{M}$	number average molar mass
M_3	number average molar mass of aggregates
M_{A3}	molar mass of *P-P-P* aggregates
M_{app}	apparent molecular weight of the solute
M_{avg}	average molar mass of terminators and propagators

M_{B3}	molar mass of *P-P-T* aggregates
M_p	average monomer molar mass of propagators
M_t	average monomer molar mass of terminators
n	number of aggregates
n_1	number of moles of solvent
n_2	number of moles of solute
o-DCB	ortho-dichlorobenzene
$p°$	vapor pressure
ΔP	reduction in vapor pressure
$P_1°$	vapor pressure of pure solvent
p_1	partial pressure of solvent in solution
P_1	propagator monomer
$[P_1]$	equilibrium concentration of propagator monomers
$[P_1]_0$	initial concentration of propagator monomers
P_k	asphaltene aggregate with k propagator monomers
P_kT	asphaltene aggregate with k propagator monomers and one terminator monomer
$[P_k]$	equilibrium concentration of aggregates, P_k
$[P_kT]$	equilibrium concentration of aggregates, P_kT
R	gas constant
T	absolute temperature
$[T]$	equilibrium concentration of terminator monomers

$[T]_0$	initial concentration of terminator monomers
T/P	initial molar ratio of terminators to propagators
ΔT	change in temperature
ΔV	change in voltage
ΔV_1	measured voltage difference of the solution
ΔV_{blank}	measured voltage difference of the pure solvent
x_1	mole fraction of solvent
x_2	mole fraction of solute
x_3	mole fraction of aggregates
x_{A3}	mole fraction of *P-P-P* aggregates
x_{B3}	mole fraction of *P-P-T* aggregates
x_P	mole fraction of propagators
x_T	mole fraction of terminators

Greek Symbols

Δ	represents a change
v	solvent molar volume

Subscripts

0	refers to initial conditions
app	indicates apparent molar mass
avg	indicates average molar mass

A	refers to asphaltenes
A3	*P-P-P* aggregates
blank	refers to blank run performed during VPO measurements
B3	*P-P-T* aggregates
i	refers to coefficients in the equation of VPO response
insol	refers to insoluble fraction
k	refers to number of monomers in the aggregate
o	refers to sucrose
p, *P*	propagators
s	refers to SDS
t, *T*	terminators
v	refers to vaporization

Superscripts

o	refers to vapor pressure

Chapter 1

Introduction

There has been a constant decline in the availability of conventional light oils as these reserves were the first to be put on production and are now depleted. As a result, the oil industry's focus has shifted to the utilization of heavier crudes or offshore fields. However, the production and processing of heavy crudes requires the introduction of diluents or increase in temperature to reduce viscosity. Solvent addition can cause asphaltenes (the heaviest fraction of a crude oil) to precipitate. Asphaltenes can also precipitate with a drop in pressure, for example, during offshore production in the Gulf of Mexico. Asphaltene precipitation can foul equipment or the reservoir increasing operating costs and reducing permeability.

Asphaltenes are defined as a solubility class of bitumen/heavy oil, which are soluble in toluene and insoluble in n-alkanes such as n-pentane or n-heptane. This operational definition of asphaltenes is used because asphaltenes contain about 10^5 to 10^6 molecules of different shapes and sizes (Wiehe and Liang, 1996) and hence it is impossible to define any asphaltene purely by its chemical structure.

The numerous models available today to predict asphaltene precipitation assume a fixed average molar mass or molar mass distribution of asphaltenes. However, in recent years researchers (Moschopedis and Speight, 1976; Ravey et al., 1988, Mohamed et al., 1999; Petersen et al., 1987 etc.) have shown that asphaltenes self-associate and this self-

association, depends on temperature, pressure and composition. Hence, before one develops a model to predict the precipitation of asphaltenes one needs to predict the molar mass distribution of asphaltenes as a function of temperature, pressure and composition.

1.1 Problems Related to Asphaltene Precipitation

Crude oil production is often reduced when asphaltenes precipitate as they can block the pores of reservoir rocks and can also plug the wellbore tubing, flowlines, separators, pumps, tanks and other equipment. At reservoir conditions, the adsorption of asphaltenes to mineral surfaces causes a reversal in wettability of the reservoir from water-wet to oil-wet and also results in in-situ permeability reductions. Both factors reduce oil production. Apart from the production loss, the cost of removing precipitated asphaltenes from equipment and flowlines can be very expensive and significantly alter the economics of a project. Examples of these cases have been reported in the Prinos Field, Greece; Hassi-messaoud Field, Algeria; Ventura Avenue Field, California, and other places throughout the world (Leontaritis and Mansoori, 1987).

Crude oil residues are produced in oil refineries by vacuum distillation of virgin crude oils and of streams that have already undergone processing. These residues contain asphaltenes. Agglomeration of asphaltenes plays an important role in residue processing and influences product properties. The asphaltenes (which contain some metals) are known to cause catalyst deactivation by metal deposition on the catalyst and also by coke deposition.

Asphaltene precipitation can cause major problems during the transportation of bitumen and heavy oil. The flow of paraffin diluted bitumen through transportation pipelines and processing equipment can result in deposition of precipitated asphaltenes. This deposition causes higher pumping rates and can lead to a buildup of internal pipeline pressure.

Thus it can be seen that there is a need for predicting the thermodynamic conditions for asphaltene precipitation.

1.2 Objectives of the Present Work

As mentioned earlier, asphaltene molecular association has been cited in the literature to depend upon temperature, pressure and composition. It is important to account for the change in molar mass of asphaltenes (the degree of self-association) with thermodynamic changes in order to model asphaltene deposition accurately.

The data on the effect of solvent and temperature on asphaltene association in the literature is scarce. Moreover, it is not clear what properties of the solvent affect the association of asphaltenes. The role of other petroleum constituents is also not clear. For example, resins are also known to decrease the association of asphaltenes dramatically. To date, there has been little or no effort to quantify the change in the degree of association due to changes in temperature and pressure or composition of the system.

The objectives of this thesis are as follows:

- Measure the molar mass of asphaltenes in different solvents and at different concentrations using a Vapor Pressure Osmometer.

- Investigate the effect of temperature on asphaltene association.
- Investigate the effect of solvent on asphaltene association.
- Investigate the effect of asphaltene-resin interactions on asphaltene association.
- Develop a theoretical model to predict asphaltene association.

1.3 Thesis Structure

The relevant literature is reviewed in Chapter 2. A description of asphaltene structure is provided and the implications of the structure on self-association are discussed. The evidence of self-association and also the role of other oil constituents such as saturates, aromatics and resins on the association of asphaltenes is discussed. The implications of self-association on the prediction of asphaltene precipitation is also discussed.

Chapter 3 describes the experimental methods employed in this study. This includes an overview of extraction methods such as SARA fractionation and asphaltene extraction for obtaining various samples used during the course of this research. Also the Vapor Pressure Osmometer (VPO) is described in detail as it was the major experimental tool used to measure the association of asphaltenes under different conditions.

Chapter 4 describes the Asphaltene Association Model developed to predict the aggregation state of asphaltenes. Different schemes are discussed and a detailed modeling procedure outlined. In Chapter 5, the experimental results obtained from the VPO are shown along with discussions on model performance. The implications on solubility modeling of asphaltenes are also discussed.

Chapter 6 summarizes the findings of the study and provides recommendations for additional research required to extend the model to other solvent and temperature conditions. Also the importance of a clear industry standard for experimental techniques involved during asphaltene and resin extraction is emphasized.

Chapter 2

Literature Review

Crude oils can be fractionated and classified in a number of ways. Classification by solubility is the most relevant to asphaltene association and solubility modeling. There are four major solubility fractions: saturates, aromatics, resins and asphaltenes. Details of the methods used to separate them are given in Chapter 3. Saturates are markedly different from the other three fractions as they mainly contain paraffins and naphthenes and hence, are deemed nonpolar. On the other hand, aromatics, resins and asphaltenes form a continuum with increasing polarity, molar mass and heteroatom content (Figure 2.1). Asphaltenes can self-associate and/or precipitate from the crude oil upon a change in temperature, pressure or composition. The self-association and precipitation is mediated by other solubility fractions particularly the resins. Hence it is evident that petroleum is a delicately balanced physical system where the asphaltenes depend on the other fractions for complete mobility and phase stability (Speight, 1999).

Asphaltenes are a complex group of compounds and have proven difficult to characterize. Consequently, the development of theoretical models to predict asphaltene association and precipitation has been limited. In fact, until the mid 1980's, research was largely limited to experimental characterizations. This literature review focuses on the molecular structure of asphaltenes and gives some insight into why asphaltene molecular association occurs. The evidence on the self-association of asphaltenes and various

possible association mechanisms are discussed. Interactions between resins and asphaltenes are reviewed because resins have been shown to significantly affect asphaltene association and precipitation. Finally, the advantages and limitations of the newer predictive solubility models that have appeared in the last two decades are briefly discussed.

Figure 2.1 Continuum of Aromatics, Resins and Asphaltenes in Petroleum

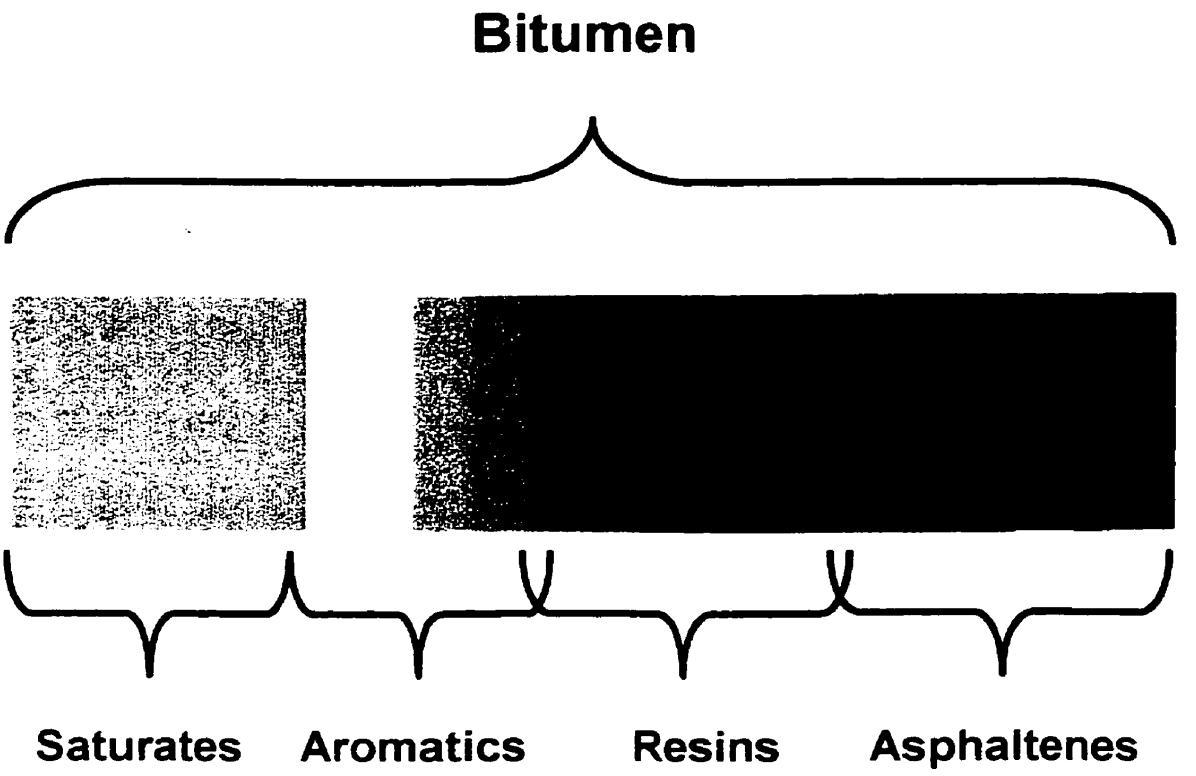

2.1 Molecular Structure and Composition of Asphaltenes

By definition, asphaltenes are a solubility class. They are precipitated from bitumens and petroleums by the addition of a normal alkane such as pentane or heptane.

The part of the precipitate that remains soluble in toluene is deemed the asphaltenes. Asphaltenes are dark brown to black friable solids that have no definite melting point and, when heated, decompose and leave a carbonaceous residue. The amount of asphaltenes in petroleum varies with source, depth of burial, the specific gravity of crude oil and the sulfur content of the crude.

The molecular nature of the asphaltene fractions of petroleums and bitumens has been subject to numerous investigations. However, determining the actual structure of the constituents of the asphaltene fraction has proven to be difficult because they are a mixture of many thousands of molecular species. Nevertheless, the various investigations have brought to light some significant facts about asphaltene structure. There are indications that asphaltenes consist of condensed aromatic nuclei, which carry alkyl, and alicyclic systems with heteroatoms (that is, nitrogen, oxygen and sulfur) scattered throughout in various, aliphatic and heterocyclic locations. With increasing molar mass of the asphaltene fraction, both aromaticity and proportion of the heteroelements increase (Koots & Speight, 1975).

Attempts have been made to describe the total structure of asphaltenes in accordance with the nuclear magnetic resonance (NMR) data and results of chemical analyses (Witherspoon & Winniford, 1968). Strausz et al (1992) identified a host of structural units in Alberta asphaltenes from detailed chemical and degradation studies. He also showed that the extent of aromatic condensation is low and that highly condensed pericyclic aromatic structures are present in very low concentrations. From his work he concluded that petroleum asphaltenes were mainly derived through the catalytic

cyclization, aromatization and condensation of n-alkanoic (probably fatty acids) precursors. He came up with a hypothetical asphaltene molecule consisting of large aromatic clusters.

Petroleum asphaltenes have a varied distribution of heteroatom (N, O, S) functionality. Nitrogen exists as varied heterocyclic types but the more conventional primary, secondary and tertiary aromatic amines have not been established as being present in petroleum asphaltenes (Moschopedis and Speight, 1976b). There are also reports in which the organic nitrogen has been defined in terms of basic and nonbasic types (Nicksic and Jeffries-Harris, 1968). Spectroscopic investigations (Moschopedis and Speight, 1979) suggest that carbazoles occur in asphaltenes, which supports, earlier mass spectroscopic evidence (Clerk and O'Neal, 1969) for the occurrence of carbazole nitrogen in asphaltenes. The application of X-ray absorption near-edge structures (XANES) spectroscopy to the study of asphaltenes has led to the conclusion that a large portion of the nitrogen is present in aromatic systems, but in pyrrolic rather than pyridinic form (Mitra-Kirtley et al., 1993). Other studies (Schmitter et al., 1984) have brought to light the occurrence of four-ring aromatic nitrogen species in petroleum.

Oxygen has been identified in carboxylic, phenolic and ketonic (Petersen et al., 1974) locations but is not usually regarded as being located primarily in heteroaromatic ring systems. Some evidence for the location of oxygen within the asphaltene fraction has been obtained by infrared spectroscopy. Examination of dilute solutions of the asphaltenes in carbon tetrachloride show that at low concentration (0.01% wt/wt) of asphaltenes a band occurs at 3585 cm^{-1}, which is within the range anticipated for free

nonhydrogen-bonded phenolic hydroxyl groups. In keeping with the concept of hydrogen bonding, this band becomes barely perceptible, and the appearance of the broad absorption in the range 3200-3450 cm^{-1} becomes evident at concentrations above 1% wt/wt (Moschopedis and Speight, 1976a,b).

Other evidence for the presence and nature of oxygen functions in asphaltenes has been derived from infrared spectroscopic examination of the products after interaction of the asphaltenes with acetic anhydride. Thus, when asphaltenes are, heated with acetic anhydride in the presence of pyridine, the infrared spectrum of the product exhibits prominent absorptions at 1680, 1730 and 1760 cm^{-1}. These observations suggest acetylation of free and hydrogen-bonded phenolic hydroxyl groups present in the asphaltenes (Moschopedis and Speight, 1976a,b).

Sulfur occurs as benzothiophenes, dibenzothiophenes and naphthelene-benzothiophenes (Drushel, 1970). More highly condensed thiophene-types may also exist but are precluded from identification by low volatility. Other forms of sulfur that occur in asphaltenes include the alkyl-alkyl sulfides, alkyl-aryl sulfides and aryl-aryl sulfides (Yen, 1974).

Nickel and vanadium occur as porphyrins but whether or not these are an integral part of asphaltene structure is not known (Baker, 1969). Some of the porphyrins can be isolated as a separate stream from petroleum (Branthaver, 1990).

Differences in the composition of asphaltenes have not been addressed in detail in the literature. The nature of the source material and subtle regional variations in the maturation conditions serve to differentiate one crude oil (and hence one asphaltene)

from another. The elemental composition of asphaltenes isolated by use of excess volumes of n-pentane as the precipitating medium show that the amounts of carbon and hydrogen usually vary over only a narrow range (Speight, 1999) as shown in Table 2.1. These values correspond to a hydrogen-to-carbon atomic ratio of 1.15 ± 0.5%.

Table 2.1 Elemental Composition of Asphaltenes from World Sources (Speight, 1999)

Source	Composition (wt %)					Atomic ratios			
	C	H	N	O	S	H/C	N/C	O/C	S/C
Canada	79.0	8.0	1.0	3.9	8.1	1.21	0.011	0.037	0.038
Iran	83.7	7.8	1.7	1.0	5.8	1.19	0.017	0.009	0.026
Iraq	80.6	7.7	0.8	0.3	9.7	1.15	0.009	0.003	0.045
Kuwait	82.2	8.0	1.7	0.6	7.6	1.17	0.017	0.005	0.035
Mexico	81.4	8.0	0.6	1.7	8.3	1.18	0.006	0.016	0.038
Sicily	81.7	8.8	1.5	1.8	6.3	1.29	0.016	0.017	0.029
USA	84.5	7.4	0.8	1.7	5.6	1.05	0.008	0.015	0.025
Venezuela	84.2	7.9	2.0	1.6	4.5	1.13	0.020	0.014	0.020

In contrast to the carbon and hydrogen contents of asphaltenes, notably variations occur in the proportions of the hetero elements, in particular in the proportions of oxygen and sulfur. Oxygen contents vary from 0.3 to 4.9% and sulfur contents vary from 0.3 to 10.3%. On the other hand, the nitrogen content of the asphaltenes has a somewhat lesser degree of variation (0.6-3.3%).

The use of n-heptane as the precipitating medium yields a product that is substantially different from the n-pentane-insoluble material (Table 2.2). For example, the hydrogen-to-carbon atomic ratio of the n-heptane precipitate is lower than that of the n-pentane precipitate. This indicates a higher degree of aromaticity in the n-heptane precipitate. Nitrogen-to-carbon, oxygen-to-carbon, and sulfur-to-carbon ratios are usually higher in the n-heptane precipitate, indicating higher proportions of the heteroelements in this material (Speight, 1999).

The large variety of functional groups and heteroatom content in the asphaltenes indicates that asphaltene molecules have the potential to form links with other similar molecules in a number of ways. These links may be formed through acid-base interactions, aromatics (π-π) stacking, hydrogen bonding, dipole-dipole interactions or even weak van der Waal's interactions. However, π-π bonding is considered the prevalent theory (Yen, 1974).

2.2 Asphaltene Molar Mass

Numerous techniques have been, employed to measure the molar mass of asphaltenes. However, there are many discrepancies with these techniques. For example, ultracentrifuge studies give molar masses up to 300,000 while an osmotic pressure method indicated molar masses of 80,000 and a molecular film method yielded values of 80,000 to 140,000 (Speight, 1999). However, other procedures have yielded lower values: 2500 to 4000 by the ebullioscopic method; 600 to 6000 by the cryoscopic method; 900 to 2000 by viscosity determinations; 1000 to 4000 by light absorption

coefficients; 1000 to 5000 by vapor pressure osmometry; and 2000 to 3000 by an isotonic or equal vapor pressure method (Speight, 1999).

Table 2.2 Elemental Composition of Various Asphaltenes (Speight, 1999)

Source	Solvent Medium	Composition (wt %)					Atomic ratios			
		C	H	N	O	S	H/C	N/C	O/C	S/C
Canada	n-pentane	79.5	8.0	1.2	3.8	7.5	1.21	0.013	0.036	0.035
	n-heptane	78.4	7.6	1.4	4.6	8.0	1.16	0.015	0.044	0.038
Iran	n-pentane	83.8	7.5	1.4	2.3	5.0	1.07	0.014	0.021	0.022
	n-heptane	84.2	7.0	1.6	1.4	5.8	1.00	0.016	0.012	0.026
Iraq	n-pentane	81.7	7.9	0.8	1.1	8.5	1.16	0.008	0.010	0.039
	n-heptane	80.7	7.1	0.9	1.5	9.8	1.06	0.010	0.014	0.046
Kuwait	n-pentane	82.4	7.9	0.9	1.4	7.4	1.14	0.009	0.014	0.034
	n-heptane	82.0	7.3	1.0	1.9	7.8	1.07	0.010	0.017	0.036

The measurement of the molar mass of petroleum asphaltenes is not an exact science. The problem appears to be that asphaltenes self-associate and form aggregates. These aggregates have been, detected by small-angle X-ray (Kim and Long, 1979) and neutron (Overfield et al., 1989) scattering as will be discussed later. The techniques that measure molar mass in solution often measure the aggregate molar mass and hence give high values. On the other hand the low volatility of asphaltenes interferes with mass spectrometry techniques and produces molar mass measurements that tend to be low.

The two techniques that have gained the most favor are Gel Permeation Chromatography (GPC) and Vapor Pressure Osmometry (VPO). However, the strong tendency of asphaltenes to adsorb throws off the calibration used for GPC techniques producing misleading results. VPO is now the preferred technique of many researchers due to its high accuracy, ease of use and relatively lower error of measurement. Nonetheless, VPO experiments have to be interpreted carefully.

Speight and Moschopedis (1976) showed that asphaltenes tend to self-associate even in dilute solutions and there has been considerable conjecture about the actual molar masses of these materials. They studied asphaltene molar masses by vapor pressure osmometry and showed that molar masses of various asphaltenes was dependent on the concentration of asphaltenes in the solvent. The self-association also depends on the nature of the solvent and on the solution temperature at which the determinations were performed. They showed that when the measured molar mass of asphaltenes was plotted against the dielectric constant of the solvent, a limiting value was reached for solvents of high dielectric constant such as nitrobenzene. The limiting molar masses were consistent with the molar mass anticipated on the basis of structural determinations by proton magnetic resonance spectroscopy. Experiments performed in pyridine showed that at infinite dilution a molar mass of 1800 g/mol was observed. Figure 2.2 shows these observations for Athabasca asphaltenes at 37° C.

Figure 2.2 Molar Mass Data for Athabasca Asphaltenes (Speight and Moschopedis, 1976)

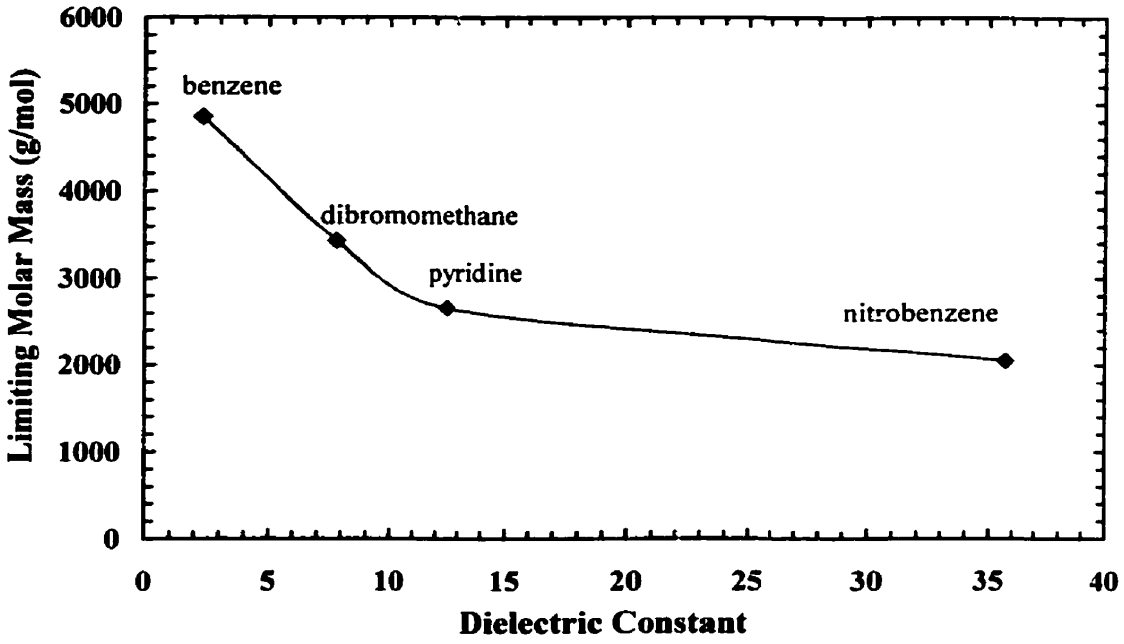

Speight (1989) performed numerous experiments with a Vapor Pressure Osmometer with Athabasca asphaltenes extracted from the bitumen using pentane, heptane, decane and hexadecane as solvents. The solvents used in the VPO were a relatively nonpolar solvent such as benzene as well as more polar solvents such as dibromomethane, nitrobenzene and pyridine. He showed that molar masses in benzene are significantly higher than those in nitrobenzene or pyridine. He used an asphaltene concentration of 2.5 % w/w and temperature of 37° C. These results are, summarized in Table 2.3.

In another supporting work by Ali et al (1989), the chemical structure of Qiayarah asphaltenes in heavy oils was investigated by nuclear magnetic resonance (n.m.r) technique. They measured the ^{1}H and ^{13}C n.m.r spectra of asphaltenes separated from heavy crude oil using n-pentane at different temperatures. In the three hypothetical

structures they proposed using average molecular parameters and n.m.r measurements, the calculated molar masses of unit sheets of asphaltenes ranged from 1400 to 2200 g/mol.

Table 2.3 Variation of Asphaltene Molar Mass with the Solvent Polarity, VPO Method (Moschopedis and Speight, 1976)

Solvent used to extract asphaltene*	Solvent used for VPO Measurement**			
	C_6H_6	CH_2Br_2	C_5H_5N	$C_6H_5NO_2$***
Pentane	8450	6340	2850	2320
Heptane	8940	7120	4380	2980
Decane	10050	7630	4840	3180
Hexadecane	12490	8800	5100	3210

* Feedstock: Athabasca bitumen
** Asphaltene concentration: 2.5 % w/w, 37° C
*** Data obtained at three higher temperatures and extrapolated to 37° C

Wiehe and Liang (1996) measured the average molar mass of asphaltenes from Arabian crude oil using vapor pressure osmometry. They chose o-dichlorobenzene as the solvent. They showed that at the highest temperature of commercial instruments, 130° C, the molar mass was independent of asphaltene concentration. By extrapolating the molar mass measurement at 70° C to zero concentration, the same value, 3390, within experimental error was obtained. However, one drawback in this work was that all the measurements were carried out at concentrations above 14 kg/m^3. However, the concentration dependence of molar mass occurs at lower concentrations as will be

explained in detail in Chapter 5 where similar experiments were performed with Athabasca asphaltenes.

2.3 Evidence for Asphaltene Self-Association

Measurement of asphaltene molar mass by the various methods described in the previous section was the first indication of asphaltene self-association. Solvent, temperature and asphaltene concentration have been shown to affect the molar mass of asphaltenes. However, there have been other techniques used by researchers to establish this phenomenon.

Herzog et al. (1988) performed small-angle X-ray scattering (SAXS) experiments using a synchrotron X-ray source for some asphaltene dispersions in organic solvents as well as natural solvents (maltenes). They interpreted asphaltene species were thin, large and porous particles with varying radius and a lateral extension possibly greater than 800 A°. This interpretation has been supported by several other experimental observations including those by Xu et al. (1995), who used SAXS to demonstrate the existence of particles with sizes ranging from 30 to 150 A° in crude oils diluted in aromatic solvents. Small angle neutron scattering (SANS), used by Ravey et al. (1988), revealed particle sizes in this same size range. Also they concluded that the physical dimensions and shape of the asphaltene aggregates was a function of solvent and temperature of investigation.

Mohamed et al. (1999) measured the surface and interfacial tensions (IFT) versus water in systems formed by Brazilian crude oil, n-pentane insolubles, and n-heptane

insolubles in the aromatic solvents toluene, pyridine, and nitrobenzene. IFT measurements were taken at room temperature using the ring method and employing an automatic tensiometer. Their results showed a cmc (critical micelle concentration) of asphaltenes indicating possible asphaltene aggregation. They proposed a plane wise adsorption of asphaltene molecule on the water-hydrocarbon interface. Rogel et al. (2000) used a similar technique and observed asphaltene cmc's in the range of 1 to 30 kg/m^3 depending on the asphaltene type and the solvent used. Sheu et al. (1996) studied the self-association of asphaltenes in pyridine and nitrobenzene through surface tension experiments. A discontinuous transition in the surface tension as a function of asphaltene concentration was interpreted as the critical asphaltene concentration above which self-association occurs.

Thus, the association of asphaltenes has been established through the numerous techniques used by researchers. Now let us consider possible mechanisms proposed in order to explain this association.

2.4 Mechanism of Asphaltene Self-Association

The precise mechanism of association has not been, conclusively established in literature. Hydrogen bonding, acid-base interactions, dipole-dipole interactions and π-π stacking of aromatic ring clusters have been proposed as possible mechanisms.

Leon et al (1998) performed surface tension and stability measurements to study the self-association behavior of two different asphaltene samples, one from a stable crude oil (non-precipitating) and the other from an unstable (precipitating) crude oil.

Asphaltenes from unstable crude oils were characterized by high aromaticity, low hydrogen content, and high condensation of the aromatic rings. Asphaltenes from stable crude oils showed low aromaticity, high hydrogen content, and low condensation of their aromatic rings. They showed that these structural and compositional characteristics of the asphaltenes strongly influence their self-associating behavior. They found that asphaltenes from unstable oils begin to aggregate at lower concentrations than asphaltenes from stable oils. Self-association appears to be related to a high content of condensed aromatics, which supports a π-π bonding mechanism. However, the role of heteroatoms in asphaltene self-association was not investigated by this group of researchers.

In the solid state, asphaltenes or aromatic clusters stack upon each other through π-π bonding in the same way graphite sheets stack (Yen, 1974). Hence, one possible mechanism for asphaltene self-association is π-π bonding. Brandt et al. (1995) proposed that the formation of stacked aromatics from single sheets is the first step in the process of aggregation. They used computer-aided molecular modeling to calculate parameters for an association model. They predicted that a high degree of stacking occurs at low asphaltene concentrations in neutral and poor solvents. However, with increasing asphaltene concentration they found that the stack size decreases and a limiting stack size of five units/stack was reached. Even in very good solvents, they found a limited ordering of the sheets into stacks. Their model also predicted a phase split beyond a critical poor solvency. The two phases are an asphaltene-rich phase with almost constant stack sizes and an asphaltene-lean phase with stack sizes strongly varying with the

temperature-dependent phase composition. The model also predicts a strong destabilizing effect when the asphaltene-to-solvent molecular-volume ratio decreases. They also showed that solid-asphaltenes had the same limiting stack size irrespective of the method of preparation (evaporation or precipitation). However, their results have yet to be verified experimentally.

Petersen (1967) investigated the presence of intermolecular and intramolecular hydrogen bonding in asphaltenes using infrared spectrophotometry. He examined the OH and NH stretching bands of whole and diluted asphaltene samples. Phenolic and/or alcoholic OH and pyrrole-type NH were found to exist largely as hydrogen-bonded complexes. He found that asphaltenes were more difficult to dissociate in carbon tetrachloride and exhibited more intramolecular bonding than maltenes. He suspected that in addition to oxygen and nitrogen atoms, π-bases were important in hydrogen bonding. Also since the association forces of hydrogen bonding are large, these forces probably play an important role in the properties and behavior of asphaltenes.

In another recent work, Rogel (2000) showed through molecular modeling that the stabilization energies obtained for asphaltene and resin associates were due mainly to the van der Walls forces between the molecules. Comparatively, the contribution of hydrogen bonding to the stabilization energy was very low.

Maruska and Rao (1987) studied the involvement of dipoles in asphaltene association and concluded that interactions between heteroatoms are responsible for asphaltene association. They quantified the dipole moment of asphaltenes by applying dielectric spectroscopy to several heavy oils with different asphaltene concentrations.

The response of the permanent dipoles was measured as a function of concentration and temperature. They showed that as the concentration of asphaltenes exceeded 10% the dielectric constant exhibited substantial negative deviation from linearity, signifying the onset of intermolecular interactions. They also noted that raising the temperature increased the dielectric constant, indicating dissociation of the aggregates. They established that asphaltenes have dielectric constants ranging from 5 to 7. Their model calculations indicated more than one dipole per asphaltene molecule. The diameter of the dipole center was assessed to be 3 to 6 A°.

Maruska and Rao concluded that polar interactions, such as between acid-base functionalities, are involved in the aggregation of asphaltene molecules to form high molar mass oligomers. These molecules contain more than one heteroatom each and the heteroatoms are responsible for giving the molecule its polar character. In a dilute solution the separation of the polar species allows the existence of monomers. As the concentration is raised, they encounter one another and form pairs to lower the local net dipole field. If a molecule has more than one dipole then it can continue the interaction to form higher oligomers. However, in the most concentrated cases, not all the dipolar field is effectively cancelled. Also they proposed that as the molecules associate and form a complex interacting system, the local mobility is affected and hence the viscosity increases.

Thus, it is, seen that different researchers have proposed different mechanisms to explain asphaltene aggregation. However, there is no consensus yet among all the postulated theories due to the complex nature of petroleum asphaltenes and resins.

2.5 Interactions of Asphaltenes with Resins

The behavior of asphaltenes in petroleum has been complicated by another solubility class called the resins which are structurally similar to asphaltenes. Petroleum resins are defined as those materials that remain soluble when petroleum or asphalt is dispersed in pentane but adsorb on a surface-active material such as Fuller's earth. As mentioned earlier, resins are structurally very similar to asphaltenes but have a higher H/C ratio and lower heteroatom content, polarity and molar mass. Hence, the number of links they can form through hydrogen bonding, aromatic stacking or acid-base interactions is lower than those formed by asphaltenes.

Koots and Speight (1975) noted that the association of resins does not occur to anywhere near the same extent as asphaltenes and the molar masses of these materials in benzene appear to be those of unassociated entities. They measured molar masses ranging from about 700 to 1000 g/mol for a whole range of resins extracted from Canadian and Middle East crude oils.

Rogel (2000) carried out molecular mechanics and dynamics calculations for asphaltenes and resins from crude oils of different origins. She used average structural models of the resins obtained from analytical techniques. The average resin molar mass ranged from 600 to 1000 g/mol.

Speight (1999) isolated a suite of petroleum resins and studied their elemental composition (Table 2.4). He showed that the proportions of carbon and hydrogen, like those of asphaltenes, vary over a narrow range: 85 ± 3% carbon and 10.5 ± 1% hydrogen. The proportions of nitrogen (0.5 ± 0.15%) and oxygen (1.0 ± 0.2%) also appear to vary

over a narrow range, but the amount of sulfur (0.4 to 5.1%) varies over a much wider range. There are notable increases in the H/C ratios of the resins, relative to those of the asphaltenes. Presumably this indicates that aromatization is less advanced in the resins than in the asphaltenes. There is also a tendency to decreased proportions of nitrogen, oxygen, and sulfur in the resins relative to the asphaltenes.

Table 2.4 Elemental Composition of Petroleum Resins (Koots and Speight, 1975)

Source	Composition (wt %)					Atomic ratios			
	C	H	O	N	S	H/C	O/C	N/C	S/C
Canada	86.1	11.9	1.1	0.5	0.4	1.66	0.009	0.005	0.002
Iraq	77.5	9.0	3.1	0.3	10.1	1.39	0.03	0.003	0.048
Italy	79.8	9.7	7.2	trace	3.3	1.46	0.067	-	0.016
Kuwait	83.1	10.2	0.6	0.5	5.6	1.47	0.005	0.005	0.025
USA	85.1	9.0	0.7	0.2	5.0	1.27	0.006	0.002	0.022
Venezuela	79.6	9.6	--4.5--		6.3	1.45	-	-	0.030

The majority of investigators have been inclined to focus their attention on the asphaltene and oil fraction of the crude oil, while studies on the function of resins has only been briefly documented in the literature. For example, Sanchanen and Wassiliew (1972) noted that molar masses of resins depended on the molar masses of the crude oils from which they were derived. Witherspoon and Munir (1960) briefly noted that resins were required for asphaltenes to dissolve in the distillate portion of the crude oil. More

specific mention of their function was made by Dickie and Yen (1967) who consider that petroleum resins provide a transition between the polar (asphaltene) and the relatively non-polar (oil) fractions in petroleum thus preventing asphaltene self-association.

Koots and Speight (1975) investigated the role of resins in a crude oil by performing a series of tests based on the dissolution of asphaltenes in various crude oil fractions. The results confirmed that petroleum asphaltenes are not soluble in their corresponding resin-free oil fractions. Also they found that petroleum asphaltenes were insoluble in oil fractions of other crudes. It was only possible to bring about dissolution of the asphaltenes by the addition of the corresponding resins. However, while resins were able to dissolve asphaltenes from the same source crude in the oil fraction of any crude oil, it was much more difficult to bring about asphaltene dissolution by interchanging various asphaltenes and resin fractions. In all cases, dissolution did eventually occur but the resulting synthetic 'crude oils' were found to be unstable and deposited granular asphaltene material on standing overnight. Also the general indications are that the degree of aromaticity and the proportion of heteroatoms in the resins play an important part in the ability of these materials to solubilize asphaltenes in oil.

Moschopedis and Speight (1976) showed that dilute solutions (0.01-0.5% w/w) of Athabasca asphaltenes in a variety of non-polar organic solvents exhibit the free hydroxyl absorption band (c.3585 cm^{-1}) in the infrared. At higher concentration (>1% w/w) this band becomes less distinguishable, with concurrent onset of the hydrogen-bonded hydroxyl absorption (c.3200-3450 cm^{-1}). Upon addition of a dilute solution (0.1-1%

w/w) of the corresponding resins to the asphaltene solutions, the free hydroxyl absorption was reduced markedly or disappeared, indicating the occurrence of intermolecular hydrogen bonding between the asphaltenes and resins. Hence when resins and asphaltenes are present together hydrogen bonding may be one of the mechanisms by which resin-asphaltene interactions are achieved. Also resin-asphaltene interactions appear to be stronger that asphaltene-asphaltene interactions. Thus in petroleums and bitumens it is believed that asphaltenes exist not as agglomerations but as single entities that are dispersed by resins.

Ignasiak et al (1977) confirmed the earlier work of Moschopedis et al. (1976) by showing that intermolecular hydrogen bonding was, involved in asphaltene association and has a significant effect on observed molar masses. He proposed that asphaltenes might exist as sulfur polymers.

In a recent work by Murgich et al. (1999), the conformation of lowest energy of an asphaltene molecule of the Athabasca sand oil was calculated through molecular mechanics. Molecular aggregates formed from the asphaltene with nine resins from the same oil, in an n-octane and toluene medium were studied. The resins showed higher affinities for the asphaltene than toluene and n-octane and also exhibited a noticeable selectivity for some of the external sites of the asphaltene. They showed that this selectivity depended on the structural fit between the resins and the site of the asphaltene. The selectivity explains why resins of one oil may not solubilize asphaltenes from other crudes. They concluded that both enthalpic and entropic contributions to free energy should be considered when the stability of the asphaltene and resin molecular aggregates

is examined. These results are significant because they demonstrate that asphaltene molecules, especially the large ones, are not necessarily two-dimensional flat disks but they have the capacity to fold upon themselves into a complex 3-D structure.

Chang and Fogler (1994) investigated the stabilization (disaggregation and dispersion) of crude oil asphaltenes in apolar alkane solvents using a series of alkylbenzene-derived amphiphiles as the asphaltene stabilizers. They assessed the influence of the chemical structure of these amphiphiles on the effectiveness of asphaltene solubilization and on the strength of asphaltene-amphiphile interaction using both UV/vis and FTIR spectroscopies. They showed that the polarity of the amphiphile's head group and the length of the amphiphile's alkyl tail primarily controlled the effectiveness of the amphiphile in stabilizing asphaltenes. Increasing the acidity of the amphiphile's head group could promote the amphiphile's ability to stabilize asphaltenes by increasing the acid-base attraction between asphaltenes and amphiphiles. On the other hand, although decreasing the amphiphile's tail length increased the asphaltene-amphiphile attraction slightly, it still required a minimum tail length for amphiphiles to stabilize the asphaltenes. They also found that additional acidic side groups of amphiphiles could further improve the amphiphile's ability to stabilize asphaltenes. They also studied the role of solvent on the amphiphile stabilization of asphaltenes. Thus they proposed that two factors were important to stabilize asphaltenes by amphiphiles, the adsorption of amphiphiles to asphaltene surfaces and the establishment of a stable steric alkyl layer around asphaltene molecules.

In another supporting work, Chang and Fogler (1996) studied the interactions between asphaltenes and resins. In their study, two types of oil soluble polymers, dodecylphenolic resin and poly (octadecene maleic anhydrite) were synthesized and used to prevent asphaltenes from flocculating in heptane media through the acid-base interactions with asphaltenes. The results indicated that these polymers could associate with asphaltenes to either inhibit or delay the growth of asphaltene aggregates in alkane media. However, multiple polar groups on a polymer molecule make it possible to associate with more than one asphaltene molecule, resulting in hetero-coagulation between asphaltenes and polymers. It was found that the size of the asphaltene-polymer aggregates was strongly affected by the polymer-to-asphaltene weight ratio. At low polymer-to-asphaltene weight ratios, asphaltenes were found to flocculate among themselves and with polymers until the flocs precipitated out of solution. On the other hand, at high polymer-to-asphaltene weight ratios, small asphaltene-polymer aggregates formed that remained fairly stable in solution.

2.6 Asphaltenes in Crude Oils

The preceeding sections have shown that asphaltenes self-associate and that other oil constituents especially resins, influence the association. The associated asphaltenes can be considered as micelles, colloidal particles and/or macromolecules.

2.6.1 Micelle/Colloid Concept

An early hypothesis of the physical structure of petroleum (Pfeiffer and Saal, 1940) indicated that asphaltenes are the centres of micelles or colloids formed by association or possibly adsorption of part of the maltenes (i.e., resins) onto the surfaces or into the interiors of the asphaltene aggregates.

The term "micelle", "colloid" and "aggregate" are often used interchangably in the literature. Strictly speaking, a micelle refers to an aggregate of surfactant molecules that forms above a certain concentration, the critical micelle concentration. The aggregation is driven by hydrophobic/hydrophillic interactions; for example, the surfactant molecules of a micelle in an oil medium are arranged so that the hydrophillic part of the molecules reside inside the micelle away from the oil.

In the micellar view of asphaltenes, asphaltene monomers form micelles above a cmc. Researchers have focussed on identifying a cmc with interfacial tension measurements (Mohamed et al., 1999; Sheu et al., 1996; Rogel et al., 2000). However, Yarranton et al. (2000) demonstrated that asphaltene self-association occurs in the absense of any evidence of micelle formation. Recent work (Alboudwarej et al., 2001) suggest that apparent asphaltene cmc's may result simply from a change in asphaltene molar mass, without involving the micelle model. Hence, the micelle model is not supported by strong experimental evidence.

A better supported model of asphaltene structure is the colloidal model. According to the colloidal view (Leontaritis and Mansoori, 1988), a crude oil is composed of asphaltene molecules (colloids with their surface covered by resin

molecules) suspended in the crude oil. The adsorbed resins prevent aggregation and disperse the asphaltenes. The colloids can aggregate upon a change in the system temperature , pressure and composition that causes resins to desorb from the asphaltenes. The colloidal view is consistent with SANS and SAXS evidence of asphaltene aggregates in the nanometer size range. The colloidal model is the prevalant view of asphaltenes in crude oils.

2.6.2 Polymer/Macromolecule Concept

According to this alternative school of thought, asphaltenes exist as free molecules in a non-ideal solution (Hirschberg et al., 1984). Hirschberg et al. assumed that "pure" asphaltenes aggregate by a linear "polymerization" process. The asphaltene monomer they considered corresponded to the asphaltene sheet defined by Yen (1972). They proposed that in crude oil the polymerization is blocked (reduced) by the association of asphaltenes with similar but less polar hetero-components, the resins.

The greatest difference between the polymer/macromolecular view and micelle/colloidal view of asphaltenes is the fact that the latter considers asphaltene aggregates to be solid particles. There is no convincing evidence to explain which if any of the views correctly describe the nature of the asphaltenes. However, due to the relative simplicity of the macromolecular/polymer concept of asphaltenes, this has been used to model the aggregation of asphaltenes in this thesis and will be discussed in detail in Chapter 5.

2.7 Asphaltene Solubility

The different views of an asphaltene aggregate have led to two types of asphaltene solubility models: the colloidal models and the continuous thermodynamic models. In all these models, a number of parameters are tuned to obtain best fits to the experimental data. One significant parameter for both models is the molar mass of the asphaltenes. However, the existing models do not fully account for asphaltene self-association. All of them use a fixed average molar mass and molar mass distribution of asphaltenes. But, as shown previously, asphaltene molar mass varies significantly with temperature, solvent and concentration. Hence to predict asphaltene solubility it is necessary to model asphaltene self-association in order to predict the molar mass distribution.

Chapter 3

Experimental Methods

In this work, asphaltene association is assessed by measuring the molar mass of asphaltene-resin mixtures at various conditions. Asphaltenes and resins were obtained from Athabasca and Cold Lake bitumens by SARA fractionation. Molar masses were measured with a vapor pressure osmometer (VPO). Details are provided below.

3.1 Materials

All experiments with the VPO were performed using high purity solvents and chemicals. Toluene (99.96% purity) was obtained from VWR and o-dichlorobenzene (99% HPLC grade), distilled water, light mineral oil, octacosane and sodium dodecyl sulphate was obtained from Sigma Aldrich Co. Sucrose octaacetate was obtained from Jupiter Instrument Co. For asphaltene extractions and SARA fractionation, reagent-grade solvents were used. n-Pentane, n-heptane and toluene were obtained from Phillips Chemical Co.; acetone, methanol and dichloromethane from BDH Inc. Attapulgus clay was obtained from Engelhard Corporation, New Jersey and silica gel (grade 12, 28-200 mesh size) was obtained from Sigma Aldrich Co.

Athabasca bitumen was obtained from Syncrude Canada Ltd. and Cold lake bitumen from Imperial Oil. The Athabasca bitumen is an oil sand processed to remove sand and water. The Cold Lake bitumen is produced from an underground reservoir through cyclic steam injection and has also been processed to remove sand and water.

3.2 SARA Analysis of Petroleum Crudes

SARA fractionation is a technique for the separation of petroleum crudes into different fractions based on their solubility. This method, referred to as Clay-Gel Absorption Chromatography (ASTM D 2007), is a procedure for classifying oil samples of initial boiling point of at least 260° C (500° F) into hydrocarbon types of polar compounds, aromatics and saturates. The following terms refer to the hydrocarbon types separated by this test method:

a) *asphaltenes*, or *n-pentane insolubles* – insoluble matter that precipitates from a solution of oil in n-pentane under the conditions specified.

b) *resins* or *polar compounds* – material retained on adsorbent clay after percolation of the sample in n-pentane eluent under the conditions specified.

c) *aromatics* – material that, on percolation, passes through a column of adsorbent clay in an n-pentane eluent but adsorbs on silica gel under the conditions specified.

d) *saturates* – material that, on percolation in an n-pentane eluent, is not adsorbed on either the clay or silica gel under the conditions specified.

In the present work asphaltenes and resins are extracted using this technique and used thereafter for VPO measurements.

3.2.1 Extraction and Purification of Asphaltenes

The first step of SARA fractionation is to precipitate asphaltenes from a crude oil with the addition of n-pentane. In the standard procedure, 40 volumes of pentane are

added to one volume of bitumen. The mixture is sonicated using an ultrasonic bath for 45 minutes and left overnight. Next day, the mixture is filtered using a Whatman's No.2 (8μm) filter paper. The filter cake is mixed with 4 volumes of solvent, sonicated for 45 minutes and left overnight. The mixture is again filtered and subsequently washed with pentane for 5 days until no coloration of the solvent is observed. The solvent is recovered from the solvent-maltene (deasphalted oil) mixture using a rotovap at 40° C. The asphaltenes and maltenes are dried in a vacuum oven at 50° C until no change in weight is observed. These asphaltenes are referred to as C5-asphaltenes since n-pentane (a C5 n-alkane) was used for the extraction. The maltenes were further separated into saturates, aromatics and resins as discussed in the next section.

Note that, since an 8μ filter paper was used for asphaltene extraction, asphaltenes smaller than 8μm may pass through the filter paper and become a part of the maltenes. These then became a part of the resin fraction after SARA fractionation is completed. To estimate the asphaltene loss, resins were added to n-pentane and the weight of the insoluble fraction was measured. This was about 2-3 % of the original bitumen. The C5-asphaltenes typically contain some resinous material that is insoluble in n-pentane but may be soluble in a higher n-alkane such as n-heptane. It was desired to test asphaltenes with less resinous material. Therefore, asphaltenes were also extracted from the bitumens using n-heptane. The same procedure was used as for n-pentane and the resulting asphaltenes are referred to as C7-asphaltenes.

From Table 3.1 it can be seen that C5-asphaltenes make up approximately 17.5% of bitumen whereas C7-asphaltenes make up approximately 13.5%. Since C7-

asphaltenes make up less of the bitumen, it is likely that these asphaltenes contain less resinous material. It is for this reason that only maltenes obtained from the extraction of C5-asphaltenes were used for the rest of the SARA fractionation. The significance of lower proportion of resinous material in C7-asphaltenes will be discussed in detail in Chapter 5.

Table 3.1 Composition of Athabasca and Cold Lake Bitumen

	Present Work		Literature*	
Bitumen Fraction	**Athabasca**	**Cold Lake**	**Athabasca**	**Cold Lake**
Saturates	16.3	17.3	19.4	20.7
Aromatics	39.8	39.7	38.1	39.7
Resins	26.4	25.8	26.7	24.8
C5-asphaltenes	17.5	17.3	15.8	15.3
C7-asphaltenes	13.4	14.5	11.3	-
toluene insolubles (weight fraction of C5-asphaltenes)	6.5	-	-	-
toluene insolubles (weight fraction of C7-asphaltenes)	7.8	6.3	2.3	-

* Peramanu et al. (1999)

The dried C5- or C7-asphaltenes were purified to remove any non-asphaltenic solids (consisting of clay, sand, and some adsorbed hydrocarbons) that co-precipitated along with the asphaltenes. To remove these solids, the asphaltenes were dissolved in toluene, typically at a concentration of 0.01 g of asphaltene/cm^3 of toluene. The mixture was centrifuged at 3500 rpm (900g's) for 5 minutes. The supernatant was removed and

dried in a rotary evaporator at 70° C under vacuum. The fractions of the C5- and C7-asphaltenes that did not dissolve in toluene are reported in Table 3.1.

To investigate further the effect of removing resins, a Soxhlet apparatus was used to obtain ultra pure asphaltenes. This method is used for continuous extraction of analytes from a solid into an organic solvent. A schematic of the Soxhlet apparatus is shown in Figure 3.1. A flask containing the solvent and the non-volatile extract is heated so that pure solvent vapor rises in the larger outside tube, enters the water-cooled condenser and liquifies. The pure solvent drips through the solid material, in effect continuously washing the solid. This method of extraction is equivalent to infinite washing stages.

Figure 3.1 Soxhlet Apparatus

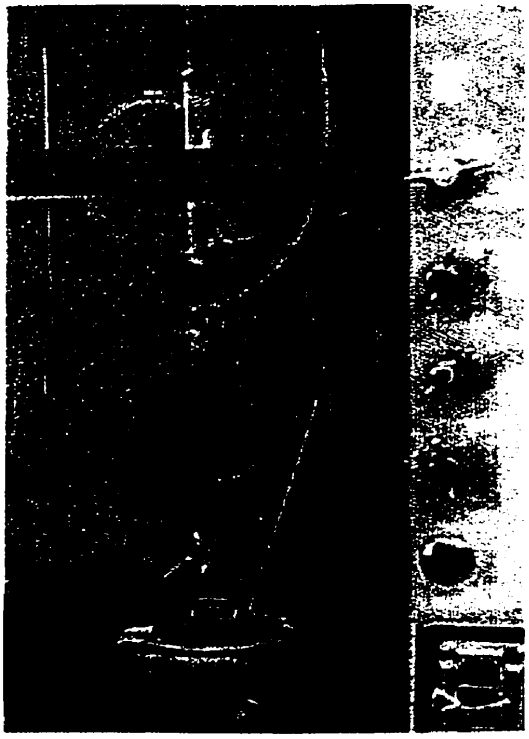

3.2.2 Fractionation of Maltenes

The maltenes from the pentane extraction are used for fractionation into saturates, aromatics and resins. The separation into these petroleum fractions is performed using the Clay-Gel Adsorption Chromatography method (ASTM D2007M). This technique is described in detail below.

Clay and Gel Activation

Approximately 200 g of Attapulgus clay is washed in a beaker with methylene chloride 2-3 times until the wash is colorless. The procedure is repeated with methanol and then with distilled water until the pH of the water is 6-7. The washed clay is evenly spread on a metal tray and dried in an oven overnight at 80° C under vacuum. Activation of the silica gel only requires heating. Approximately 200 g of silica gel is spread evenly on a tray and dried in an oven overnight at 145° C. After this procedure the dried silica gel and clay are activated and ready for use in chromatography.

Chromatographic procedure

The adsorption column consists of two identical glass sections assembled vertically as shown in Figure 3.2. 100 g of freshly activated Attapulgus clay is placed in the upper adsorption column. 200 g of activated silica gel is placed in the lower column. 50 g of Attapulgus clay is added on top of the gel. It is important that the adsorbents in each column be packed at a constant level. A constant level of packing of the adsorbent is achieved with a minimum of ten taps with a soft rubber hammer at different points up and down the column. A piece of glass wool (of about 25 mm loose thickness) is placed over the top surface of the clay in the upper column to prevent agitation of the clay while

charging the eluents. The two columns are assembled together (clay over gel) after lubricating the joint with hydrocarbon-insoluble grease.

Figure 3.2 Clay-Gel Adsorption Columns

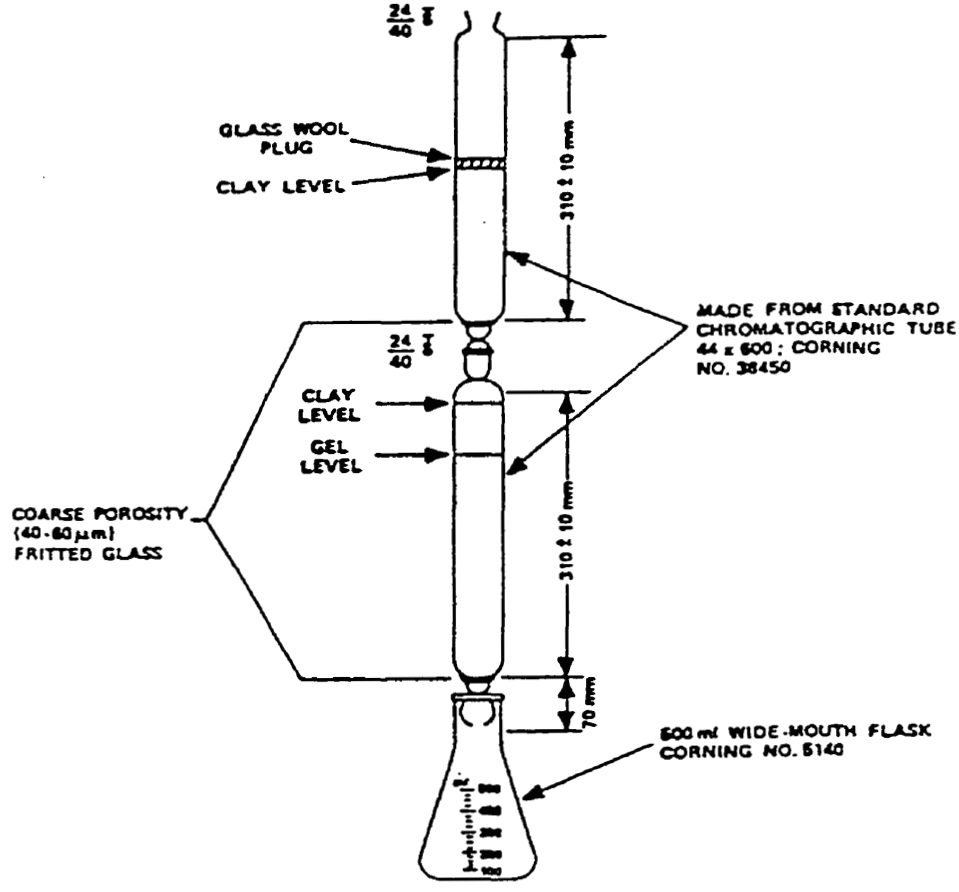

5 g of maltene sample is weighed in a beaker, diluted with 25 ml of pentane and swirled to ensure a uniform sample. Prior to sample addition, 25 ml of pentane is added to the top of the clay portion of the assembled column with the help of a funnel and allowed to percolate into the clay. When all the pentane has entered the clay, the diluted sample is charged to the column. The sample beaker is washed 3-4 times with pentane

and the washings are added to the column. After the entire sample has entered the clay, the walls of the column above the clay are washed free of the sample with pentane. After all the washings have entered the clay, pentane is added to maintain a liquid level well above the clay bed until saturates are washed from the adsorbent. Approximately 280 ± 10 ml of pentane effluent is collected from the column in a graduated, 500 ml wide mouth conical flask. After the collection is finished, the flask is replaced with another flask for collection of aromatics and put away until the solvent is to be removed.

Immediately after all the pentane has eluted, a solvent mixture of pentane and toluene (50:50) in the amount of 1560 ml is added to the column through a separatory funnel. The column is allowed to drain. At this point, resins are adsorbed on the clay in the upper column and aromatics are adsorbed on the gel in the lower column. The two column sections are disconnected carefully so that no sample or solvent is lost.

In order to extract the aromatics, the bottom section is placed in an extraction assembly. Toluene in the amount of 200 ± 10 ml is placed in a 500 ml 3-neck flask and refluxed at a rate of 8-10 ml/min for 2 hours as shown in Figure 3.3. The toluene reflux is measured by collecting the reflux flow for one minute in a graduated cylinder (the solution in the flask is later combined with the rest of the aromatic fraction).

To recover the resins, a solvent mixture of toluene and acetone (50:50) in the amount of 400 ml is charged slowly to the top clay column section. The effluent is collected in a separate flask. If the sample contains moisture, the effluent is collected in a 500 ml separatory funnel, shaken well with approximately 10 g of anhydrous calcium chloride granules for 30 sec, allowed to settle and filtered through an 8μ size filter paper.

Figure 3.3 Extraction Apparatus for Aromatics

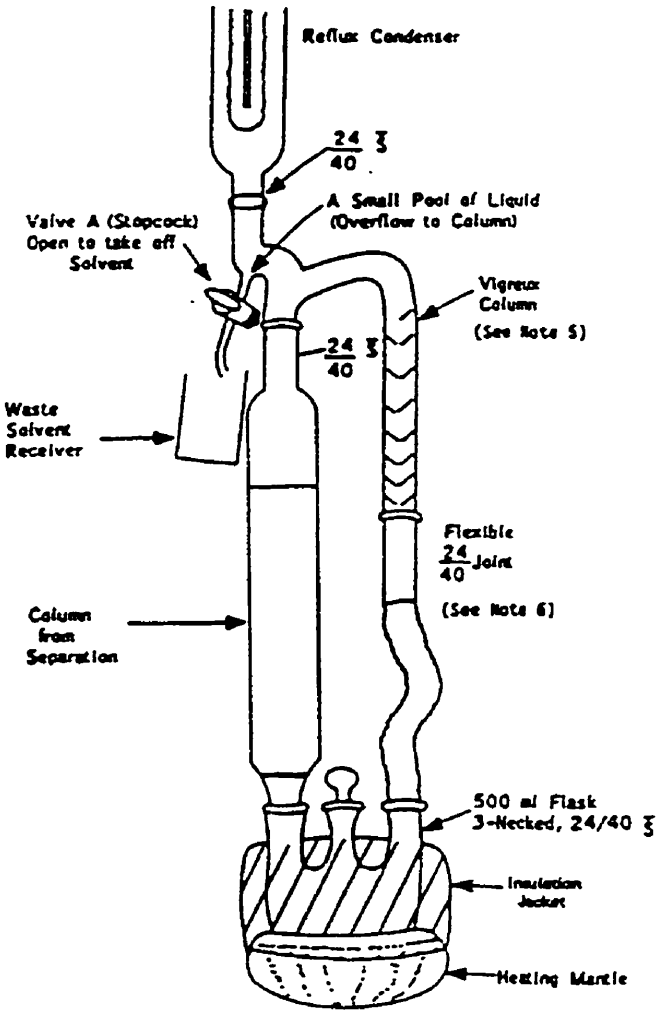

Solvent Removal

The saturate/pentane solution from the 500 ml wide mouth conical flask is transferred to a 500 ml round bottom flask. The conical flask is rinsed 3-4 times with pentane to get all the Saturates out into the round bottom flask. The solvent is evaporated using a rotovap with the water bath set at a temperature of 35° C.

Similarly, the resin/acetone/toluene and aromatic/pentane/toluene effluents are transferred to respective round bottom flasks and solvent is removed with the rotovap with water bath temperature set at 65° C under vacuum. After solvent evaporation each fraction is transferred into glass vials. The fractions are dried in the fume hood until no change in weight is observed.

Selection of sample size

SARA fractionation in our case is limited by the capacity of the columns to adsorb resins. Hence, the sample size was determined based on the resins content in the sample according to the guideline given in Table 3.2. Also if 5 g of sample is chosen (high resin content), two upper columns are used in conjunction with a single bottom column to optimize the fractionation.

Table 3.2 Selection of Sample Size for SARA Fractionation

Resins Content Range (wt percent)	Sample size, g
0-20	10 ± 0.5
Above 20	5 ± 0.2

Results of SARA fractionation

The SARA analysis in weight percent of Athabasca and Cold Lake bitumen and is compared with those found in literature in Table 3.1. It was observed that the average yield was about 93 to 94%. The loss is attributed to resins that remained adsorbed in the

clay section. Since, resins are known to adsorb strongly, especially the higher molar mass constituents, the missing 6-7% was assigned to the resin fraction.

3.3 Experimental Techniques for Molar Mass Measurements

Several methods have been used for asphaltene molar mass determination. These can be divided into absolute methods that yield the absolute molar mass without the use of any standard and relative methods that require calibration with a material of known molecular weight. Molecular weight determination methods are also classified into those that give an average value (number or mass average) and those that give a complete distribution. In the category of absolute methods, membrane osmometry, cryoscopy, eulliometry and light scattering measure the average molar mass while equilibrium ultracentrifuge measures the molecular weight distribution. In the category of relative methods, viscosity and vapor pressure osmometry (VPO) measure the average molar mass and gel permeation chromatography (GPC) measures the molecular weight distribution. Among these methods, VPO and GPC have been extensively used because relative methods requiring calibration are generally easier and faster than absolute methods.

GPC (also known as size exclusion chromatography) is an attractive method for determining molar-average molecular weight distribution of petroleum fractions. However, it is important to realize that petroleum contains constituents that have a wide range of polarities and types and each particular type interacts with the gel surface to a different degree. The strength of the interaction increases with increasing polarity of the

constituents and with decreasing polarity of the solvent. For example, asphaltenes are made up of polynuclear aromatics with a strong tendency to adsorb on polystyrene gel. Hence, due to the lack of realistic standards of known number-average molecular weight distribution for calibration purposes, this technique poses problems in interpretation of the obtained distributions.

Mass Spectroscopic techniques such as Plasma Desorption Mass Spectroscopy (PDMS) have also been used but the molar masses obtained from these methods are suspect because of the low volatility of asphaltenes.

VPO on the other hand is a popular technique, as it appears to accurately measure the number-average molar mass under the correct set of temperature and solvent conditions. This technique was used to collect average molar mass data of asphaltenes and resins in different solvents, and at different temperatures and solute concentrations.

3.4 Description and Operation of the Vapor Pressure Osmometer (VPO)

Vapor Pressure Osmometry (VPO) is a technique based on the difference in vapor pressure between a pure solvent and a solution. The vapor pressure difference is manifested as a temperature difference, which can be measured very precisely with thermistors. When calibrated with a suitable standard material, the temperature difference can be converted to a molar concentration and thus to molecular weight. The theory is described in detail in the forthcoming section. A Model 833 VPO from Jupiter Instrument Company was used. This osmometer has a detection limit of 5×10^{-5} mol/L when used with toluene or chloroform.

A VPO consists of two thermistors in a temperature-controlled chamber containing saturated solvent vapor, as shown in Figure 3.4. The two thermistors are placed in the measuring chamber with their glass-enclosed, sensitive bead elements pointed up. Small pieces of fine stainless steel screen are formed into "caps" that are placed over the thermistors to hold a small volume of liquid on each bead. These thermistors are connected in an AC bridge. The voltage difference between the thermistors is measured with a synchronous detector system.

Figure 3.4 Schematic of Vapor Pressure Osmometer (VPO)

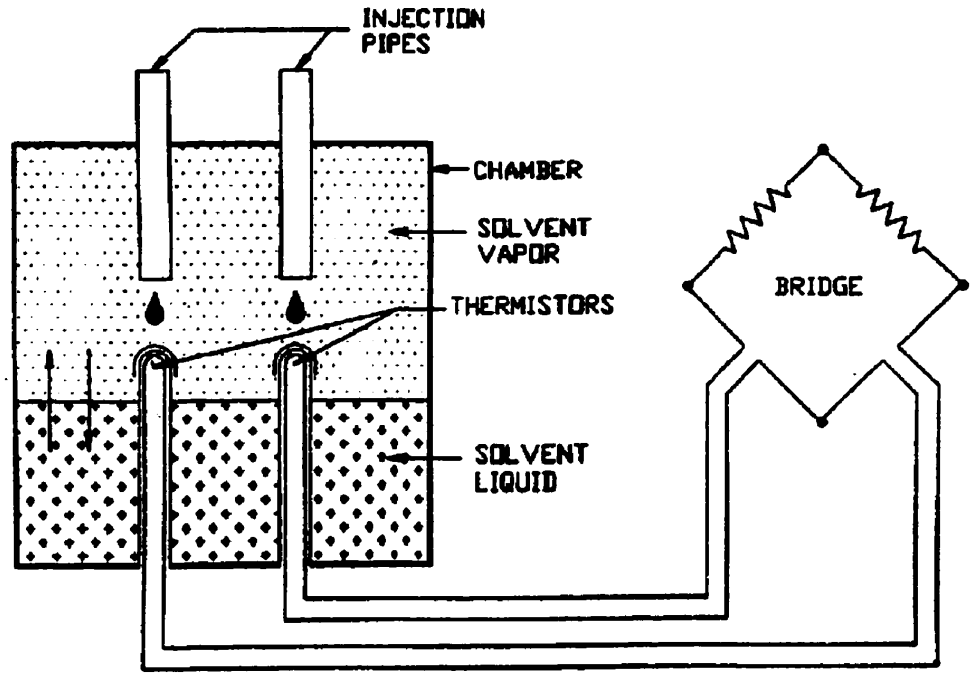

The chamber contains a reservoir of solvent and two wicks to provide a saturated solvent atmosphere around the thermistors. Temperature is controlled by a closed loop

control system to maintain a stable, uniform chamber temperature. Under these conditions, if pure solvent is placed on both thermistors, they will be at the same temperature and the bridge can be adjusted to zero to establish a "reference" condition.

If the pure solvent on one thermistor is then replaced by solution, condensation into the solution from the saturated solvent atmosphere will proceed due to lower vapor pressure of the solution. But solvent condensation releases heat, so this process will warm the thermistor. In principle, condensation will continue until the thermistor temperature is raised enough to bring the solvent vapor pressure of the solution up to that of pure solvent at the surrounding chamber temperature. Thus a temperature difference will be attained between the two thermistors, which is directly related to the vapor pressure of the solution. If the solute concentration is known, this temperature difference can be used to calculate the molecular weight as follows.

In a sufficiently dilute solution, the vapor pressure of the solvent is, given by Raoult's Law:

$$p_1 = P_1^0 x_1 \tag{3.1}$$

where p_1 is the partial pressure of solvent in solution, P_1^0 is the vapor pressure of pure solvent and x_1 is the mole fraction of solvent.

Also for a binary mixture, $x_1 = 1\text{-}x_2$ where x_2 is the mole fraction of solute. Hence,

$$p_1 = P_1^0 (1\text{-}x_2) \tag{3.2}$$

$$\Delta P = P_1^0 - p_1 = P_1^0 x_2 \tag{3.3}$$

where ΔP is the reduction in vapor pressure. The pressure change is related to the temperature change through the Clausius-Clapeyron equation.

$$\frac{dp^0}{dT} = \frac{p^0 \Delta H_v}{RT^2} \tag{3.4}$$

where $p°$ is the vapor pressure, T is the absolute temperature, ΔH_v is the enthalpy of vaporization and R is the gas constant. Eq. 3.4 can be integrated to yield

$$\Delta T = \frac{RT^2 \Delta P}{p^0 \Delta H_v} \tag{3.5}$$

For the very small temperature changes encountered in the vapor pressure osmometer, it is assumed that T, ΔH_v and $p°$ are constant. Substitution of Eq. 3.3 into Eq. 3.5 yields

$$\Delta T = \frac{RT^2 P_1^0 x_2}{p^0 \Delta H_v} \tag{3.6}$$

For small pressure changes $P_1{}^0 \approx p°$. Hence,

$$\Delta T = \frac{RT^2 x_2}{\Delta H_v} \tag{3.7}$$

Now by definition,

$$x_2 = n_2/(n_1+n_2)$$

where n_1 is the number of moles of solvent and n_2 is the number of moles of solute.

For very small n_2, $x_2 \approx n_2/n_1$ and hence

$$\Delta T \approx \frac{RT^2}{\Delta H_v} \frac{n_2}{n_1} \tag{3.8}$$

or

$$\Delta T \approx \frac{RT^2}{\Delta H_v} \frac{C_2}{m_2} \frac{m_1}{1000} \tag{3.9}$$

where C_2 is the solute concentration (w/w), m_2 is the solute molecular weight *and* m_1 is the solvent molecular weight. Then

$$\Delta T \approx K_1 \frac{C_2}{m_2} \tag{3.10}$$

where K_1 includes all the constant terms in Eq. 3.9.

In the VPO, a voltage change ΔV is observed, which is proportional to the temperature difference ΔT.

$$\Delta V = \Delta V_1 - \Delta V_{blank} = K_2 \Delta T \tag{3.11}$$

where ΔV_1 is the measured voltage difference of the solution and ΔV_{blank} is the measured voltage difference of the pure solvent. From Eq.'s 3.10 and 3.11 and combining the constants, a relationship between ΔV and m_2 is obtained.

$$\Delta V \approx K_0 \frac{C_2}{m_2} \tag{3.12}$$

Eq. 3.12 is the basis for all calculations related to the VPO. The calibration factor K_0 is determined for each set of experimental conditions (solvent and temperature) by measuring ΔV and C_2 for one or more materials of known molecular weight m_2. By reversing the procedure, unknown molecular weights are determined using the factor K_0. The calibration factor also includes heat lost by radiation, conduction, and convection. For finite solute concentrations when the assumption of ideal solution is not valid, the relation is given by (Peramanu et al., 1999):

$$\frac{\Delta V}{C_2} = \frac{K_0}{M_{app}} = K_0 \left(\frac{1}{M_2} + A_2 C_2 + A_3 C_2^2 + ... \right) \tag{3.13}$$

where M_{app} is the apparent molecular weight of the solute and A_i are the coefficients. Most solutes form nearly ideal solutions with the solvent at low concentrations and it is sufficient to include only the first power of concentration in Eq. 3.13. Hence,

experimental data can be fit to a straight line for extrapolation to a zero concentration as follows:

$$\frac{\Delta V}{C_2} = \frac{K_0}{M_{app}} = K_0\left(\frac{1}{M_2} + A_2 C_2\right) \tag{3.14}$$

Note that a plot of $\Delta V/C_2$ versus C_2 gives a straight line with a slope of K_0A_2 and an intercept of K_0/M_2. For an ideal system, a plot of $\Delta V/C_2$ versus C_2 gives a line of a constant value of K_0/M_2.

3.5 VPO Calibration Curves and Verification of the Detection of Aggregation.

In order to check if the VPO was able to detect aggregation, VPO measurements were performed on a typical surfactant system, sodium dodecyl sulphonate (SDS) in water. This system is known from literature to form micelles above a critical micelle concentration (cmc) of 2.3 kg/m^3 at 25° C. The VPO was first calibrated using sucrose (M = 342.2 g/mol) in water at 50° C. The calibration curves are shown in Figure 3.5 where, the VPO response, $\Delta V/C_0$ is plotted versus the concentration of sucrose, C_0. A straight line was obtained and the instrument constant was calculated from the intercept. Two such calibrations were performed and an average value of 2519 mV-litre/mol was found for the constant.

Figure 3.6 shows the results obtained for the SDS/water system at 50° C. On the left axis, the results are presented as $\Delta V/C_s$ versus SDS concentration, C_s. The value of $\Delta V/C_s$ is nearly constant until the cmc of 2.8 kg/m^3 is reached. The cmc of 2.8 kg/m^3 was confirmed with interfacial tension (IFT) measurements performed by Yarranton et al.

(2000) using SDS in water versus light mineral oil. With a nearly constant VPO response, a truncated form of Eq. 3.14 was used to calculate the apparent molar mass,

$$M = \frac{K_0 C_s}{\Delta V} \tag{3.15}$$

Figure 3.5 Calibration Curves for Sucrose in Water at 50 °C

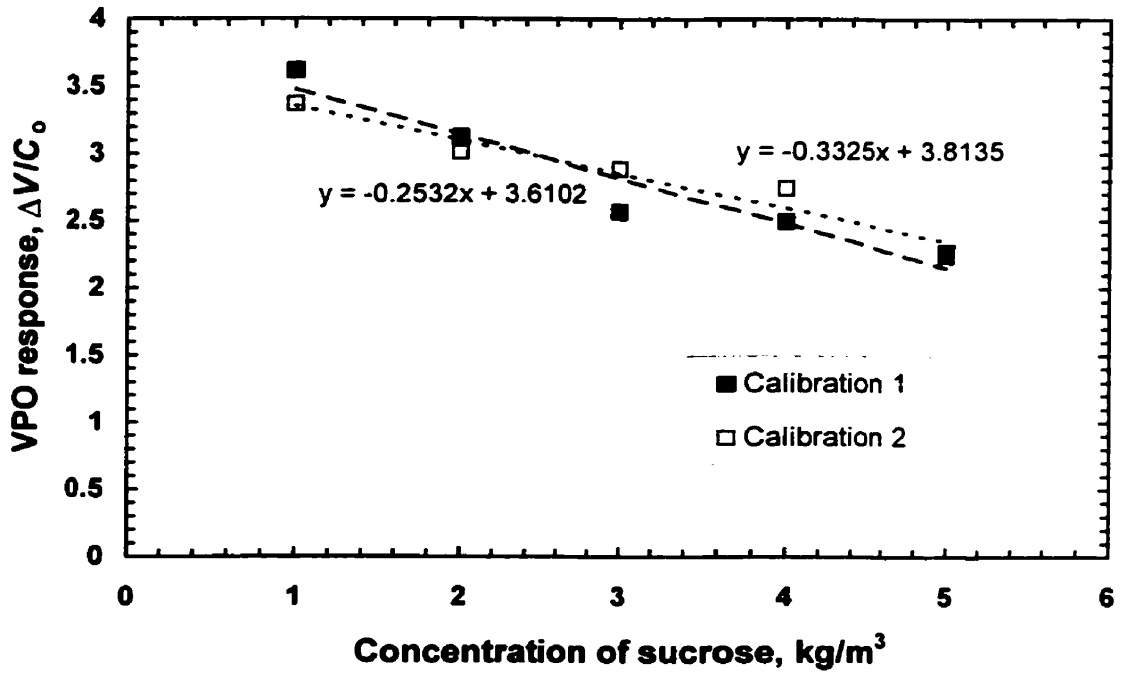

The number average molar mass for the SDS/water system is expected to equal the monomer molar mass below the cmc and to be an average of the monomer and micelle molar mass above the cmc. At sufficiently high concentrations, the number of micelles will far exceed the number of monomers and the average molar mass will equal the micelle molar mass. The number of monomers per micelle can then be estimated from the high concentration data and a value of 36 monomers/micelle was found here. The VPO and IFT measurements are compared with literature values in Table 3.3.

Figure 3.6 VPO Measurements of SDS in Water at 50 °C

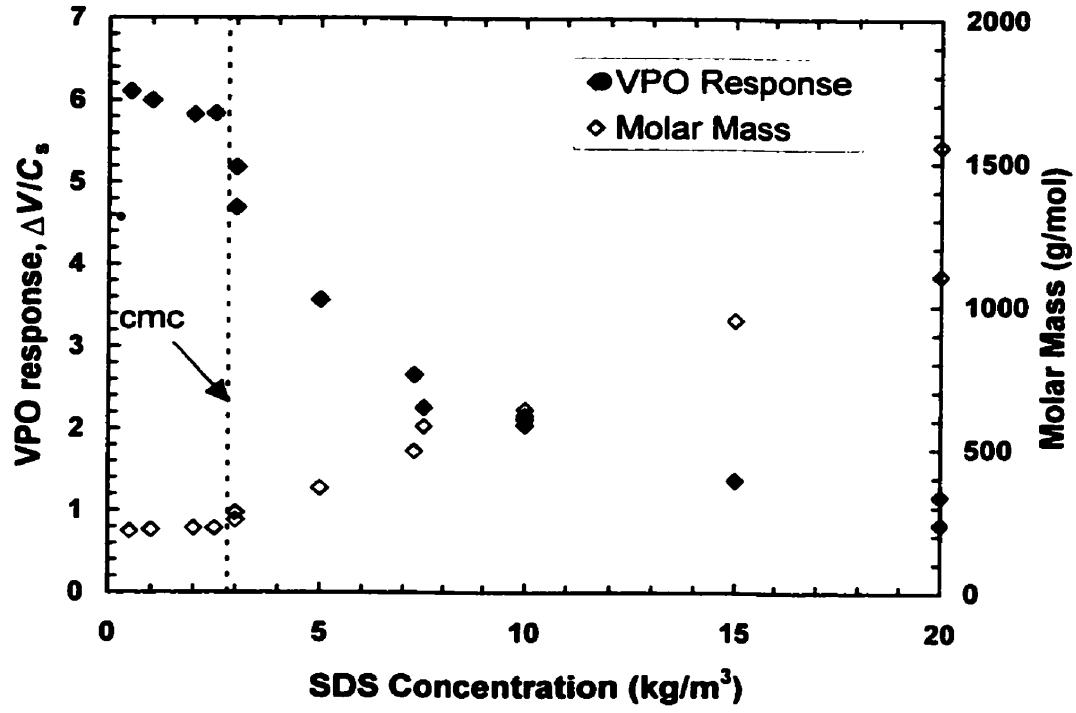

Table 3.3: Properties of SDS/water System

Property	Present Work (50° C)	Literature (25° C)
cmc from VPO (kg/m^3)	2.8±0.5	2.3
cmc from IFT (kg/m^3)	2.8±0.5	-
monomer molar mass (g/mol)	220	288
monomers per micelle	36	80

The results obtained show that the VPO is capable of detecting aggregation. The 24% discrepancy observed between experimental and literature values for the monomer

molar mass reflects the potential error in VPO measurements if few data points are collected. The error may also come from calibration; for example, if there was an error in the blank run.

3.6 Possible Sources of Error from the VPO

The VPO is a sensitive piece of equipment. In practice, a number of other thermal sources and losses contribute to the observed results. Electrical current flowing through the thermistors results in self-heating, which is kept as small as possible but cannot be eliminated entirely. In addition, heat is lost by radiation, conduction, and convection; hence, the actual measured temperature difference is not completely due to the vapor pressure differences. Careful experimental design is necessary to obtain reasonably accurate molar mass measurements of unknown samples.

For all the asphaltene/resin systems, a calibration was performed at the respective temperature and solvent conditions using sucrose octaacetate as the solute (molar mass of 679 g/mol). A typical calibration is shown in Figure 3.7. Octacosane (395 g/mol) was used to check the calibration. The measured molar mass of octacosane was found to be within 2% of the correct value. From the intercept of the plot of $\Delta V/C$ versus C, the instrument constant K_0 was calculated and used in corresponding asphaltene and resin systems. Note that the instrument constant gradually changed with time and so recalibration was necessary at frequent intervals.

Figure 3.5 Calibration Curve for Sucroseoctaacetate in o-DCB at 75 °C

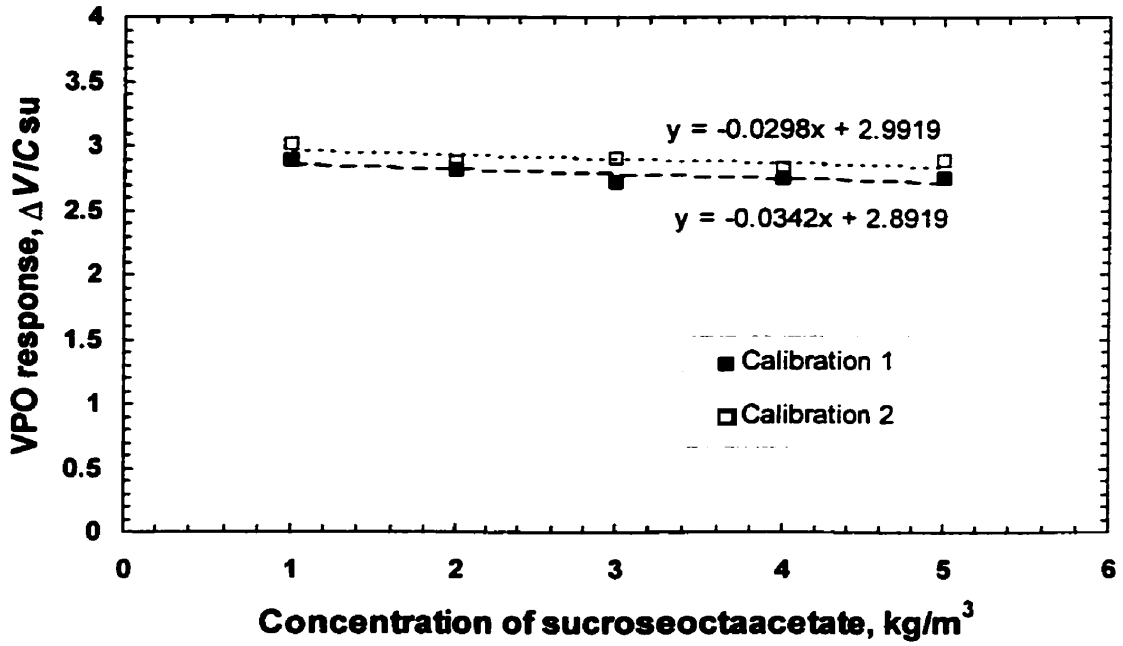

During the asphaltene experiments, there were slight fluctuations in the voltage at any given condition probably because of slight local temperature variations. A common observation during molar mass measurements in asphaltene systems was that. at low concentration (<3 kg/m^3), the voltage responses obtained were very small and there was considerable fluctuation in the voltage reading. Hence, the degree of error may be quite significant at these low concentrations. Therefore, 1 to 4 repeats were performed in this concentration zone and an average taken. On the other hand, at medium and high concentrations (>20 kg/m^3), it was found that asphaltenes tended to deposit on the needle and syringe head and hence it was important to clean them thoroughly before moving to the next concentration. Nonetheless, it was found that VPO responses at medium and high concentration (>3 kg/m^3) were quite stable and repeatable within 2-3% error. Typically, one repeat was performed in this concentration range

Chapter 4

Asphaltene Association Model

The experimental observations of the number average molar mass of asphaltenes obtained from the VPO are discussed in Chapter 5. However, some results are presented here to help explain the rationale behind the proposed association model. Asphaltenes were found to aggregate to different levels depending on temperature and solvent. Also the degree of aggregation strongly depended on asphaltene concentration until a limiting molar mass was reached. The introduction of resins into an asphaltene system reduced the degree of aggregation quite dramatically. Figure 4.1 shows the effect of temperature and solvent for C5-asphaltenes and Figure 4.2 shows the effect of adding resins on the average molar mass. A model that qualitatively accounts for all these observations can be derived starting from Strausz's view of an asphaltene molecule (1992).

Consider the hypothetical asphaltene molecule proposed by Strausz et al. (1992). This molecule consists of a number of polyaromatic ring clusters with attached aliphatic chains. Also this molecule contains heteroatoms (N, O, S) in associated functional groups such as acids, ketones, thiophenes, pyridines and porphyrins. There appears to be many ways in which this molecule can link with other similar molecules. These links can be formed through aromatic stacking, acid-base interactions or hydrogen bonding (as discussed in Chapter 2). Since asphaltenes are a mixture of many thousands of chemical species featuring a variety of functional groups, the type and strength of the potential

links may vary considerably from molecule to molecule and from site to site. Also the number of potential links that can form would likely depend on the solvent and temperature conditions. For example, in a strongly polar solvent like nitrobenzene, the asphaltene-solvent interactions tend to dominate the asphaltene-asphaltene interactions. "Strong" sites could still form asphaltene-asphaltene links but "weak" sites may not. A similar argument applies with temperature. The higher the temperature, the fewer sites are capable of forming links and the asphaltenes will tend to remain as separate entities. This idea is illustrated in Figure 4.3.

Figure 4.1 Effect of Temperature and Solvent on Molar Mass

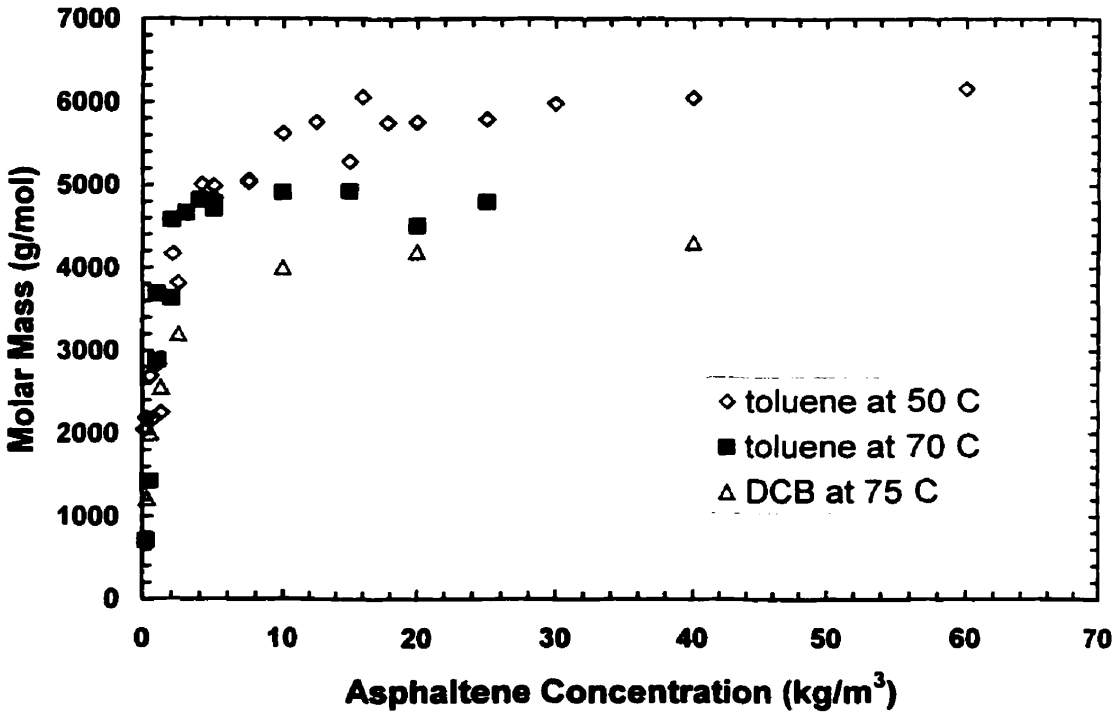

Note this view of association is a significant departure from the colloidal model where asphaltenes are assumed as being surrounded by resins that adsorb on their surface.

However, the association model developed from this concept and outlined below qualitatively accounts for all the experimental observations to be presented in Chapter 5.

Figure 4.2 Effect of Adding Resins on Molar Mass

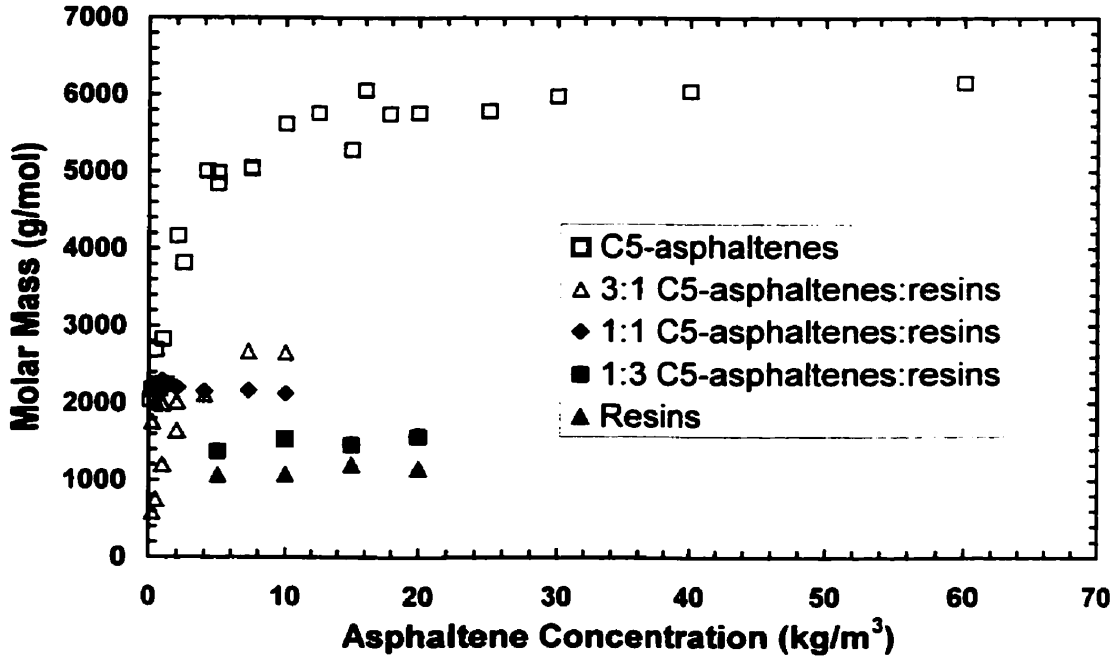

4.1 Assumptions in the Asphaltene Association Model

The association of asphaltenes illustrated in Figure 4.3 is analogous to polymerization. In this scheme asphaltenes are treated as free molecules in solution that contain multiple active sites (heteroatoms or aromatic clusters) and can interact with other similar molecules to form bigger aggregates. Hence asphaltenes can be treated as propagators in a polymerization reaction. On the other hand, resins may have a single active site and can link up with just one other molecule. Hence they can be treated as terminators in a polymerization reaction. In fact, the real difference between asphaltenes and resins may be a functional difference; that is, asphaltenes may have multiple sites and

self-associate while resins do not have sufficient sites to self-associate. This view is consistent with the similar chemical nature of asphaltenes and resins and the smaller heteroatom content, aromaticity and molar mass of the resins.

Figure 4.3 Possible Association between Asphaltene Molecules

(a) High temperature, good solvent

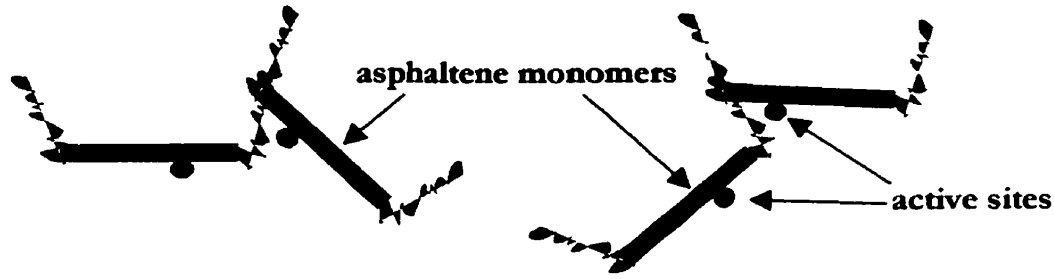

(b) Low temperature, poor solvent (linear aggregation)

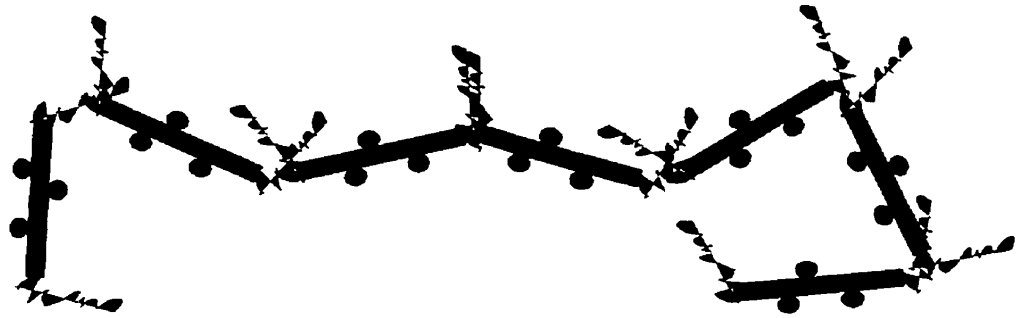

(c) *Low temperature, poor solvent (random, branched aggregation)*

Initially, asphaltene self-association and asphaltene-resin interactions analogous to linear polymerization are assumed. This might be an oversimplification but the purpose here is to test if this simple model is capable of capturing the physics involved in the aggregation phenomena. As with linear polymerization, this model is described in terms of propagators and terminators as defined below.

Propagators: A propagator is a molecule that contains multiple active sites (functional groups) and is capable of linking with other similar molecules or aggregates.

Terminators: A terminator is a molecule that contains a single active site (functional group) and is capable of linking with propagators or aggregates thus terminating association.

Neutrals: A neutral is a molecule that contains no active sites (functional groups) and is incapable of linking with other molecules and aggregates. Typically, saturates and aromatics are in this category.

Hence, the association of asphaltenes and resins can be described in terms of propagators and terminators by using an association scheme analogous to linear polymerization. It is proposed that asphaltenes consist mainly of propagators but also contain a small proportion of terminators. Resins on the other hand consist mainly of terminators but also contain a small proportion of propagators. This mixture reflects how terminators and propagators may partition during aggregation. The end result is that any precipitated material can be characterized as a mixture of varying amounts of propagators and terminators.

4.2 Model Development and Theory

A simple polymerization type scheme involving propagators and terminators is proposed. As the association is really non-reactive there is no initiation step unlike polymerization reactions. Hence, there are two steps: propagation and terminators.

4.2.1 Propagation

These "reactions" involve propagators and aggregates. A propagator monomer, denoted by P_1, can link up with another monomer or with an existing aggregate P_k (where k is the number of monomers in the aggregate). These "reactions" are assumed to be first order with respect to both the propagator monomer and the aggregate molecules and are characterized by an association constant, K, which represents equilibrium between forward and reverse association. Also the concentration of the aggregates can be expressed in terms of the association constant, K, and equilibrium concentration of propagators, $[P_1]$. The association constant is assumed to be the same for any aggregate size. The "reaction" scheme is as follows:

$$P_1 + P_1 \xleftrightarrow{K} P_2 \quad \ldots\ldots\ldots\ldots [P_2] = K[P_1]^2 \tag{4.1}$$

$$P_1 + P_2 \xleftrightarrow{K} P_3 \quad \ldots\ldots\ldots\ldots [P_3] = K[P_1][P_2] = K^2[P_1]^3 \tag{4.2}$$

$$P_1 + P_3 \xleftrightarrow{K} P_4 \quad \ldots\ldots\ldots\ldots [P_4] = K[P_1][P_3] = K^3[P_1]^4 \tag{4.3}$$

.....

.....

$$P_1 + P_n \xleftrightarrow{K} P_{n+1} \ldots\ldots\ldots\ldots [P_{n+1}] = K[P_1][P_n] = K^n[P_1]^{n+1} \quad (4.4)$$

where P_k is an aggregate of k monomers.

4.2.2 Termination

The other set of "reactions" involve terminators and aggregates. A terminator monomer can link up with a propagator or an existing aggregate thus terminating association. Again these "reactions" are assumed to be first order with respect to both the terminator monomer and aggregate molecules and are characterized by an association constant. The concentration of the terminated aggregates can be expressed in terms of the association constant, K and the equilibrium concentration of terminator monomers, $[T]$ and propagator monomers, $[P_1]$. For simplicity, the termination of one site on the aggregate is assumed to stop further association. This assumption is discussed in more detail later and gives the following scheme:

$$P_1 + T \xleftrightarrow{K} P_1T \ldots\ldots\ldots\ldots [P_1T] = K[P_1][T] \quad (4.5)$$

$$P_2 + T \xleftrightarrow{K} P_2T \ldots\ldots\ldots\ldots [P_2T] = K[P_2][T] = K^2[P_1]^2[T] \quad (4.6)$$

$$P_3 + T \xleftrightarrow{K} P_3T \ldots\ldots\ldots\ldots [P_3T] = K[P_3][T] = K^3[P_1]^3[T] \quad (4.7)$$

.....

.....

$$P_n + T \xleftrightarrow{K} P_nT \ldots\ldots\ldots\ldots [P_nT] = K[P_n][T] = K^n[P_1]^n[T] \quad (4.8)$$

To keep the model simple it is assumed that the association constant for all reactions involved in the propagation and termination steps is the same. This means that the ease with which a monomer forms a link with another monomer is the same as that with an existing aggregate. This is a first step towards model development. Later in this chapter, the case of changing association constant with size of the aggregates is considered.

4.2.3 Solving for Equilibrium Composition

The "reactions" schemes are solved in the same manner as a polymerization reaction starting with mass balance equations for both propagators and terminators.

Mass balance of propagators:

$$[P_1]_0 = ([P_1] + 2[P_2] + 3[P_3] + 4[P_4] + \ldots\ldots\ldots\ldots\ldots\ldots) + ([P_1T] + 2[P_2T] + 3[P_3T] + 4[P_4T] + \ldots\ldots\ldots\ldots\ldots\ldots) \quad (4.9)$$

Substituting the $[P_k]$ from Eq's 4.1 to 4.4 gives:

$$[P_1]_0 = \left([P_1] + 2K[P_1]^2 + 3K^2[P_1]^3 + 4K^3[P_1]^4 + \ldots\ldots\ldots\ldots\ldots\ldots\right) +$$

$$\left(K[P_1][T] + 2K^2[P_1]^2[T] + 3K^3[P_1]^3[T] + 4K^4[P_1]^4[T] + \ldots\ldots\ldots\ldots\ldots\ldots\right)$$

$$= [P_1](1 + K[T])\left(1 + 2K[P_1] + 3K^2[P_1]^2 + 4K^3[P_1]^3 + \ldots\ldots\ldots\ldots\ldots\right) \quad (4.10)$$

This infinite series can be simplified as follows:

$$[P_1]_0 = [P_1]\frac{(1 + K[T])\left(1 + K[P_1] + K^2[P_1]^2 + K^3[P_1]^3 + \ldots\ldots\ldots\right)}{(1 - K[P_1])} \quad (4.11)$$

or

$$[P_1]_0 = \frac{[P_1](1 + K[T])}{(1 - K[P_1])^2} \tag{4.12}$$

Mass balance of terminators:

$$[T]_0 = [T] + [P_1T] + [P_2T] + [P_3T] + \ldots\ldots\ldots\ldots \tag{4.13}$$

Substituting the $[P_kT]$ from Eq's 4.5 to 4.8 gives:

$$[T]_0 = [T] + K[P_1][T] + K^2[P_1]^2[T] + K^3[P_1]^3[T] + \ldots\ldots\ldots\ldots$$

$$= [T](1 + K[P_1] + K^2[P_1]^2 + K^3[P_1]^3 + \ldots\ldots\ldots\ldots) \tag{4.14}$$

which simplifies to,

$$[T]_0 = \frac{[T]}{(1 - K[P_1])} \tag{4.15}$$

or $$[T] = [T]_0(1 - K[P_1]) \tag{4.16}$$

Hence the equilibrium concentration of terminators can be determined from the equilibrium concentration of propagators.

Calculation of equilibrium concentration of propagators and terminators

Substituting Eq. 4.16 into Eq. 4.12 and eliminating $[T]$, gives

$$[P_1]_0 = \frac{[P_1](1 + K[T]_0(1 - K[P_1]))}{(1 - K[P_1])^2} \tag{4.17}$$

The physically valid root of Eq. 4.17 is given by:

$$[P_1] = \frac{1 + K(2[P_1]_0 + [T]_0) - \sqrt{(1 + K(2[P_1]_0 + [T]_0))^2 - 4K^2[P_1]_0([P_1]_0 + [T]_0)}}{2K^2([P_1]_0 + [T]_0)} \tag{4.18}$$

The value of $[T]$ is then obtained from Eq. 4.16. Once $[T]$ and $[P_1]$ are known the concentration of any aggregate can be found from Eq's 4.1-4.8. The only remaining

unknowns then are $[P_1]_0$ and $[T]_0$ and K or alternatively the initial concentration of all monomers, ($[P_1]_0$+$[T]_0$), the initial mole ratio of terminators to propagators, T/P and K. It remains to relate these parameters to asphaltene/resin systems.

Calculation of Average Molar Mass

From the equilibrium concentration of each aggregate in solution, the average molar mass, $\bar{M}$ can be determined as follows:

$$\bar{M} = \frac{\begin{array}{l}([P_1]M_p + [P_2]2M_p + [P_3]3M_p + [P_4]4M_p + \ldots\ldots\ldots\ldots\ldots\ldots\ldots\ldots) \\ +([T]M_t + [P_1T](M_p + M_t) + [P_2T](2M_p + M_t) + [P_3T](3M_p + M_t) + \ldots\ldots)\end{array}}{\begin{array}{l}([P_1] + [P_2] + [P_3] + [P_4] + \ldots\ldots\ldots\ldots\ldots\ldots\ldots\ldots) \\ +([T] + [P_1T] + [P_2T] + [P_3T] + [P_4T] + \ldots\ldots\ldots\ldots\ldots\ldots)\end{array}} \quad (4.19)$$

Substituting the $[P_k]$ from Eq's 4.1 to 4.4 and the $[P_kT]$ from Eq's 4.5 to 4.8 gives:

$$\bar{M} = \frac{\begin{array}{l}([P_1]M_p + K[P_1]^2.2M_p + K^2[P_1]^3.3M_p + K^3[P_1]^4.4M_p + \ldots\ldots\ldots\ldots\ldots\ldots) \\ +([T]M_t + K[P_1][T](M_p + M_t) + K^2[P_1]^2[T](2M_p + M_t) + \ldots\ldots\ldots\ldots\ldots)\end{array}}{\begin{array}{l}([P_1] + K[P_1]^2 + K^2[P_1]^3 + K^3[P_1]^4 + \ldots\ldots\ldots\ldots\ldots\ldots\ldots\ldots\ldots\ldots) \\ +([T] + K[P_1][T] + K^2[P_1]^2[T] + K^3[P_1]^3[T] + K^4[P_1]^4[T] + \ldots\ldots\ldots\ldots\ldots)\end{array}} \quad (4.20)$$

Simplifying the expression for $\bar{M}$, we get:

$$\bar{M} = \frac{\dfrac{(1 + K[T])[P_1]M_p}{(1 - K[P_1])} + [T]M_t}{([P_1] + [T])} \quad (4.21)$$

where $[P_1]$ is obtained from Eq. 4.18 and $[T]$ is obtained from Eq. 4.16.

Procedure for using the model

Note that all experimental measurements are made in terms of mass of asphaltenes and resins. These measurements must be converted to moles of terminators

and propagators to use the model. Now, the molar mass of asphaltenes and resins can be measured. However, the *T/P* ratio in each fraction is unknown a priori. Therefore, the mole fraction of terminators and propagators cannot be calculated directly. An iterative method was developed to calculate the *T/P* molar ratio for any given mixture of asphaltenes and resins until molar mass data from the VPO is matched. To use the model, we must obtain $[P_1]_0$ and $[T]_0$ from *T/P*. The procedure is outlined below.

1) Guess (*T/P*) and calculate the mole fraction of terminators.

$$\text{Since, } \frac{x_T}{x_P} = \frac{T}{P} \qquad \Rightarrow x_T = \frac{(T/P)}{1+(T/P)} \tag{4.22}$$

where x_T is the mole fraction of terminators and x_P is the mole fraction of propagators.

2) If M_{avg} is the average molar mass of terminators and propagators in any sample mixture of asphaltenes and resins, and if the mole fraction of terminators in the sample is x_T, then

$$M_{avg} = x_T * M_t + (1-x_T) * M_p \tag{4.23}$$

where M_t and M_p are the average monomer molar mass of terminators and propagators respectively.

3) Consider a sample mixture containing terminators, propagators and one litre of solvent at a particular temperature. Let m_o be the mass of asphaltenes and resins (which is also the mass of terminators and propagators) in the given volume of solvent. If the solvent molar volume, *v* is known at the given temperature one can find the total moles of the sample mixture on a one litre solvent basis:

$$tot\_moles/L\ solvent = m_o/M_{avg} + 1/v \tag{4.24}$$

4) From Equation 4.24 the initial mole fraction of asphaltene and resins (or propagators and terminators) can be obtained as follows:

$$[P_1]_0 + [T]_0 = \frac{(m_0 / M_{avg})}{(tot\_moles)} \tag{4.25}$$

5) Thus, the mole fraction of propagators or terminators in the system can be obtained in terms of the initial mole ratio of terminators and propagators (denoted by *T/P*) as follows:

$$[P_1]_0 = \frac{(m_0 / M_{avg})}{(tot\_moles).(1 + T/P)} \tag{4.26}$$

and $$[T]_0 = [P_1]_0.(T/P) \tag{4.27}$$

6) The model is run with the calculated $[P_1]_0$ and $[T]_0$. The fit of the average molar mass with experimental data is checked by inspection. If the fit is not satisfactory a new guess for the *T/P* ratio is made and steps 2 to 6 are repeated.

Typically, about three to four simulations were required to obtain the curve fits using the model for each asphaltene/resin system over a wide range of solute concentrations (0.1 to 70 kg/m^3). The coding of the model development described above was done using C++ in the Visual environment of Microsoft Developer Studio. The C++ code for the model is provided in the Appendix at the end of the thesis.

4.2 Estimated Parameters for the Association Model

Two estimated parameters are required for the model: the average monomer molar mass of terminators, M_t; and monomer molar mass of propagators, M_p. The

monomer molar mass for the propagators can be estimated from the data obtained from the VPO for the various asphaltene systems in different solvents and different temperatures by extrapolating to zero concentration (or infinite dilution). As will be discussed in Chapter 5, molar masses of 800 g/mol and 1800 g/mol were used for the terminators and propagators, respectively. A sensitivity analysis of the monomer molar masses is also included.

Note that it is an oversimplification to use an average monomer molar mass to describe terminators and propagators as in reality there would be a distribution of monomer molecules of varying sizes. But as mentioned previously, the number of parameters used in the model is to be minimized to make the model more robust.

4.4 Fit Parameters for the Association Model

Since the initial concentration of monomers is known, and M_t and M_p are estimated beforehand, the asphaltene association model in effect requires two fit parameters: the association constant, K; and the molar ratio of terminators to propagators, T/P. Typical curve fits using model parameters are shown in Figures 4.4 and 4.5. The system used is Athabasca C5-asphaltenes in toluene at 50 °C. Figure 4.4 shows the effect of changing K at constant T/P and Figure 4.5 shows the effect of changing the T/P ratio at constant K. It is clear from the two figures that the association constant, K essentially determines the concentration at which the limiting molar mass is reached and the T/P ratio determines the value of the limiting molar mass.

Figure 4.4 **Effect of K at Constant $T/P = 0.33$**
System: C5-asphaltenes in Toluene at 50° C

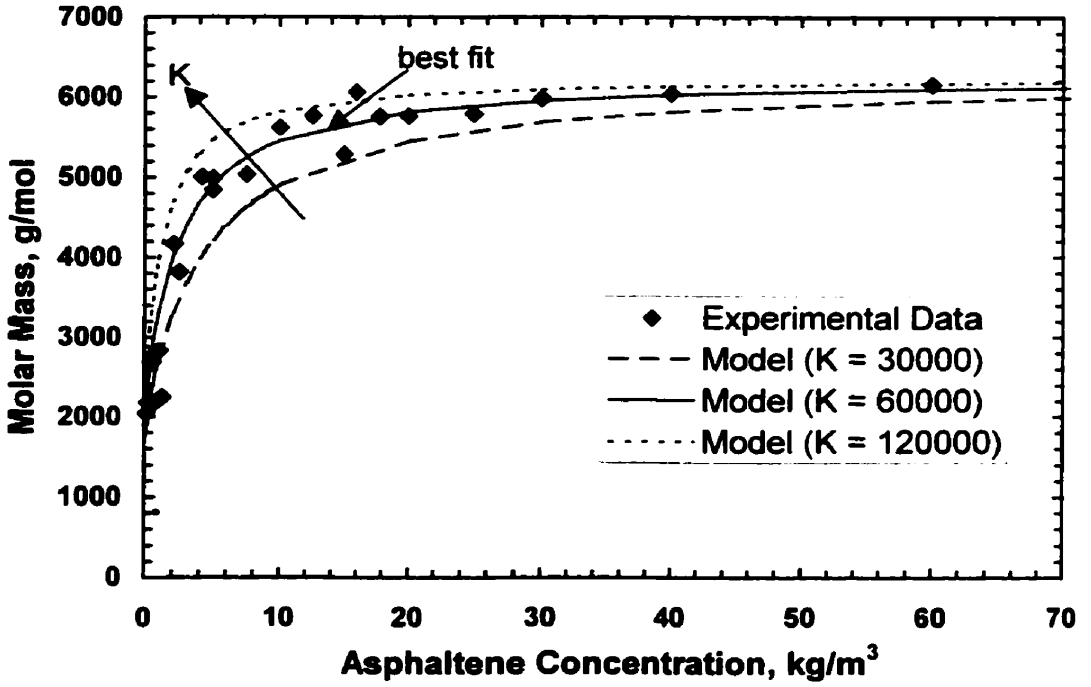

Figure 4.5 **Effect of T/P Ratio at Constant $K = 60000$**
System: C5-asphaltenes in Toluene at 50° C

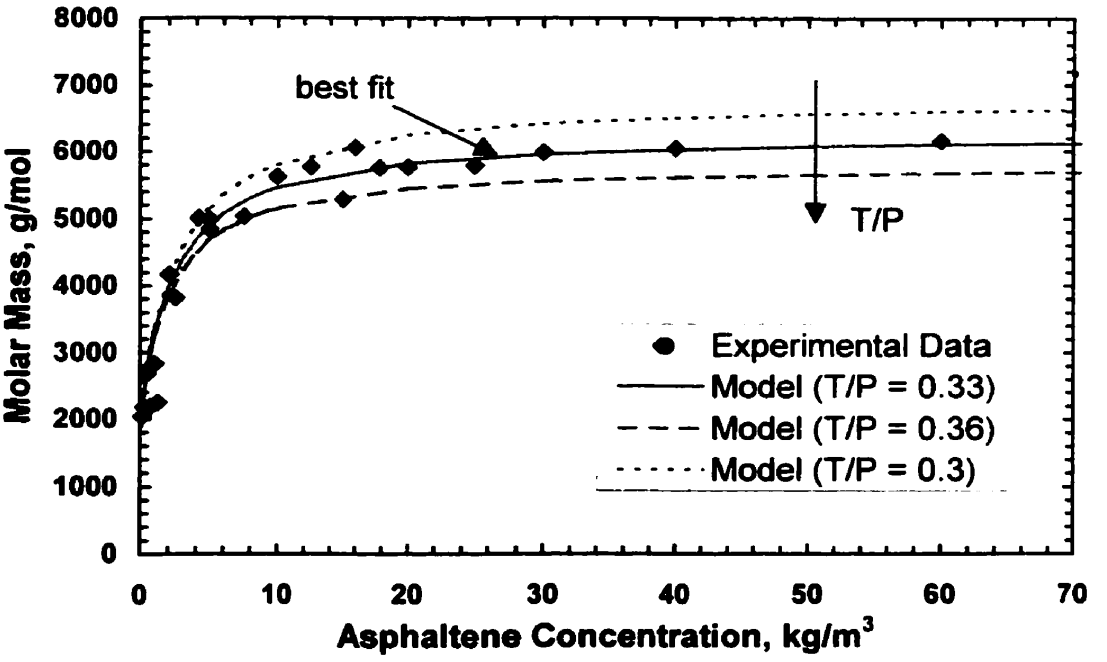

From Figure 4.4 it is apparent that increasing K decreases the concentration at which the limiting molar mass is reached. From Figure 4.5 it is evident that increasing the T/P ratio reduces the value of limiting molar mass. These trends are consistent with the assumptions in the association model.

4.3 Calculation of the Molar Mass Distribution

For any given system, a molar mass distribution can be obtained once the equilibrium concentration of propagators and terminators is determined. Since the molar mass of the propagators and terminators differs, a lumping method was used to obtain the molar mass distribution as follows:

For aggregates of any given size (eg. 3 monomers/aggregate) there will be two types of aggregates (*P-P-P* and *P-P-T*) each with a different molar mass. The mole fraction of each type is obtained from the model. Let x_{A3} be the mole fraction of *P-P-P* aggregates, M_{A3} be the molar mass of *P-P-P* aggregates, x_{B3} be the mole fraction of *P-P-T* aggregates and M_{B3} be the molar mass of *P-P-T* aggregates. The mole fraction of 3-monomer aggregates is $x_3 = x_{A3} + x_{B3}$ and the average molar mass of these aggregates is given by

$$M_3 = \frac{x_{A3}M_{A3} + x_{B3}M_{B3}}{x_3} \tag{4.28}$$

The above calculation is performed for each set of aggregates containing up to n monomers. The mole fraction of the lumped aggregates is converted to a mass fraction and since the initial mass of terminators and propagators is known, a weight percent for each of the lumped aggregates can be obtained and plotted against the molar mass to give

a molar mass distribution. Note that the choice of n is made large enough to account for the largest aggregates in the system.

4.6 Model Refinement – Introduction of a new fit parameter, *i*

The model results will be discussed in detail in Chapter 5. It was found that with the model set up described in the previous sections, the asphaltene association model fit the VPO data very well and also gave good predictions for average molar mass of asphaltene-resin systems. However, the molar mass distributions obtained from the model were very broad, i.e. the upper limit of the distributions was large ($\approx$ 50,000 g/mol). This large value may be unrealistic since previous researchers have estimated an upper limit of about 10,000 to 20,000 g/mol (Kawanaka et al., 1991; Yarranton and Masliyah, 1996; Mannistu et al., 1997) for asphaltene molar mass distributions. However, the upper limit of these distributions is still debated in the literature. To make the model more flexible and to achieve the small upper limits obtained by other researchers, another parameter called the diminution parameter was introduced into the model. This parameter empirically accounts for possible steric hindrance in adding a monomer to an existing aggregate. In other words, the association constant can be made a function of the size of the aggregates. The model development with this new parameter is shown below:

Propagation

Eq's 4.1 to 4.4 are modified with the addition of a diminution parameter, i as shown below. The diminution parameter is a fraction and can take values between 0 and 1 only.

$$P_1 + P_1 \xleftrightarrow{K} P_2 \ldots\ldots\ldots\ldots [P_2] = K[P_1]^2 \tag{4.29}$$

$$P_1 + P_2 \xleftrightarrow{iK} P_3 \ldots\ldots\ldots\ldots [P_3] = iK[P_1][P_2] = iK^2[P_1]^3 \tag{4.30}$$

$$P_1 + P_3 \xleftrightarrow{i^2K} P_4 \ldots\ldots\ldots\ldots [P_4] = i^2K[P_1][P_3] = i^3K^3[P_1]^4 \tag{4.31}$$

.....

.....

$$P_1 + P_n \xleftrightarrow{i^{(n-1)}K} P_{n+1} \ldots\ldots\ldots\ldots [P_{n+1}] = i^{(n-1)}K[P_1][P_n] = i^{\frac{(n-1)(n+1)}{2}}K^n[P_1]^{n+1} \tag{4.32}$$

Termination

The termination "reactions", Eq's 4.5 to 4.8, are modified in the same manner.

$$P_1 + T \xleftrightarrow{K} P_1T \ldots\ldots\ldots\ldots [P_1T] = K[P_1][T] \tag{4.33}$$

$$P_2 + T \xleftrightarrow{iK} P_2T \ldots\ldots\ldots\ldots [P_2T] = iK[P_2][T] = iK^2[P_1]^2[T] \tag{4.34}$$

$$P_3 + T \xleftrightarrow{i^2K} P_3T \ldots\ldots\ldots\ldots [P_3T] = i^2K[P_3][T] = i^3K^3[P_1]^3[T] \tag{4.35}$$

.....

.....

$$P_n + T \xleftrightarrow{i^{(n-1)}K} P_nT \ldots\ldots\ldots\ldots [P_nT] = i^{(n-1)}K[P_n][T] = i^{\frac{(n-1)(n+1)}{2}}K^n[P_1]^n[T] \quad (4.36)$$

Once we have the concentration of each aggregate we can write mass balance equations for both propagators and terminators as follows:

Mass balance of propagators:

$$[P_1]_0 = ([P_1] + 2[P_2] + 3[P_3] + 4[P_4] + \ldots\ldots\ldots\ldots) + ([P_1T] + 2[P_2T] + 3[P_3T] + 4[P_4T] + \ldots\ldots\ldots\ldots) \quad (4.37)$$

Substituting for $[P_2]$, $[P_3]$, $[P_4]$ and so on from Eq's 4.29 to 4.32 an expression for $[P_1]_0$ is obtained.

$$[P_1]_0 = ([P_1] + 2K[P_1]^2 + 3iK^2[P_1]^3 + 4i^3K^3[P_1]^4 + \ldots\ldots\ldots\ldots) + (K[P_1][T] + 2iK^2[P_1]^2[T] + 3i^3K^3[P_1]^3[T] + 4i^6K^4[P_1]^4[T] + \ldots\ldots\ldots\ldots) \quad (4.38)$$

$$[P_1]_0 = ([P_1] + 2K[P_1]^2 + 3iK^2[P_1]^3 + 4i^3K^3[P_1]^4 + \ldots\ldots\ldots\ldots) + [T](K[P_1] + 2iK^2[P_1]^2 + 3i^3K^3[P_1]^3 + 4i^6K^4[P_1]^4 + \ldots\ldots\ldots\ldots) \quad (4.39)$$

This infinite power series cannot be summed directly because it includes the term $[T]$, which has not yet been found.

Mass balance of terminators:

$$[T]_0 = [T] + [P_1T] + [P_2T] + [P_3T] + \ldots\ldots\ldots\ldots \quad (4.40)$$

Substituting for $[P_1T]$, $[P_2T]$, $[P_3T]$ and so on from Eq's 4.33 to 4.36 an expression in terms of $[P_1]$ is obtained.

$$[T]_0 = [T] + K[P_1][T] + iK^2[P_1]^2[T] + i^3K^3[P_1]^3[T] + \ldots\ldots\ldots\ldots$$

$$= [T]\left(1 + K[P_1] + iK^2[P_1]^2 + i^3K^3[P_1]^3 + \ldots\ldots\ldots\ldots\right) \quad (4.41)$$

Eq. 4.41 is rearranged to solve for $[T]$ as follows:

$$[T] = \frac{[T]_0}{\left(1 + K[P_1] + iK^2[P_1]^2 + i^3K^3[P_1]^3 + \ldots\ldots\ldots\ldots\right)} \quad (4.42)$$

The denominator of the RHS expression above is an infinite power series, which includes $[P_1]$. Eq's 4.42 and 4.39 have two unknowns, $[P_1]$ and $[T]$.

Calculation of equilibrium concentration of propagators and terminators

Substituting Eq. 4.42 into Eq. 4.39 and eliminating $[T]$, an expression based on $[P_1]$ is obtained.

$$[P_1]_0 = \left([P_1] + 2K[P_1]^2 + 3iK^2[P_1]^3 + 4i^3K^3[P_1]^4 + \ldots\ldots\ldots\ldots\right)$$

$$+ [T]_0 \frac{\left(K[P_1] + 2iK^2[P_1]^2 + 3i^3K^3[P_1]^3 + 4i^6K^4[P_1]^4 + \ldots\ldots\ldots\ldots\right)}{\left(1 + K[P_1] + iK^2[P_1]^2 + i^3K^3[P_1]^3 + \ldots\ldots\ldots\ldots\right)}. \quad (4.43)$$

An analytical solution for Eq. 4.43 does not exist. Hence, a Newton-Raphson convergence technique is employed with an initial guess for $[P_1]$ from the simple two-parameter model; that is

$$[P_1]_{initial} = \frac{1 + K(2[P_1]_0 + [T]_0) - \sqrt{(1 + K(2[P_1]_0 + [T]_0))^2 - 4K^2[P_1]_0([P_1]_0 + [T]_0)}}{2K^2([P_1]_0 + [T]_0)} \quad (4.44)$$

The Newton-Raphson convergence technique was chosen to solve Eq. 4.44 since the derivative of the equation with respect to $[P_1]$ can be determined analytically. The remainder of the model is developed as before once the equilibrium concentration of terminators and propagators is obtained. Note that when the value of the diminution parameter is set to 1, the model reduces to the two-parameter model.

Chapter 5

Results and Discussion

In this Chapter, the model developed in Chapter 4 is tested on molar masses of Athabasca and Cold Lake asphaltenes/resin systems measured with the VPO at different temperatures and in two different solvents. Monomer molar masses of 1800 g/mol and 800 g/mol for propagators and terminators respectively, were used for testing the association model on the various systems. A sensitivity analysis for the monomer molar masses is included. Molar mass distributions obtained from the model are discussed. Also, the implications towards solubility modeling of asphaltenes are discussed at the end of the chapter.

5.1 Experimental and Model Results of Molar Masses of Asphaltenes

In Chapter 3 it was shown that the VPO was capable of detecting aggregation. Once this was established, the molar masses of C5-asphaltenes, C7-asphaltenes and resin systems were measured in toluene and o-dichlorobenzene at varying temperatures and concentrations. Molar mass measurements in the concentration range of 0.25 to 60 kg/m^3 for the systems shown in Table 5.1 was performed using the VPO. The VPO molar mass of each system was typically measured over three concentration ranges: low concentration (0.25 to 10 kg/m^3), intermediate concentration (5 to 25 kg/m^3) and high concentration (10 to 60 kg/m^3). Hence there was significant overlap over these

concentration ranges in order to check for repeatability of results. The symbol 'X' in Table 5.1 represents experiment performed under specified conditions.

Table 5.1 Experiments Performed with the Vapor Pressure Osmometer

System	Solvent used			
	Toluene		o-DCB	
	50° C	70° C	75° C	130° C
Athabasca C5-asphaltenes	X	X	X	X
Athabasca C7-asphaltenes	X	X	X	X
Cold Lake C5-asphaltenes	X			
Cold Lake C7-asphaltenes	X			
Athabasca C5-asphaltenes+resins*	X			
Athabasca Resins	X			
Cold Lake Resins	X			

* C5-asphaltenes:resin mass ratios of 3:1, 1:1 and 1:2.5

A typical plot of VPO response, $\Delta V/C_A$ versus asphaltene concentration for Athabasca C5-asphaltenes in toluene is given in Figure 5.1. The apparent molar mass from Eq. 3.17 is shown on the same plot. There is a linear decrease in $\Delta V/C_A$ (or increase in apparent molar mass) as the asphaltene concentration increases, but a limiting value is reached at a concentration of about 20 kg/m^3. The change in $\Delta V/C_A$ could be caused by non-ideal solution behavior. However, with non-ideal behavior, departures from ideality are expected to be minimal at low concentration and significant at high concentrations.

The VPO measurements show the opposite behavior. Hence, it is more likely that the change in VPO response reflects a change in the asphaltene molar mass; that is, some form of association occurs. More supporting evidence for association of asphaltenes is discussed in sections 5.5 and 5.6.

Figure 5.1 VPO Measurements of Athabasca Asphaltenes in Toluene at 50 °C

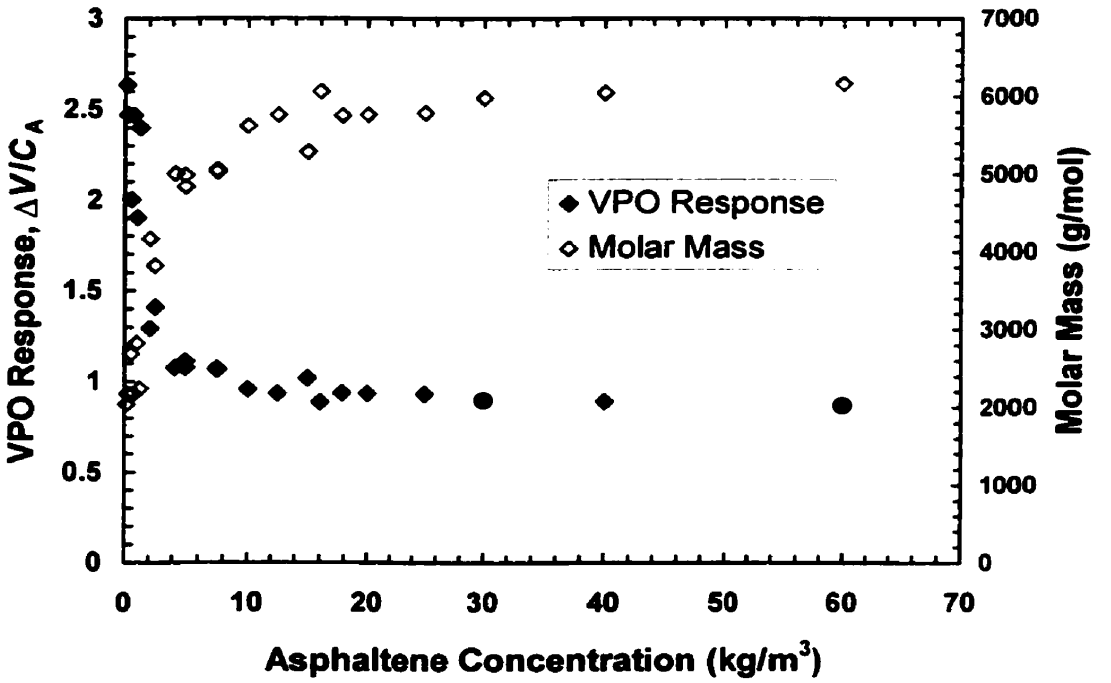

Assuming ideal solution behavior, Eq. 3.12 was used to calculate molar mass from the measured voltage difference. The VPO apparent molar mass of Athabasca C5- and C7-aphaltenes in toluene at 50° C is shown in Figure 5.2. The symbols represent experimental data and the lines indicate model curve fits. It is seen that the asphaltenes show an increase in apparent molar mass as the asphaltene concentration increases but reach a limiting molar mass.

Figure 5.2 VPO Molar Masses of C5- and C7-asphaltenes in Toluene at 50° C

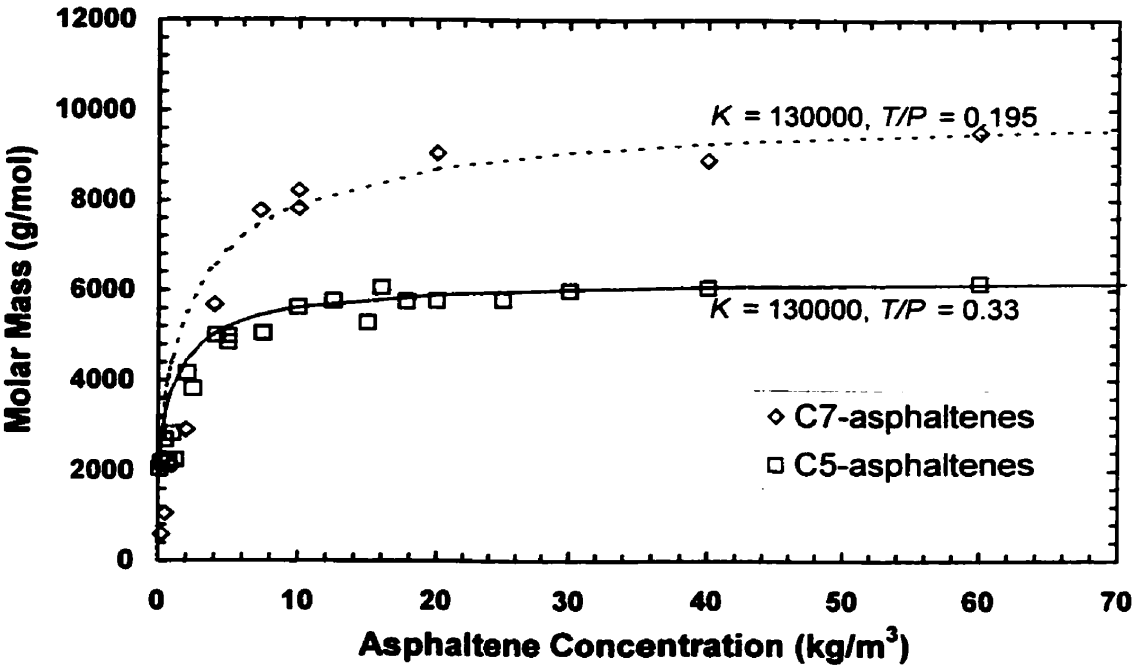

The change in apparent molar mass may explain why VPO experiments have yielded different results for different researchers. Typically, to obtain the molar mass of asphaltenes, the measured molar mass is linearly extrapolated to zero concentration. Now consider Figure 5.2. If the molar masses of the C5-asphaltenes were measured in toluene at 50° C from concentrations between 20 and 50 kg/m^3 (2-5 wt%), then a molar mass of about 6000 g/mol would be estimated from the linear extrapolation. On the other hand, an extrapolation over concentrations from 1 to 5 kg/m^3, would give a molar mass of about 1500 g/mol. In fact, different researchers have used both concentration ranges. Some of the variations in reported asphaltene molar masses may be due to the different concentrations used in VPO experiments.

Note that the shape of the curves in Figures 5.2 suggest that the low-concentration extrapolation can give an estimate of the average size of an asphaltene monomer while the extrapolation at high concentration can, at best, give an idea of the average limiting size of the asphaltene aggregates. The estimated monomer molar masses is the infinitely dilute molar mass found by extrapolation of the molar masses measured at asphaltene concentrations from <3 kg/m^3 to zero concentration, as shown in Figure 5.3. The estimated aggregate molar mass is the highest molar mass measured above 20 kg/m^3 asphaltene concentration as illustrated in Figure 5.4. The extrapolations in Figures 5.3 and 5.4 are shown for, C5- and C7-asphaltenes in toluene at 50° C. All of these experimental observations were published recently (Yarranton et al., 2000).

Figure 5.3 Low Concentration Extrapolation of VPO Molar Masses in Toluene

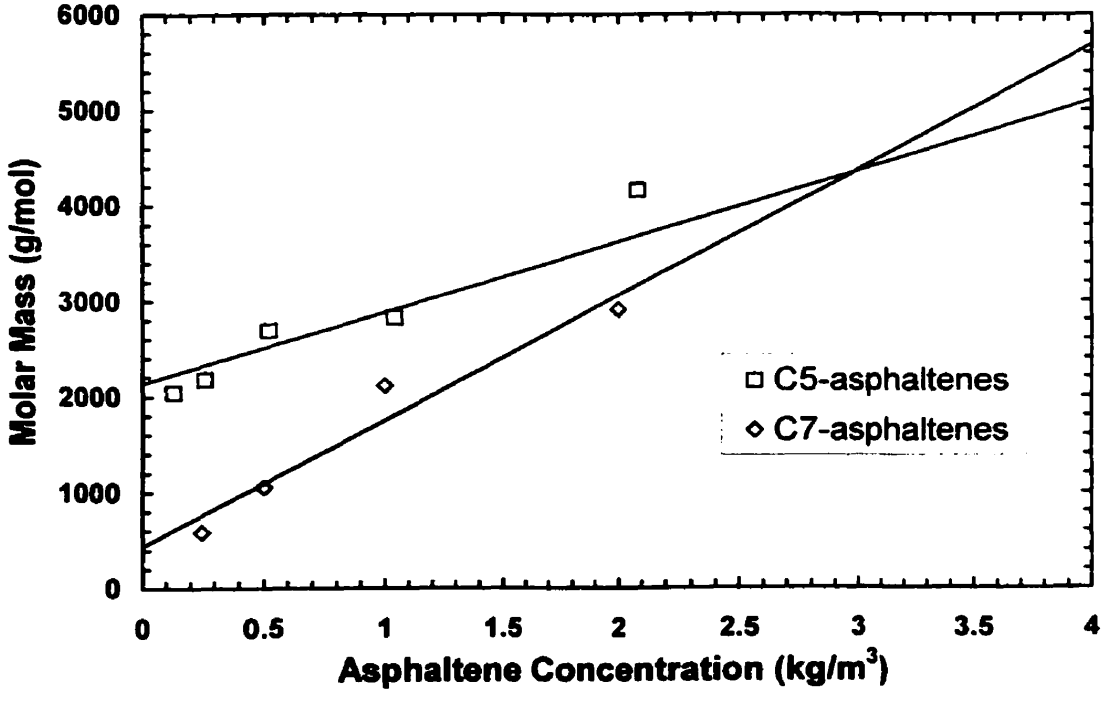

Figure 5.4 High Concentration Extrapolation of VPO Molar Masses in Toluene

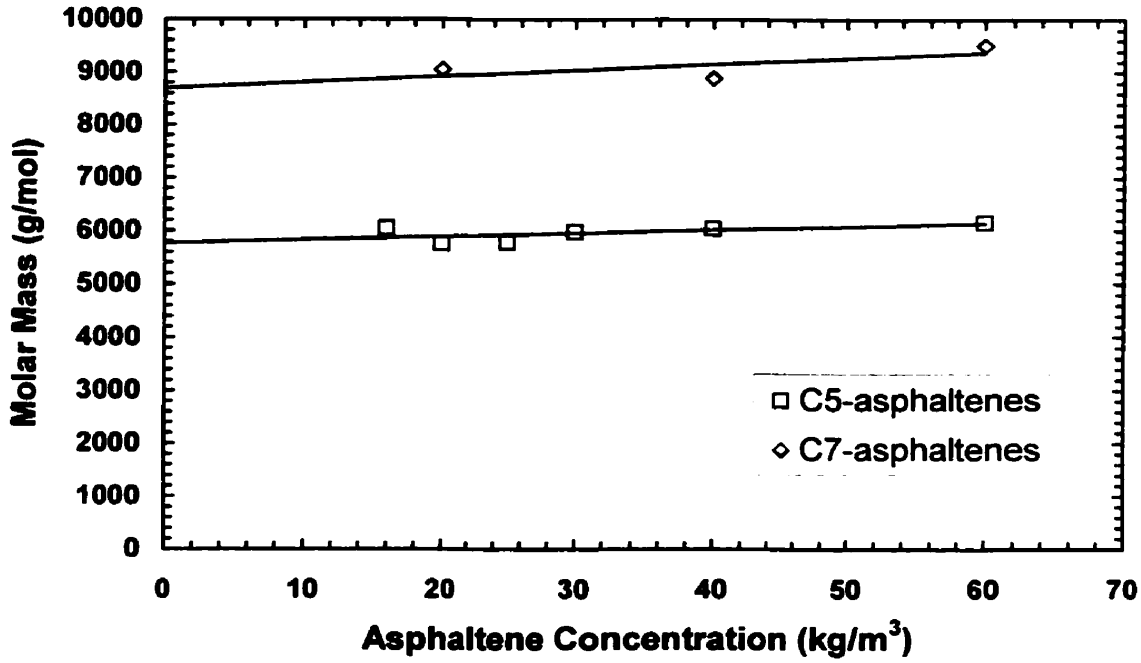

From Figure 5.2 it is evident that the molar mass of the C7-asphaltenes is higher than, that of the C5-asphaltenes. The *T/P* ratio and the association constant, *K* from the two-parameter model fit the experimental data quite well. It was found that the *T/P* ratio was higher for C5-asphaltenes than that for C7-asphaltenes. This can be explained from the properties of bitumen from which the asphaltenes are obtained. It is known that bitumen contains saturates, aromatics, resins and asphaltenes. Among these solubility classes, saturates are distinctly different in their structure and chemical properties and mainly contain paraffins and napthenes. On the other hand, as discussed in Chapter 2, the other three classes i.e., aromatics, resins and asphaltenes form a continuum with increasing molar mass, heteroatom content and polarity. When pentane is used to extract asphaltenes a bigger cut from bitumen precipitates than when heptane is used. Hence,

pentane extracted (C5) asphaltenes contain more resinous material. Since resins have more terminators the C5-asphaltenes have a higher *T/P* ratio and the degree of asphaltene association is reduced. Results for resins are discussed later. Another interesting observation is that the same value for the association constant was used to fit the experimental data. This shows that the association constant is probably not a strong function of the type of asphaltenes.

5.2 Effect of Temperature and Solvent on Asphaltene Association

There is quite a significant effect of temperature and solvent conditions on the association of asphaltenes. Figures 5.5 and 5.6 show the effect of temperature on molar mass of C5- and C7-asphaltenes in toluene and Figures 5.7 and 5.8 in o-dichlorobenzene along with the two-parameter model fits.

Monomer and limiting molar mass estimates of Athabasca C5- and C7-asphaltenes for the different solvents and temperatures are given in Table 5.2. Monomer molar masses are obtained from linear extrapolation at low asphaltene concentrations (<3 kg/m^3) and limiting molar masses from linear extrapolation at high asphaltene concentrations (>20 kg/m^3). The apparent monomer molar mass appears to increase with temperature and shows no apparent relationship to solvent or asphaltene type. There is considerable scatter in the data and hence the relationship to temperature may be a coincidence. However, the limiting aggregate molar mass clearly depends on the solvent, temperature, and asphaltene type. The aggregate molar mass decreases as temperature and polarity of the solvent increase. The observations presented in Table 5.2 suggest that

asphaltenes have an average monomer molar mass of approximately 1800 g/mol and can associate into aggregates of 2 to 6 monomers on average, depending on the composition, solvent and temperature.

Table 5.2 Estimated Monomer and Limiting Aggregate Molar Masses for Athabasca Asphaltenes

Asphaltene type	Solvent	Temperature (°C)	Molar mass (g/mol)	
			Monomer	Aggregate
C5-asphaltenes	toluene	50	1900	6200
	toluene	70	900	5000
	o-dichlorobenzene	75	1500	4300
	o-dichlorobenzene	130	2400	3600
C7-asphaltenes	toluene	50	400	10000
	toluene	70	2500	8300
	o-dichlorobenzene	75	900	6000
	o-dichlorobenzene	130	3000	5300

It was found that, for a given asphaltene, a higher *T/P* ratio fit the experimental data quite well at higher temperature. The rise in the *T/P* ratio suggests that some propagators become terminators as temperature increases. In other words, the weakest association sites on a given asphaltene molecule may not be able to form a link with another molecule as thermal motion increases.

Figure 5.5 **VPO Molar Mass of Athabasca C5-Asphaltenes in Toluene (M_p = 1800, M_t = 800)**

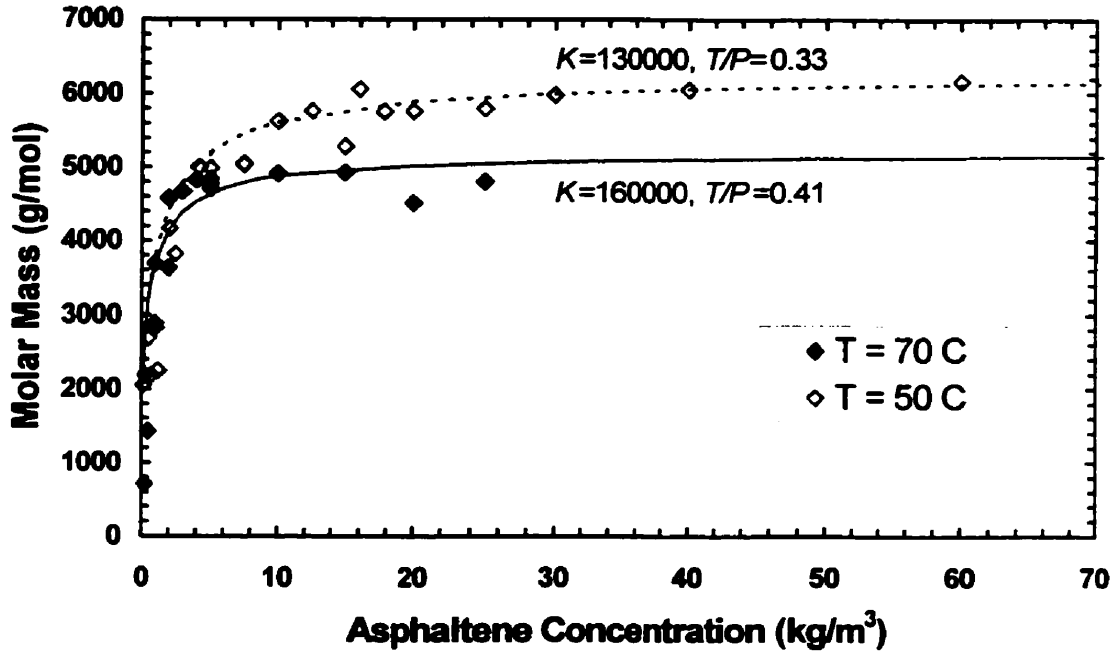

Figure 5.6 **VPO Molar Mass of Athabasca C7-Asphaltenes in Toluene (M_p = 1800, M_t = 800)**

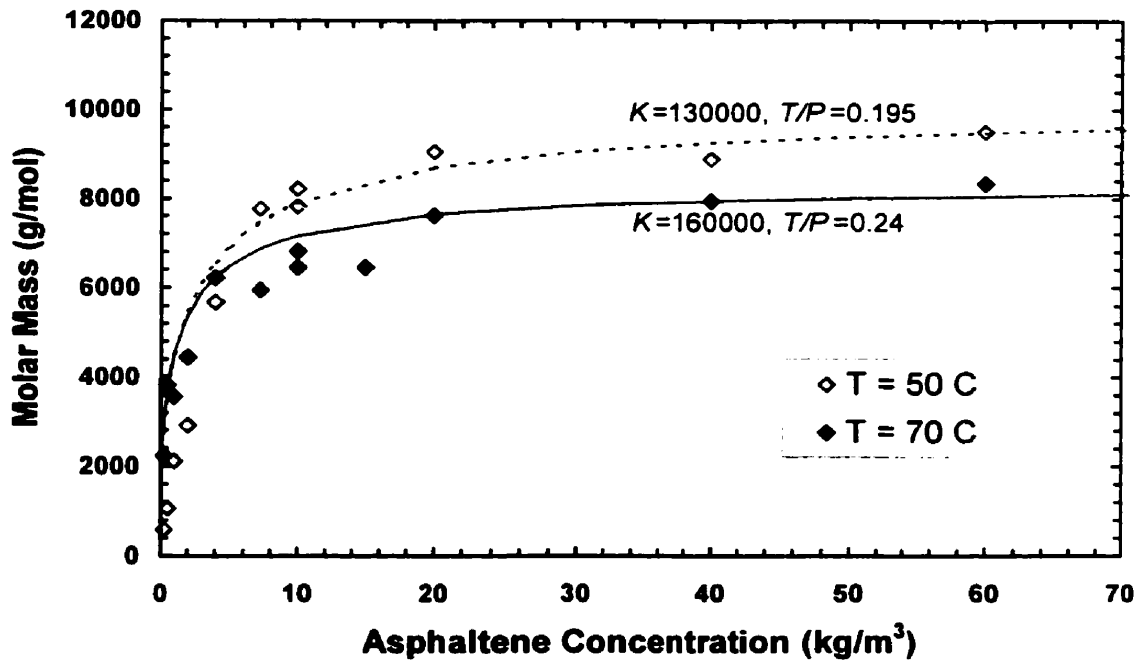

Figure 5.7 **VPO Molar Mass of Athabasca C5-Asphaltenes in o-dichlorobenzene (M_p = 1800, M_t = 800)**

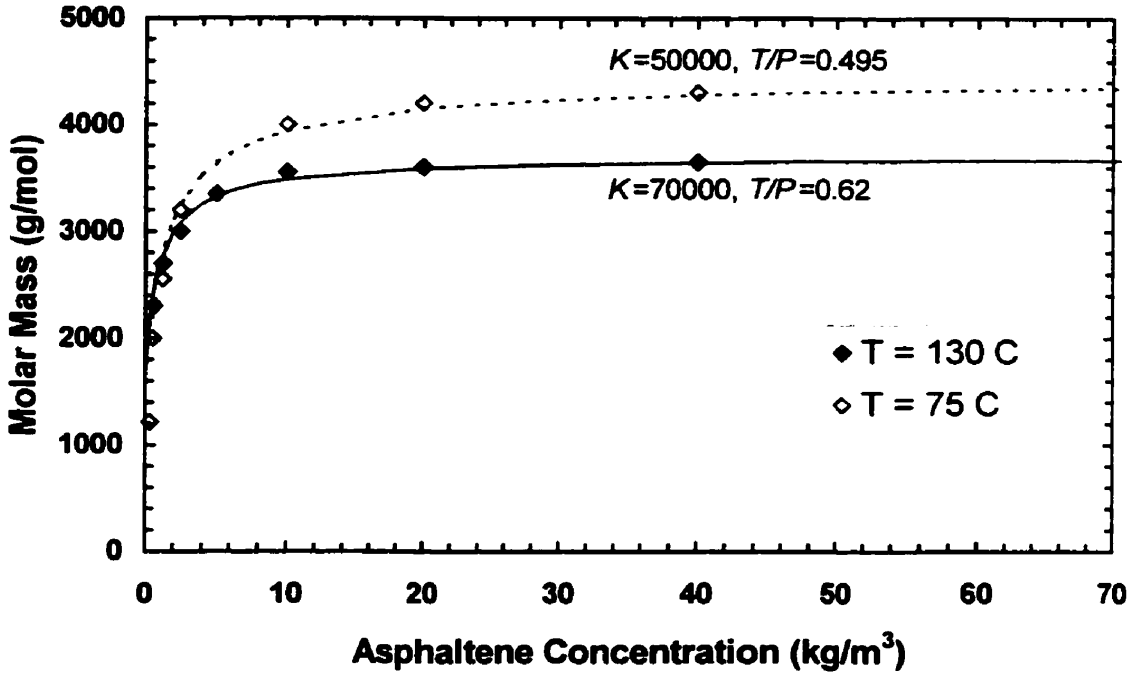

Figure 5.8 **VPO Molar Mass of Athabasca C7-Asphaltenes in o-dichlorobenzene (M_p = 1800, M_t = 800)**

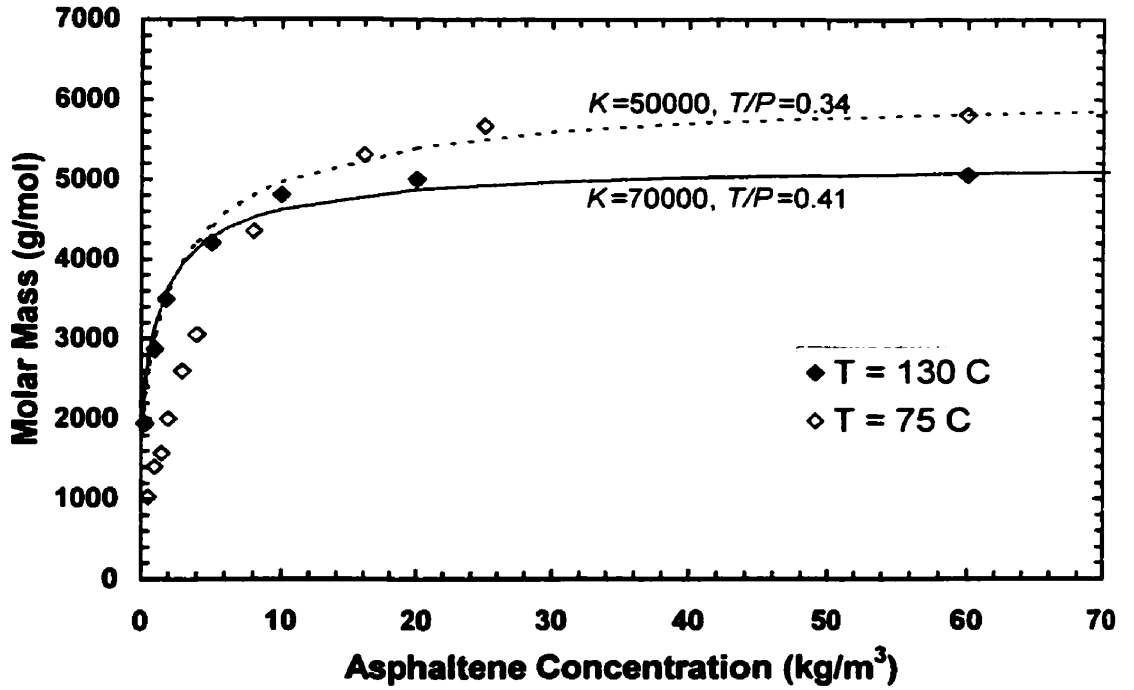

The effect of solvent polarity is shown in Figures 5.9 and 5.10 for, C5- and C7-asphaltenes, respectively at nearly fixed temperature (≈ 70° C). Note that 75° C was the lowest temperature stable VPO measurements could be obtained in o-dichlorobenzene and 70° C was the highest temperature stable measurements could be obtained in toluene. It was found that, for a given asphaltene, a higher *T/P* ratio fit the experimental data quite well for a solvent of higher polarity. This may be because as the "power" of the solvent increases, asphaltene-solvent interactions tend to dominate as compared to asphaltene-asphaltene interactions. Hence, fewer association sites are able to form links with other asphaltenes.

Figure 5.9 Effect of Solvent Polarity on Molar Mass of C5-asphaltenes at ≈ 70°C (M_p = 1800, M_t = 800)

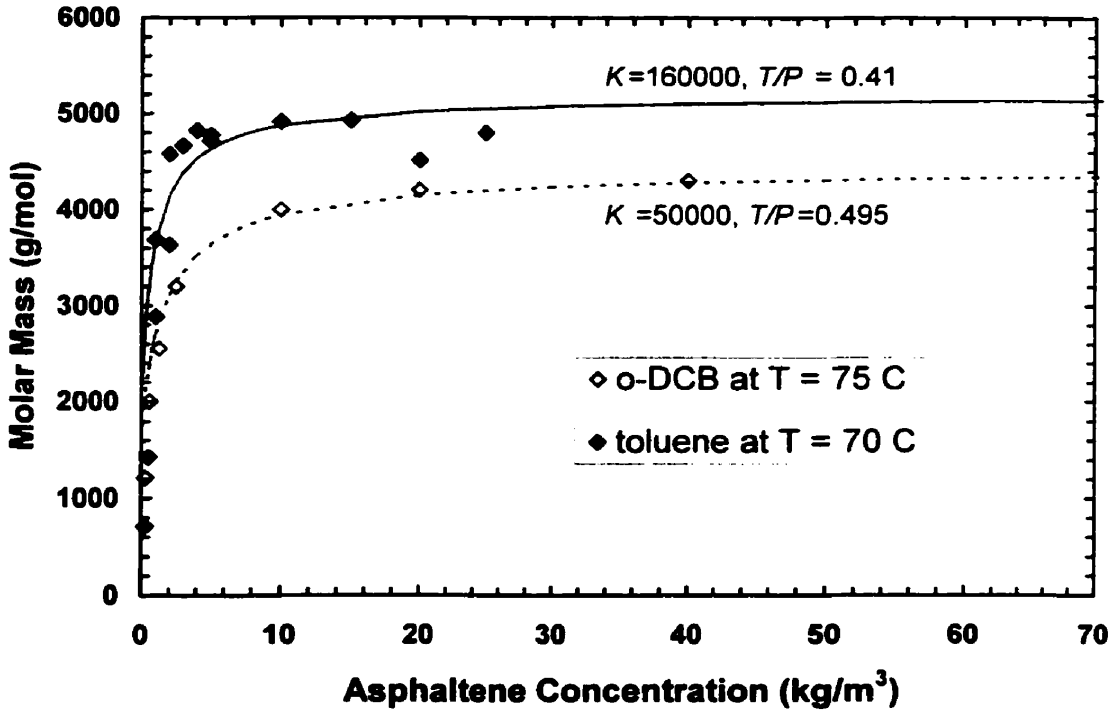

Figure 5.10 Effect of Solvent Polarity on Molar Mass of C7-asphaltenes at ≈ 70°C (M_p = 1800, M_t = 800)

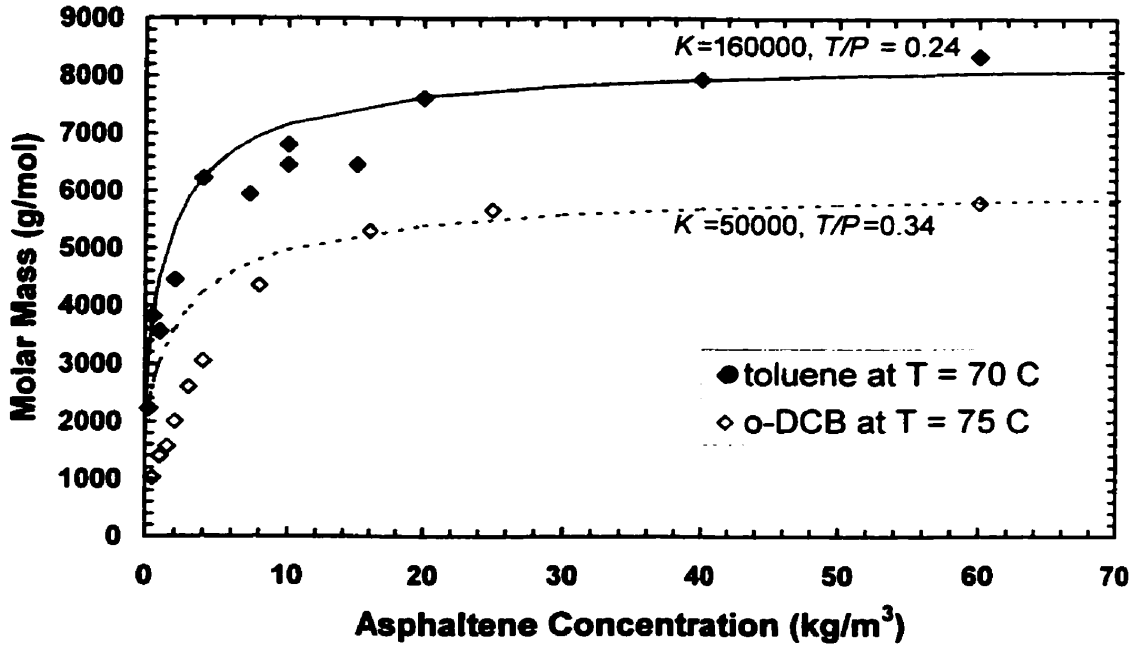

The model parameters, K and T/P, from the two-parameter model are summarized in Table 5.3. As temperature increases, K and T/P both increase. As the solvent "power" increases, K decreases and T/P increases. To explain these trends, it is necessary to recognize that the model is an averaging approach to thousands of individual "reactions". In a conventional approach, each reaction can be expressed in terms of free energy

$$K = e^{\frac{-\Delta G^o}{RT}} \tag{5.1}$$

where $\Delta G°$ is the standard Gibb's free energy of solution, R is the gas constant, K is the association constant and T is the temperature. Since association is favored, $\Delta G°$ is negative and as temperature increases, the association constant is expected to decrease. However, in the proposed model the T/P ratio is increased as the temperature increases and in effect some reactions are removed from consideration, as some propagators

become terminators. Hence the $\Delta G°$ of the averaged reactions can change. Since $\Delta G°$ in effect changes with temperature the value of K does not necessarily decrease with temperature. Note that as temperature increases, the combined effect of increasing T/P and K is to decrease the aggregate size, which is consistent with Eq. 5.1. The effect of increasing solvent power is to reduce the $\Delta G°$ of association, which is accounted for by higher T/P and lower K.

The standard Gibb's energy, $\Delta G°$ is computed using Eq. 5.1 and is reported in Table 5.3 for the various systems. It was interesting to note that the standard Gibb's energy varied over a fairly small range, –37.39 to –31.32 kJ/mol for the various systems.

Table 5.3 Summary of Association Constant and *T/P* Ratios for Various Asphaltene Systems from the Two-Parameter Model

Solvent	Temperature (° C)	Association Constant, *K*	Standard Gibb's Energy, kJ/mol	*T/P* ratio (C5-asphaltenes)	*T/P* ratio (C7-asphaltenes)
Toluene	50	130000	-31.63	0.33	0.195
	70	160000	-34.19	0.41	0.24
o-DCB	75	50000	-31.32	0.495	0.34
	130	70000	-37.39	0.62	0.41

Note that an average value for the association constant was used to describe all association "reactions" including termination and propagation for any system. This assumption was used so as to reduce the number of parameters in the model. In reality, termination "reactions" probably have a higher association constant than propagation

"reactions" (Hirschberg and Hermans, 1984) since resin-asphaltene interactions appear to be stronger than asphaltene-asphaltene interactions (Moschopedis and Speight, 1976). However, the assumption of an average association constant does not appear to have a significant influence on the average molar mass of asphaltenes.

Note that since VPO measurements were subject to greater degree of error (as high as 100%) at low asphaltene concentrations (<3 kg/m^3) as discussed in Chapter 3, the criteria used to fit the curves in all cases was a match at asphaltene concentrations above 3 kg/m^3. In general there was about 3-4% error in the VPO measurements in this concentration range. With this criteria, the value of the association constant was not found to be dependent on the type (C5 or C7) of asphaltenes for a system defined by solvent and temperature. Hence the same value for the association constant was used to fit the experimental VPO data at a particular temperature and solvent regardless of the type of asphaltenes. It can be concluded that the association constant may not be a strong function of the asphaltene type and may be assumed to be a function of temperature and solvent properties only.

5.3 Effect of Resins on Molar Mass of Asphaltenes

As discussed in Chapter 2, resins are known to reduce the degree of asphaltene association. To determine the effect of adding resins, C5-asphaltenes and resins were mixed in different proportions and the average molar masses of the resulting systems were measured at different concentrations using the VPO. The results are presented in Figure 5.11. The symbols represent experimental data and the lines represent model fits.

It is evident from the plot that, molar mass decreases from C7-asphaltenes (which are more like "pure" asphaltenes) to C5-asphaltenes (which are more like a mixture of asphaltenes and resins) the molar mass decreases. Furthermore, in a mixture of C5-asphaltenes and resins, the molar mass decreases even further as the proportion of resins in the mixture increases.

Figure 5.11 Molar Mass of Athabasca Asphaltene & Resin Mixtures at 50 °C (M_p = 1800, M_t = 800, K = 130000)

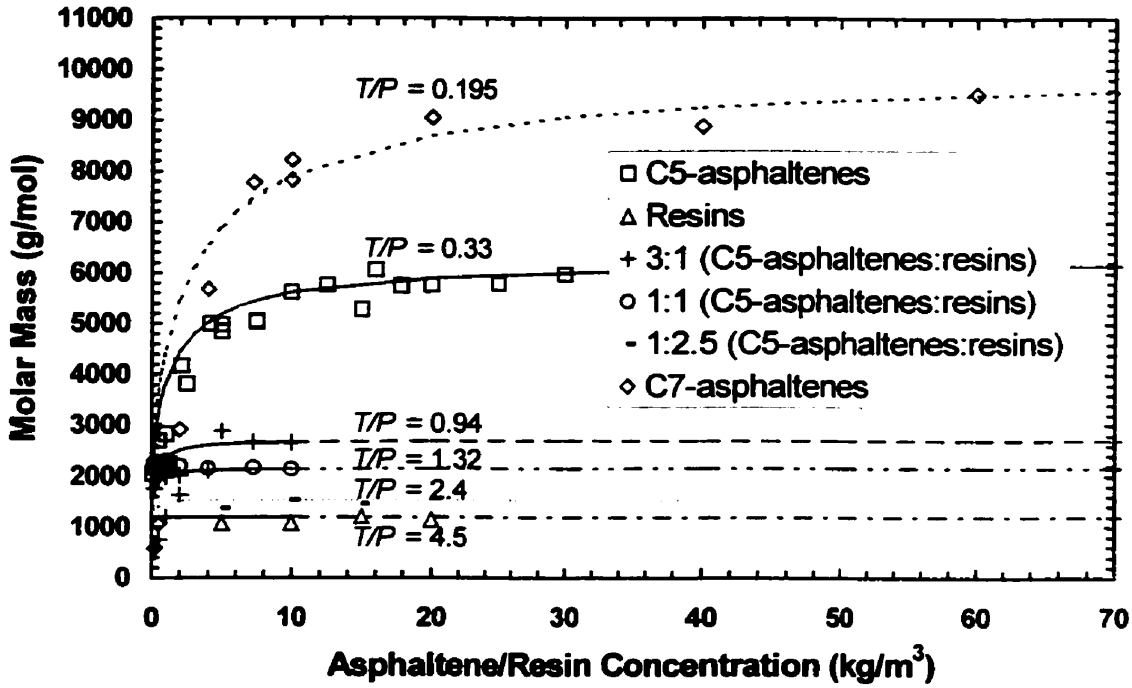

Note that the reduction in molar mass is much more than simply adding a low molar mass component to a high molar mass component. For example, consider a 3:1 (by mass) mixture of C5-asphaltenes to resins at a concentration of 10 kg/m^3. The VPO measurements indicate C5-asphaltenes have an average molar mass of 5700 g/mol and resins a molar mass of about 1200 g/mol at this concentration. Thus a 3:1 mixture would

yield a molar mass of approximately 3800 g/mol, assuming there is no association. However, the VPO measurements for this system indicate a molar mass of about 2700 g/mol. Hence the resin/asphaltene mixture molar masses are the strongest evidence that resins influence asphaltene association. This observation is supported by experiments performed in Section 5.7 where resins are removed from the asphaltenes through rigorous washing.

The asphaltene/resin mixtures also provide an opportunity to test the predictive capability of the association model. First, the association model was applied to C5-asphaltene and "pure" resin experimental data shown in Figure 5.12. An association constant of 130,000 was used and a *T/P* ratio of 0.33 for the C5-asphaltenes and a *T/P* ratio of 4.5 for "pure" resins. The *T/P* ratio for mixtures of C5-asphaltenes and resins was then calculated directly. The calculated *T/P* ratio was used to generate the model predictions shown in Figure 5.11. The predicted limiting molar masses were within 16% of the experimentally measured molar masses.

A second method for assessing the predictions is to find the *T/P* ratio that best fits the data and compare the best fit with the *T/P* ratio calculated from the known composition of C5-asphaltenes and resins. These comparisons are presented in Table 5.4. It was found that the predictions of the mole fraction terminators were within about 12% of the two-parameter model curve fit values. Considering the assumptions in the simple model, this level of agreement is very good. The success of the model in predicting the molar mass of asphaltene/resin mixtures is the strongest evidence so far that the proposed model does capture the physics of asphaltene association.

Figure 5.12 Two-parameter Model Curve Fits for Asphaltenes and Resins ($M_p = 1800$, $M_t = 800$, $K = 130000$)

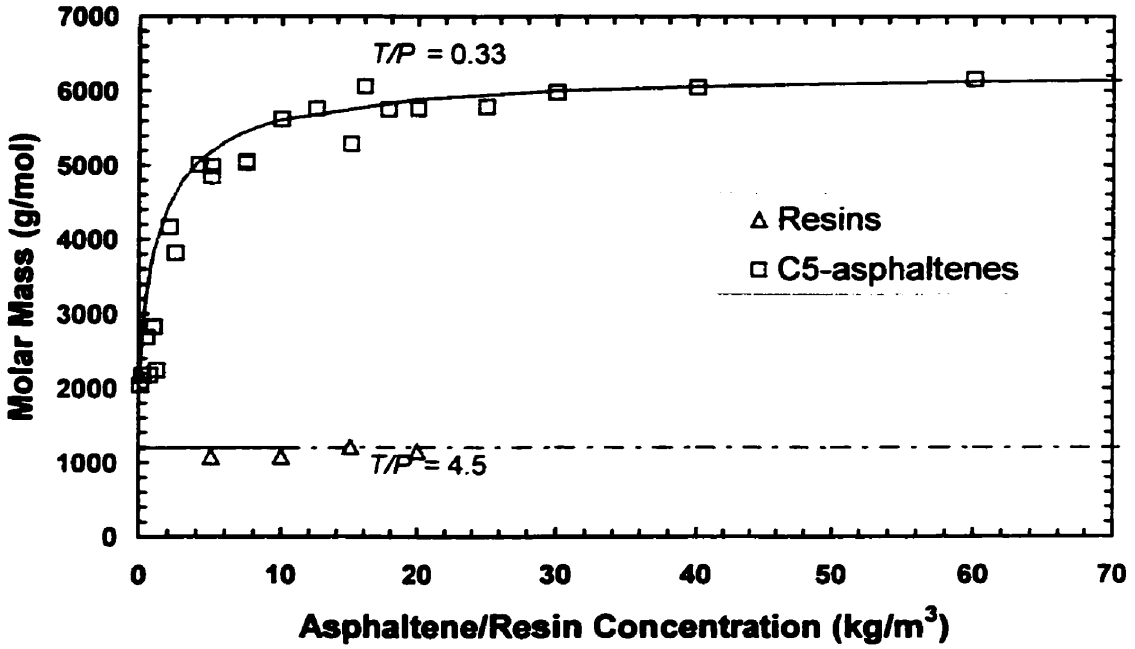

Table 5.4 Comparison of *T/P* Ratios between Predictions and Two-Parameter Model Curve Fits

System (mass ratio)	Model, *T/P*	Model mole % terminators	Mole fraction resins	Estimated mole % terminators	Estimated *T/P*	% error
C5-asphaltenes (A)	0.33	0.248				
3:1 (C5-A:R)	0.94	0.485	0.429	0.492	0.97	1.604
1:1 (C5-A:R)	1.32	0.569	0.701	0.648	1.838	12.142
1:2.5 (C5-A:R)	2.4	0.706	0.849	0.732	2.733	3.586
Resins (R)	4.5	0.818				

5.4 Comparison between Athabasca and Cold Lake Asphaltenes and Resins

VPO molar mass measurements were performed on C5-, C7-asphaltenes and resins extracted from Cold Lake bitumen in toluene at 50° C. These experiments were

performed in order to investigate if aggregation was seen in Cold Lake asphaltenes as well. Figure 5.13 shows a comparison of molar mass of Athabasca and Cold Lake C5-, C7-asphaltenes and resins in toluene at 50° C. The symbols represent experimental data and lines represent model curve fits. It is interesting to note that the aggregation behavior of the asphaltenes from the two different bitumens is similar.

Figure 5.13 Comparison between Molar Mass of Athabasca (Ath) and Cold Lake (CL) Asphaltenes and Resins

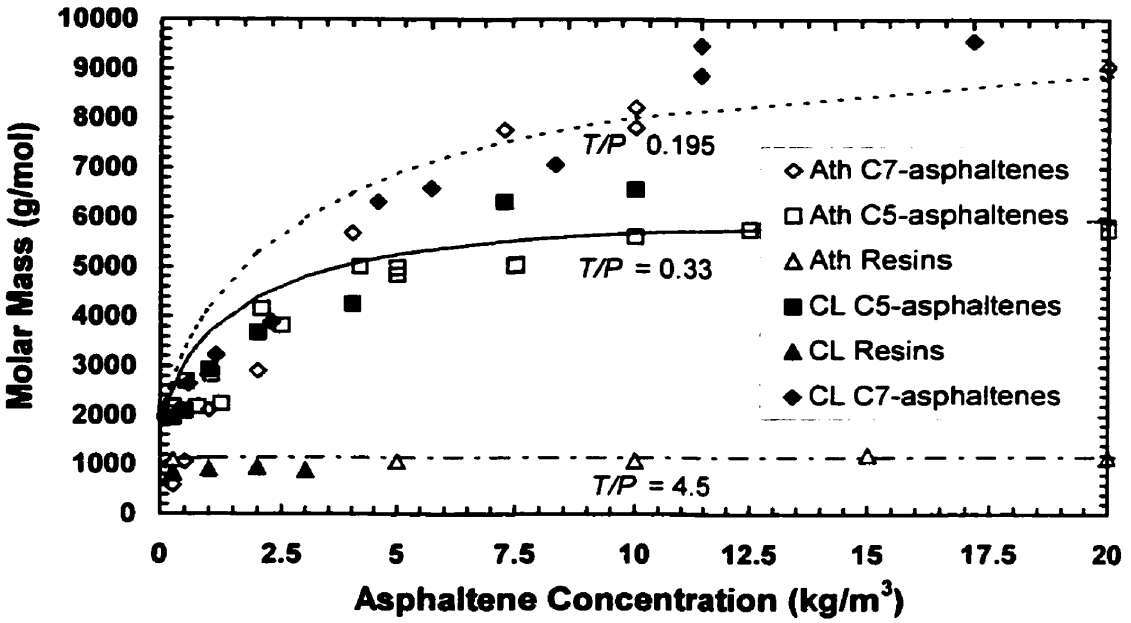

5.5 Monomer Molar Masses – A Sensitivity Analysis

As discussed in Chapter 2, there is no consensus on the monomer molar mass of asphaltenes among researchers. This may be attributed to the variations in the monomer molar mass with the source and nature of the crude oil from which these are extracted. The variations may also be due to the different techniques used by different researchers.

On the other hand there is considerable consensus on the monomer molar mass of resins as ranging from 400 to 1000 g/mol again depending upon the crude oils from which they were separated. In this section a sensitivity analysis is performed for the monomer molar mass of propagators and terminators. Different combinations of propagator and terminator monomer molar masses were used to fit the experimental data of C5- and C7-asphaltenes in toluene at 50° C. The monomer molar mass of terminators was varied from 400 g/mol to 1000 g/mol and that of propagators from 800 g/mol to 2200 g/mol. This was done in steps of 200 g/mol. In all, 32 simulations were performed using the two-parameter model. The results of the simulation are shown in Tables 5.5 and 5.6 for the *T/P* ratio and Table 5.7 for the association constant. Figure 5.14 summarizes the sensitivity analysis.

Figure 5.14 Effect of Monomer Molar Masses on the *T/P* Ratio and *K*

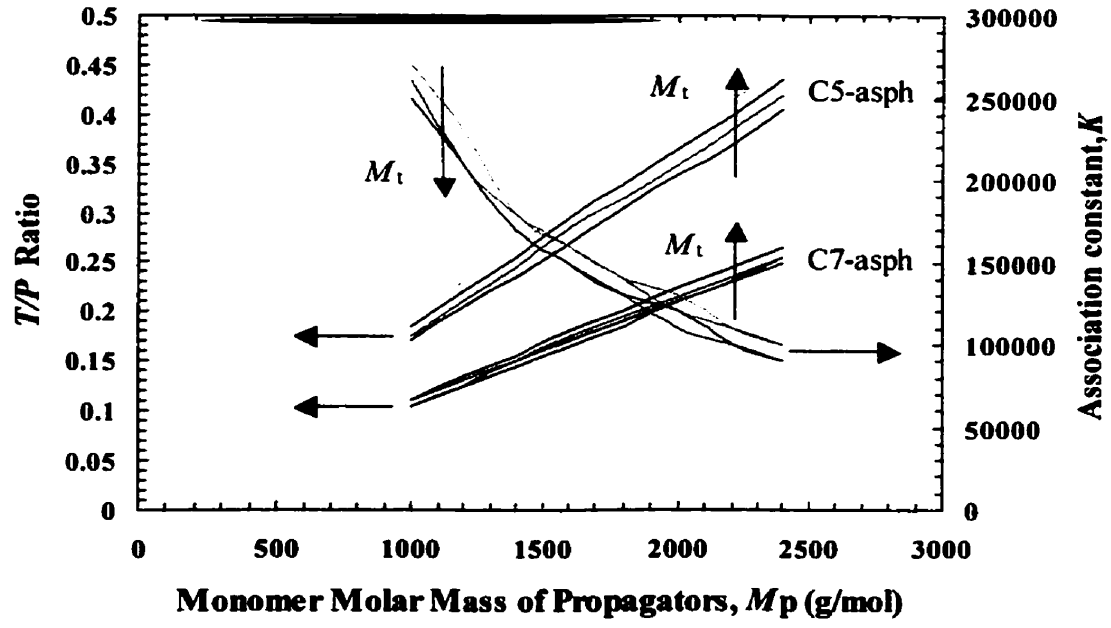

Table 5.5 ***T/P*** **Ratio of C5-asphaltenes in Toluene at 50° C**

M_t \ M_p	1000	1200	1400	1600	1800	2000	2200	2400
400	0.17	0.205	0.235	0.27	0.305	0.34	0.37	0.405
600	0.175	0.21	0.245	0.285	0.315	0.35	0.385	0.42
800	0.185	0.22	0.255	0.295	0.33	0.365	0.4	0.435
1000	0.19	0.23	0.265	0.305	0.345	0.38	0.415	0.45

Table 5.6 ***T/P*** **Ratio of C7-asphaltenes in Toluene at 50° C**

M_t \ M_p	1000	1200	1400	1600	1800	2000	2200	2400
400	0.105	0.125	0.145	0.165	0.185	0.21	0.23	0.25
600	0.105	0.125	0.15	0.17	0.19	0.21	0.23	0.255
800	0.11	0.13	0.15	0.175	0.195	0.215	0.235	0.255
1000	0.11	0.135	0.155	0.18	0.2	0.225	0.245	0.265

Table 5.7 Association Constant of C5- and C7-asphaltenes in Toluene at 50° C

M_t \ M_p	1000	1200	1400	1600	1800	2000	2200	2400
400	270000	230000	180000	160000	140000	130000	110000	100000
600	260000	210000	180000	160000	140000	120000	110000	100000
800	260000	210000	170000	150000	130000	110000	100000	90000
1000	250000	210000	170000	150000	130000	120000	100000	90000

Figure 5.15 shows the *T/P* ratio versus the monomer molar mass of propagators for different monomer molar mass of terminators (400 to 1000 g/mol in steps of 200 g/mol) for C5- and C7-asphaltenes on the primary axis. On the secondary axis is plotted the association constant for the C5- and C7-asphaltenes. It is interesting to note that the change in *T/P* ratio is more severe due to a change in propagator molar mass than due to the terminator molar mass. Also, from the slope of curves, it can be noted that the change in *T/P* ratio is more severe for C5-asphaltenes than for C7-asphaltenes. Interestingly, the association constant does not change significantly with the terminator molar mass but is sensitive to the monomer molar mass of propagators.

The molar mass of terminators and propagator monomers is assumed to be invariant. However, as shown on Figure 5.15, their molar mass depends on temperature and solvent. There is really a continuum of molar masses and the average molar mass of the terminators and propagators depends where the division between the two groups (the *T/P* ratio) falls. As temperature and solvent "power" increase, there are more terminators and the molar mass of both terminators and propagators is expected to increase. Fortunately for the range of temperatures and solvents considered in this work, neglecting the change in M_t and M_p did not significantly affect the quality of the model fits. The change in monomer molar masses should be accounted for when modeling aggregation of asphaltenes in highly polar solvents such as nitrobenzene or at very high temperatures, where essentially all of the propagators change to terminators or in other words asphaltenes remain as unassociated species (Moschopedis and Speight, 1976).

Figure 5.15 Shift in Average Monomer Molar Mass of Terminators and Propagators

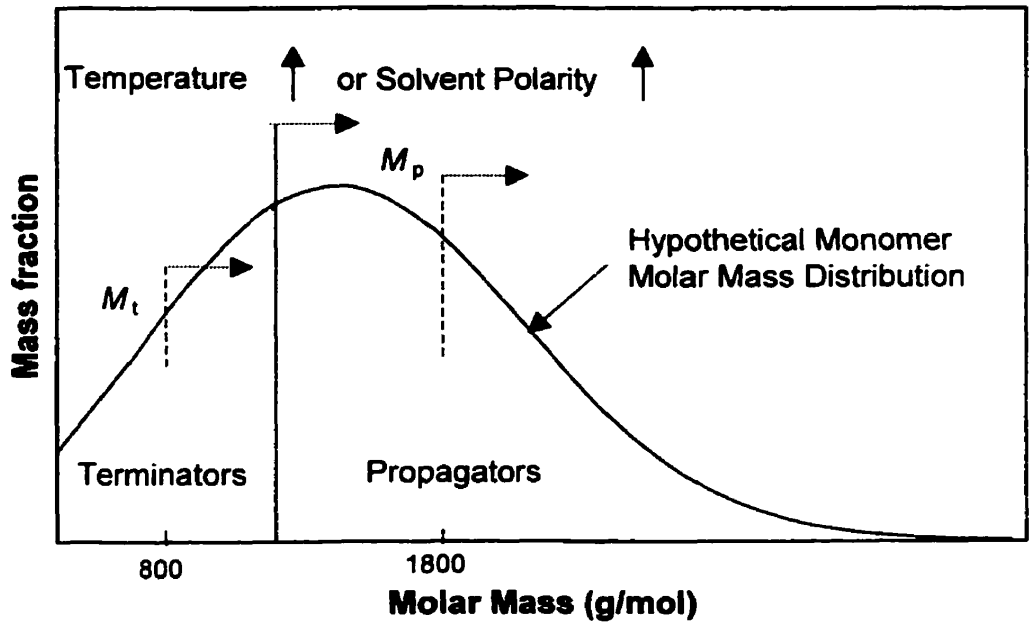

5.6 Molar Mass Distribution and Diminution Parameter

The most important output of the association model is the molar mass distribution of the asphaltenes. This is an important physical property of the asphaltenes, which serves as input to the numerous models available to predict the phase behavior of asphaltenes. The molar mass distributions of four asphaltene/resin systems in toluene at 50° C from the two-parameter model are shown in Figures 5.16 to 5.19. The molar mass distribution is plotted as mass percent of asphaltenes versus the molar mass. There is a dramatic effect of concentration on the distribution over the concentrations where the asphaltene average molar mass increases. As expected, for concentrations beyond which the limiting molar mass is reached, the molar mass distribution does not change. The molar masses range up to 50,000 g/mol.

Figure 5.16 Molar Mass Distribution of C7-asphaltenes in Toluene at 50° C

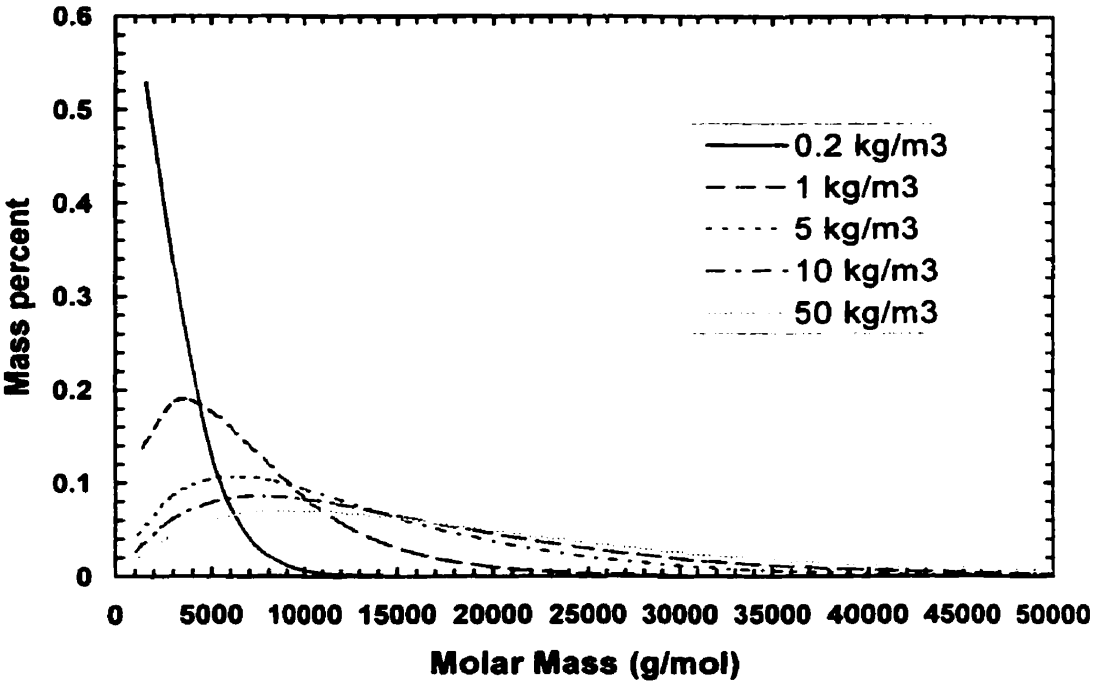

Figure 5.17 Molar Mass Distribution of C5-asphaltenes in Toluene at 50° C

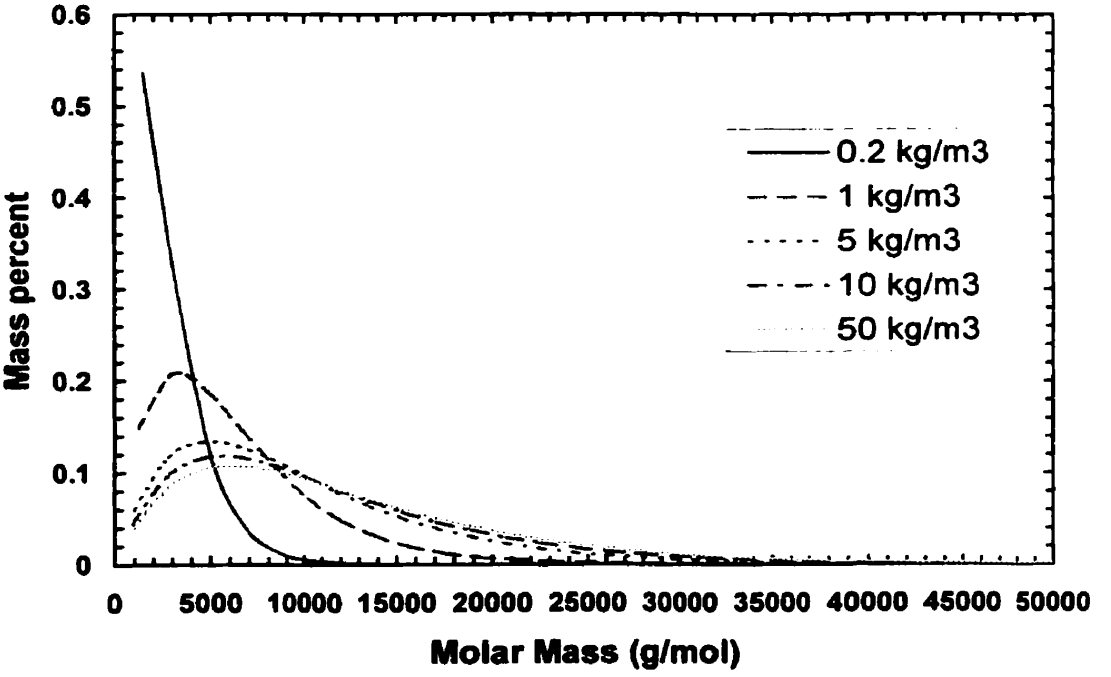

Figure 5.18 Molar Mass Distribution of 3:1 C5-asphaltenes:resins in Toluene at 50° C

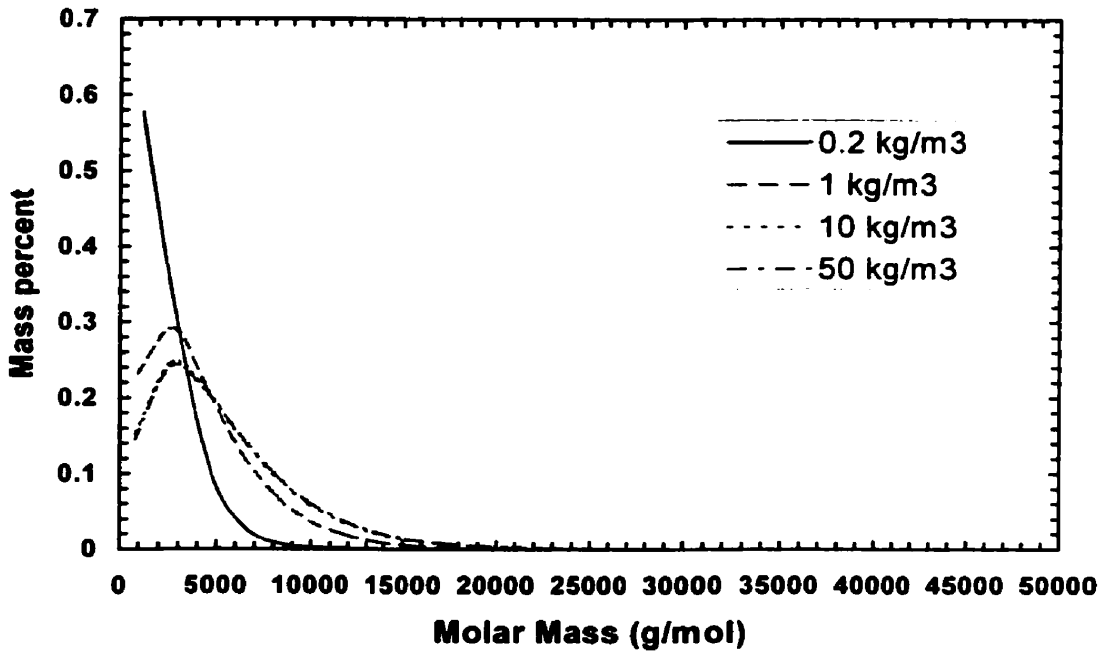

Figure 5.19 Molar Mass Distribution of 1:1 C5-asphaltenes:resins in Toluene at 50° C

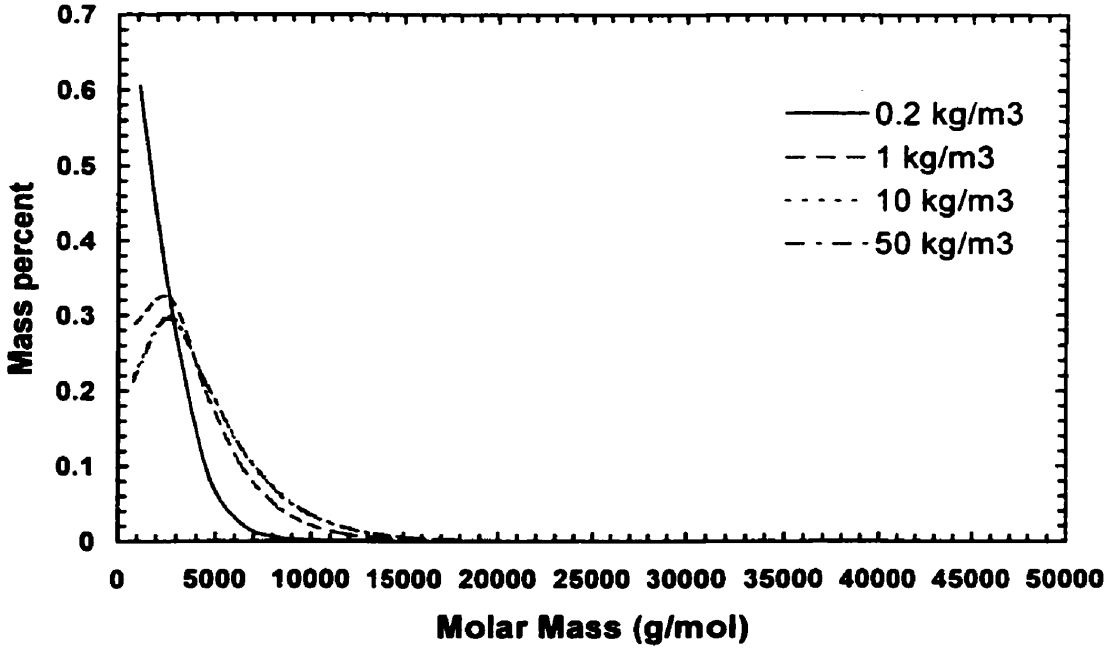

It is evident from the plots that as the proportion of resins in the system increases, the molar mass distribution changes and gives rise to a more narrow distribution. Or in other words the upper limit of the distribution reduces due to the formation of smaller aggregates.

It is interesting to note that the shape of the molar mass distribution obtained from the model is very similar to those obtained from Gel Permeation Chromatography (GPC) measurements (Peramanu et al., 1999; Kawanaka et al., 1991; Dabir et al., 1996). However, the upper limits of the asphaltene molar mass distribution used by researchers ranged from 8,500 g/mol (Yarranton and Masliah, 1996), 10,000 g/mol (Ferworn, 1996), 14,000 (Kawanaka et al., 1991), 35,000 (Dabir et al., 1996) to 100,000 (Peramanu et al., 1999). In order to have more control over the upper limit of the asphaltene molar mass distributions, a diminution parameter was introduced as discussed in Chapter 4.

The three-parameter model was tested with a value of 0.82 for the diminution parameter. The association constant was changed to fit the experimental data. Figure 5.20, demonstrates that the upper limit of the molar mass distribution can be reduced for any system by decreasing the diminution parameter from 1 towards 0. The comparison is shown for C5-asphaltenes in toluene at 50° C and a concentration of 10 kg/m^3 where the upper limit reduces from about 50,000 g/mol to about 20,000 g/mol. A value of 0.82 is used for the diminution parameter.

It was interesting to note that the *T/P* ratios for the various systems did not change significantly and hence the model predictions for the asphaltene-resin systems remained unchanged. However, it was seen that there was a dramatic change in the molar mass

distribution. Thus with a fractional value for the diminution parameter, the upper limit of the distribution can be adjusted anywhere from 10,000 g/mol to 50,000 g/mol.

Figure 5.20 Effect of Diminution Parameter on Molar Mass Distribution

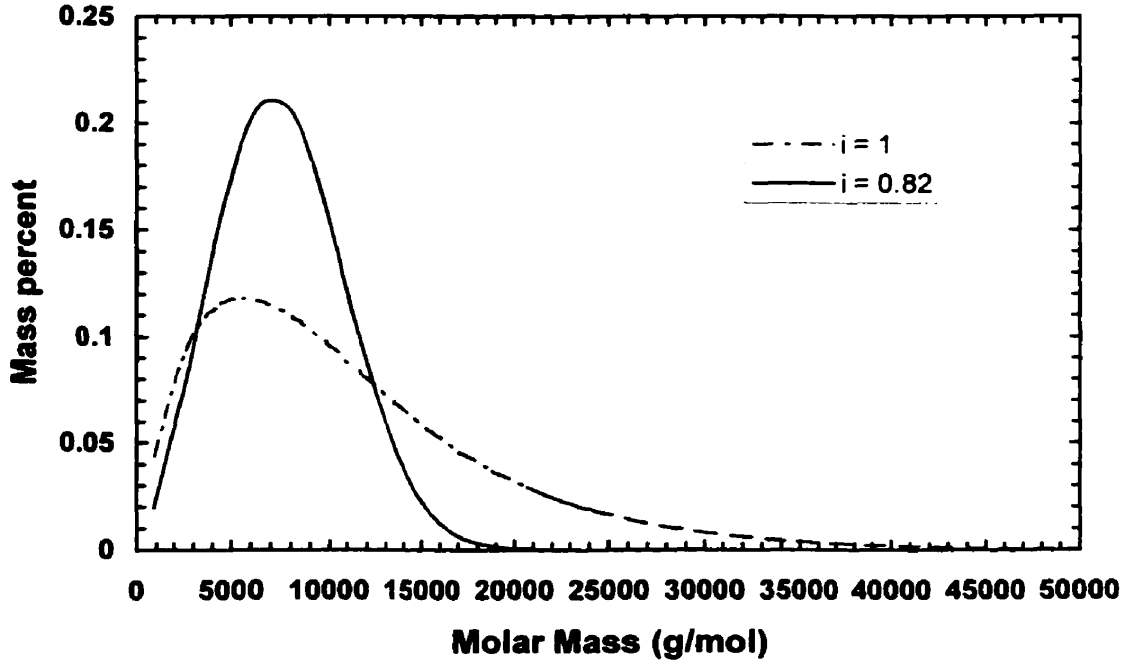

5.6 Implications of the Asphaltene Association Model on Solubility Modeling of Asphaltenes

The molar volume of asphaltenes is an important parameter necessary for modeling their phase behavior. Molar volume, which depends on the molar mass and specific gravity distributions, is still treated as a fit parameter in most approaches since accurate characterization data for asphaltenes is not available. Moreover, the models available today do not account for the change in molar volume with temperature, pressure, solvent and composition. The association model presented in this thesis is

based on experimentally measured molar masses and provides a method for estimating the change in molar volume with system conditions.

To demonstrate the significance that aggregation (and hence molar mass) has on the solubility of asphaltenes, two sets of experiments were performed. Athabasca C7-asphaltenes were extracted using n-heptane by the IP-143 method described in Chapter 3. However, 4 different procedures were used to clean the asphaltenes. The first asphaltene sample was unwashed; that is after contacting with heptane the asphaltenes were filtered using an 8μ filter paper and dried till there was no change in mass. It is likely that since this fraction was unwashed, a significant amount of resinous material remained with the asphaltenes. The second sample was obtained by 5-day washing described in Chapter 3. All VPO experiments described in the sections above were performed using this method. The third sample was prepared in exactly the same way as the second one except that the sample was washed for 10 days instead of 5. The additional washing is expected to remove more of the resinous material trapped in the structures formed by asphaltenes. The fourth sample was prepared by the Soxhlet method described in Chapter 3, which is equivalent to infinite washing.

The respective yields and non-asphaltenic solids content of the four samples are presented in Table 5.8. As expected, the asphaltene yield decreases with each extra washing step. It is interesting to note that there is not too much difference in the yields between the 5-day and 10-day washed samples. This shows that physically, it is possible to remove the resinous material trapped in asphaltene structures only to a certain extent by washing.

Table 5.8 Properties of Various C7-asphaltenes

C7-asphaltenes	% Yields[1]	% solids[2]	Two-parameter model *T/P*	Onset (volume fraction toluene)
Unwashed	15.3	6.3	0.24	0.44
5-day washed	14.3	7.4	0.195	0.5
10-day washed	13.7	7.8	0.175	0.64
Soxhlet	12.6	8.6	0	0.76

1 percentage of bitumen
2 percentage of toluene insoluble solids in asphaltenes

Once the four samples were completely dry, solubility experiments were performed using heptane and toluene. These experiments were performed at a fixed concentration of 10 kg/m^3 of total solvent and with varying volume ratios of toluene and heptane. These experiments are similar to those performed by Mannistu et al (1997). The volume fraction of toluene in the solvent mixture was varied from 0 to 1 and the fractional precipitation (f_{insol}) was measured and plotted against the volume fraction of toluene. The four solubility curves for the four samples were corrected for non-asphaltenic solids and are shown on a solids-free basis in Figure 5.21. The less the asphaltenes were washed (and the more resinous material present), the more heptane is required to initiate precipitation. In other words, washed asphaltenes are less soluble than unwashed asphaltenes. The difference is significant: unwashed asphaltenes begin to precipitate in ≈ 50% heptane while Soxhlet-asphaltenes begin to precipitate in only ≈ 25% heptane. It also appears that there is a large "tail" at low fractional precipitation when less resinous material is present.

Figure 5.21 Solubility Curves for Different C7-asphaltene Samples in Heptol

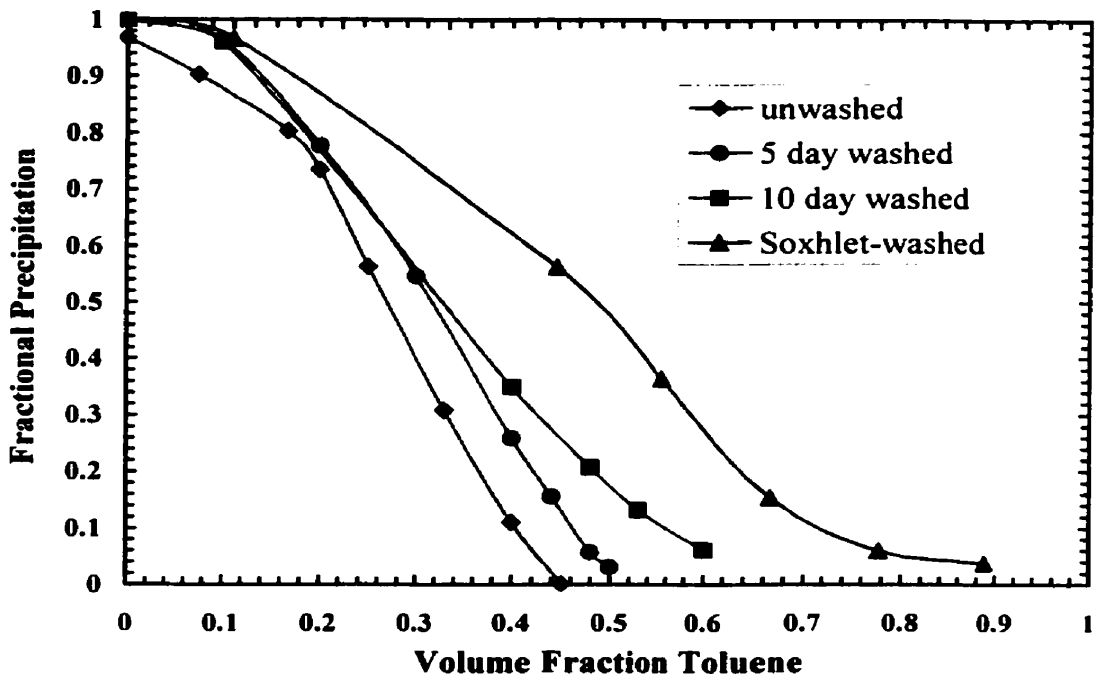

To help explain the shape of these solubility curves, VPO experiments were performed and the average molar mass of the four samples were measured in toluene over the range of 2-60 kg/m^3 at 50° C. The average molar mass of the four samples increased gradually as one went from unwashed to 10-day washed asphaltenes and increased dramatically for the Soxhlet-asphaltenes. The results are shown in Figure 5.22 along with the model fits and summarized in Table 5.8.

The low solubility clearly corresponds to higher molar mass. The "tail" observed with greater washing may reflect the broader molar mass distribution observed with these samples. Note that the solubility experiments were conducted in heptane/toluene mixtures whereas the molar mass distributions were measured in pure toluene (VPO can only be performed in a pure solvent). Hence, direct comparisons are not possible and the

above observations while suggestive are not conclusive. The molar mass distribution of the four samples is shown in Figure 5.23 at an asphaltene concentration of 10 kg/m^3 in toluene at 50° C.

Figure 5.22 Washing Effect on Molar Mass of C7-asphaltenes in Toluene at 50° C

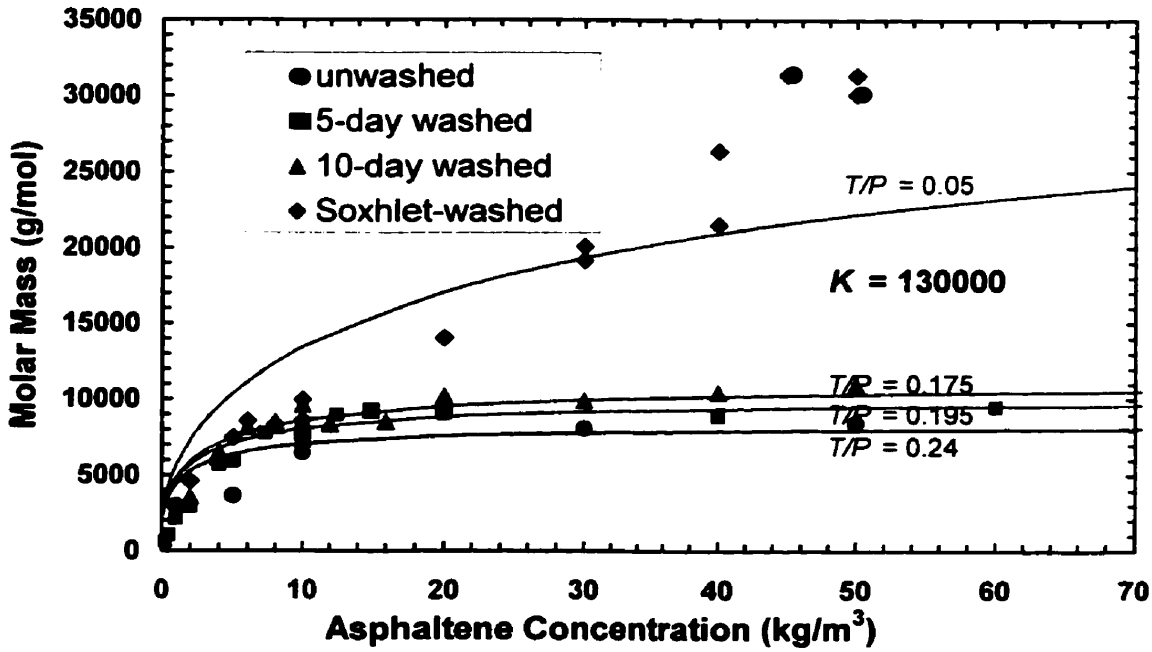

Since the VPO can only accurately detect molar masses in the range of 100 to 25,000 g/mol, there was considerable scatter in the Soxhlet washed asphaltene data at high concentrations (>30 kg/m^3). Thus the curve fit was performed using the VPO data up to 30 kg/m^3 for the Soxhlet asphaltenes. The low value of *T/P* suggests that Soxhlet washing of the asphaltenes stripped it almost completely of resinous material. Since, there were practically very few terminators present in the system to reduce the extent of asphaltene association, very large molar masses resulted. Note that the *T/P* ratio of 0.05

depends on the reaction scheme chosen. If the terminators are assumed, to be capped at both ends of a chain, then larger *T/P* ratios are required to fit the data.

Figure 5.23 Effect of Washing on the Molar Mass Distribution of C7-asphaltenes in Toluene at 50° C and Asphaltene Concentration of 10 kg/m^3

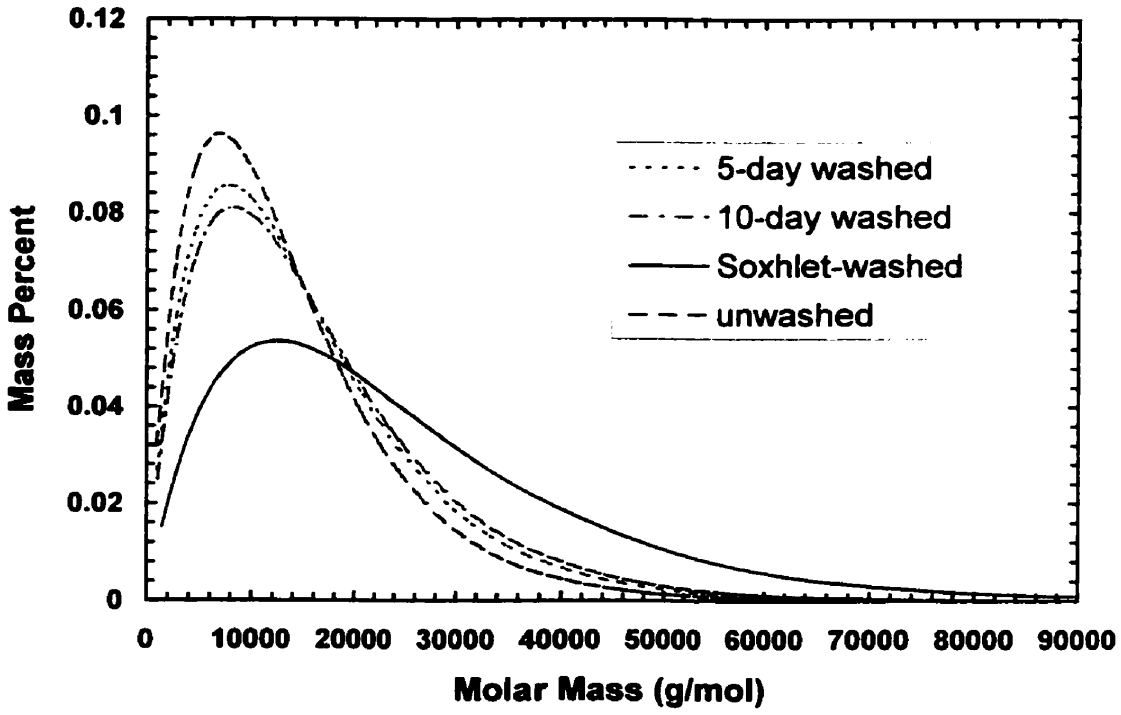

5.7 Chapter Summary

Asphaltene association and resin/asphaltene interactions were measured using a Vapor Pressure Osmometer (VPO) at different temperatures and in different solvents. The VPO experiments on Athabasca and Cold Lake asphaltenes demonstrate that the molar mass of asphaltenes increases with asphaltene concentration until a limiting molar mass is reached. The dependence of molar mass on asphaltene concentration is supported by surface tension experiments performed by Leon et al. (1998), small angle neutron

(Ravey et al., 1988) and x-ray scattering (Xu et al., 1995) experiments, VPO experiments performed by Moschopedis and Speight (1976) and those performed by Speight (1989) in dibromomethane, benzene, pyridine and nitrobenzene.

C5-asphaltenes were found to have a smaller VPO molar mass compared to C7-asphaltenes. Moschopedis and Speight (1976) showed that the VPO molar mass of asphaltenes decreases with carbon number of the n-alkane used to extract the asphaltenes. This is mainly due to the presence of a greater amount of resinous material in the low carbon number asphaltenes. These results are also supported by experiments performed by Hirschberg and Hermans (1984).

More polar solvent and higher temperature were found to reduce the measured asphaltene molar mass. The effect of solvent polarity and temperature on asphaltene association is consistent with by VPO experiments (Moschopedis and Speight, 1976) and small angle neutron scattering experiments (Ravey et al., 1988).

The VPO molar masses obtained were modeled using a scheme analogous to linear polymerization. The model requires an estimate of the molar mass of propagator and terminator molecules and has two parameters, an association constant and the molar ratio of terminators to propagators. The model successfully fit the measured molar mass data over a range of concentrations, solvents and temperatures.

A monomer molar mass of 1800 g/mol was chosen for the propagators. This value was estimated by the extrapolation of the VPO molar mass curves to zero concentration and taking an average for the various systems. A value of 1800 g/mol is consistent with previous results (Moschopedis and Speight, 1976, Peramanu et al., 1999).

A molar mass of 800 g/mol was estimated for terminators. This value falls within the range of molar masses observed for resins (Koots and Speight, 1975).

Molar masses of asphaltene-resin mixtures in toluene were measured with the VPO at 50° C. Resins dramatically lowered the average molar mass of asphaltenes by inhibiting asphaltene self-association. The predictive capability of the association model was tested by VPO experiments of asphaltene-resin mixtures. The model predictions were found to be within 16% of the experimentally measured values.

The proposed association model has a few weaknesses. The association constant used as a parameter was the same for all the association "reactions" taking place in the system. However, it has been shown by Moschopedis and Speight (1976) that asphaltene-resin interactions are favored compared to asphaltene-asphaltene interactions. This means that the association constant is probably higher for termination "reactions" compared to propagation "reactions". In fact, the aggregation model developed by Hirschberg and Hermans (1984) uses a higher value for the association between asphaltene and resin molecules.

Another problem lies in the estimation of average monomer molar masses of terminators and propagators since the monomer molar mass distribution of asphaltenes and resins is not known and is very difficult to measure experimentally due to asphaltene self-association. For more accuracy, it is necessary to estimate the change in average molar mass of terminators and propagators with temperature and solvent conditions. However, since the change in composition of terminators and propagators with temperature and solvent was not dramatic, it was reasonable to assume that the average

monomer molar masses do not change significantly. At very high temperatures and in strongly polar solvents, the shift in average monomer molar masses of terminators and propagators needs to be accounted for by assuming a monomer molar mass distribution.

Washing has a significant effect on the molar mass distribution of asphaltenes and in turn on the solubility of asphaltenes in any solvent medium. It was seen that the Soxhlet washed asphaltenes were less soluble than unwashed, 5-day washed or 10-day washed asphaltenes in heptol. Thus, the molar mass distribution of any system depends on the nature of asphaltenes, extraction method, presence of resins, solvent power and also temperature and pressure. The presence of resins in the system and the solvent power of the medium are probably the most important factors that influence the molar mass distribution of asphaltenes and in turn their solubility behavior.

One important outcome of the association model is that it can be used to estimate the molar mass distribution of asphaltenes in solvents where the dissolution of asphaltenes is not possible. Resins can be added to asphaltenes to aid in the dissolution in a given solvent. From the molar mass of asphaltene-resin mixtures the molar mass of asphaltenes can be back calculated. This can be a useful tool to estimate the molar mass distribution of asphaltenes in poor solvents such as cyclohexane and n-alkanes.

Chapter 6

Conclusions and Recommendations

6.1 Thesis Conclusions

Using a Vapor Pressure Osmometer (VPO), it was established that molar mass of asphaltenes was not fixed but depended on temperature and composition. This change in molar mass has not been accounted for in existing approaches to modeling the phase equilibrium of asphaltenes.

The self-association of asphaltenes from Athabasca and Cold Lake bitumen was measured using the VPO in toluene at 50° C and 70° C and in o-dichlorobenzene at 75° C and 130° C. The association appears to begin at concentrations below 0.5 kg/m^3. Molar mass was constant at concentrations above 10-20 kg/m^3 (approximately 1-2 wt%) suggesting that the aggregates reached a limiting size. It was found that the limiting aggregate molar mass decreases as the temperature and the polarity of the solvent increases.

Molar masses of asphaltene-resin systems were measured for eight systems with varying proportion of resins in each system. It was found that the apparent molar mass of the asphaltene-resin mixture decreased as the proportion of resins increased. It was also found that the limiting molar mass of a given asphaltene sample depended strongly on the asphaltene sample preparation and the degree of sample washing. More extensive

washing appears to remove more resinous material leading to higher measured molar masses.

The molecular association of asphaltenes, though a very complex phenomena involving millions of species of different shapes, sizes and structures, has been modeled using an aggregation mechanism analogous to linear polymerization. The polymerization "reactions" involved have been described in terms of two distinct classes: terminators and propagators. The model requires two fit parameters: the association constant and the terminator to propagator mole ratio and two estimated parameters: the monomer molar mass of terminators and propagators. The association constant determines the concentration at which the limiting molar mass is reached and the *T/P* ratio determines the limiting molar mass of aggregates. The model *fit* experimental molar masses over a range of temperatures and solvents. The model *predicted* the molar mass of asphalten-resin mixtures within ≈16% of the experimentally measured molar masses.

A variation of the polymerization model was tested that allowed greater control of the predicted molar mass distribution. A diminution parameter was introduced that related the association constant to aggregate size. In effect, the diminution parameter makes it more difficult to add a monomer to an existing aggregate. The quality of the fit to the molar mass data was similar to that of the first model. The *T/P* ratios required to obtain the fit were also similar. However, the upper limit of the molar mass distributions, were significantly lower. Hence, the diminution parameter is a useful tool for reducing the range of the molar mass distribution without losing the quality of fit to the average molar mass.

6.2 Recommendations for Future Work

The aggregation of asphaltenes has been investigated in polar solvents such as toluene and o-dichlorobenzene. However, asphaltene aggregation in non-polar and weakly polar solvents could not be investigated because asphaltenes precipitate in these solvents and VPO molar masses cannot be measured. One alternative is to measure VPO molar masses in cyclic alkanes such as decalin and cyclohexane. Asphaltenes are known to dissolve in decalin at low concentrations ($\approx$ 10 kg/m^3) but not all asphaltenes dissolve in cyclohexane. The molar mass of resin-asphaltene mixtures can be measured and asphaltene molar masses can be back calculated using the association model.

There is still uncertainty about the size of the asphaltene and resin monomers. More accurate molar masses may be obtained from VPO measurements of asphaltenes in very good solvents such as nitrobenzene. It has been postulated that in very good solvents asphaltenes remain as unassociated species at higher concentration where the VPO data is more accurate.

The upper limit of the molar mass distributions obtained from the association model needs to be confirmed. This can be done by modeling asphaltene solubility curves with regular solution and equation of state approaches. The shape of the tail of the solubility curves is likely dictated by the upper end of the molar mass distribution.

The association model described in this thesis assumes that polymer chains are capped at one end by terminators. Capping at both ends of the chain needs to be investigated since this mechanism is physically more realistic.

Asphaltene self-association needs to be verified using other measurement techniques. Differential Scanning Calorimetry (DSC) can be used to measure the change in the heats of association under different conditions. Fourier Transform–Infra Red (FT-IR) Spectroscopy can be used to determine the change in the bonding configuration in asphaltenes due to association. Also small-angle neutron (SANS) and X-ray (SAXS) scattering can be used to study the size and structure of an asphaltene system.

References

Alboudwarej, H, Akbarzadeh, K and Yarranton, H.W. Personal Communication, 2001.

Ali, L.H., Al-Ghannam, K.A. and Al-Rawi, J.M. "Chemical Structure of Asphaltenes in Heavy Crude Oils Investigated by N.M.R.", *Fuel*, 69, 1990, 520.

American Society for Testing and Material., Standard Test Method D-2007-86. "Characteristic Groups in Rubber Extender and Processing Oils and Other Petroleum Derived Oils by the Clay-Gel Absorption Chromatographic Method".

Andersen, S.I. and Birdi, K.S. "Aggregation of Asphaltenes as Determined by Calorimetry", *Journal of Colloid Interface Science*, 1991, 142(2), 497.

Brandt, H.C.A., Hendriks, E.M., Michels, M.A.J. and Visser, F. "Thermodynaic Modeling of Asphaltene Stacking", *Journal of Physical Chemistry*, 99(26), 1995, 10430.

Branthaver, J.F. "In Fuel Science and Technology Handbook", Marcel Dekker Inc., New York, 1990.

Carnahan, N.F., Quintero, L., Pfund, D.M., Fulton, J.L., Smith, R.D., Capel, M. and Leontaritis, K. "A Small Angle X-ray Scattering Study of the Effect of Pressure in the

Aggregation of Asphaltene Fractions in Petroleum Fluids under Near-Critical Solvent Conditions", *Langmuir*, 1993, 9, 2035.

Chang, V-L. and Fogler, H.S. "Stabilization of Asphaltenes in Aliphatic Solvents Using Alkylbenzene-Derived Amphiphiles. 1. Effect of the Chemical Structure of Amphiphiles on Asphaltene Stabilization", *Langmuir*, 10, 1994, 1749.

Chang, V-L. and Fogler, H.S. "Peptization and Coagulation of Asphaltenes in Apolar Media Using Oil-Soluble Ploymers", *Fuel Science and Technology International*, 14 (1&2), 1996, 75.

Dabir, B., Nematy, M., Mehrabi, A.R., Rassamdana, H. and Sahimi, M. "Asphaltene Flocculation and Deposition. III. The Molecular Weight Distribution", *Fuel*, 75,(14), 1996, 1639.

Dickie, J.P. and Yen, T.F. "Macrostructures of the Asphaltic Fractions by Various Instrumental Methods", *Journal of Analytical Chemistry*, 1967, 39, 1847.

Dickie, J.P., Haller, M.N. and Yen, T.F. "Electron Microscope Investigations of Heavy Oils", *American Institute of Chemical Engineers, Symposium Series*, 69(127), 1973, 56.

Ferworn, K.A. "Asphaltene Flocculation and Precipitation", *Ph.D Thesis*, 1992, University of Calgary, Calgary, Canada.

Handbook of Chemistry and Physics, CRC Press, 60th Edition, 1980, 216.

Herzog, P., Tchoubar, D. and Espinat, D. "Macrostructure of Asphaltene Dispersions by Small-Angle X-Ray Scattering", *Fuel*, 67, 1988, 250.

Hildebrand, J.H. "Solubility XII: Regular Solutions", *Journal of the American Chemical Society*, 51, 1929, 66.

Hirschberg, A., deJong, N.J., Schipper, B.A. and Meijer, J.G. "Influence of Temperature and Pressure on Asphaltene Flocculation", *Society of Petroleum Engineering Journal*, 1984, 24, 283.

Hirschberg, A. and Hermans, L. "Asphaltene Phase Behavior: A Molecular Thermodynamic Model", *Symposium International Lyon*, 25-27 June 1984, 492.

Ignasiak, T., Kemp-Jones, A.V. and Strausz, O.P. "Properties of Asphaltenes from various Alberta Crude Oils", *Preprints, American Chemical Society*, 22(3), 1977, 126.

Katz, D.L. and Beu, K.E. "Nature of Asphaltic Substances", *Industrial and Engineering Chemistry Research*, 37, 1945, 195.

Kawanaka, S, Park, S.J. and Mansoori, G.A. "Organic Deposition from Reservoir Fluids: A Thermodynamic Predictive Technique", *SPE Reservoir Engineering*, May, 1991, 185.

Kim, H.G. and Long, R.B. "Characterization of Heavy Residuum by a Small-Angle X-Ray Scattering Technique", *Industrial and Engineering Chemistry Research*, 18(1), 1979, 60.

Koots, J.A. and Speight, J.C. "Relation of Petroleum Resins to Asphaltenes", *Fuel*, 54, 1975, 182.

Leon, O., Rogel, E., Espidel, J. and Torres, G. "Structural Characterization and Self-Association of Asphaltenes of Different Origins", *3rd International Symposium on the Thermodynamics of Heavy Oils and Asphaltenes*, Houston, TX, December, 1998, 37.

Leontaritis, K.J. and Mansoori, G.A.: "Asphaltene Deposition During Oil Production and Processing: A Thermodynamic-Colloidal Model", SPE Paper No. 16258, *Proceedings from the 1987 SPE Symposium on Oil Field Chemistry*, Richardson, Texas.

Mannistu, K.D., Yarranton, H.W. and Masliah, J.H. "Solubility Modeling of Asphaltenes in Organic Solvents", *Energy and Fuels*, 1997, 11, 617.

Maruska, H.P. and Rao, B.M.L. "The Role of Polar Species in the Aggregation of Asphaltenes", *Fuel Science and Technology International*, 5(2), 1987, 119.

Mitra-Kirtley, S, Mullins, O.C., Branthaver, J.F., Cramer, S.P. "Nitrogen Chemistry of Kerogen and Bitumens from X-Ray Absorption Near-Edge Structure Spectroscopy", *Energy & Fuels*, 7(6),1993, 1128.

Mohamed, R.S., Ramos, A.C.S. and Loh, W. "Aggregation Behavior of Two Asphaltene Fractions in Aromatic Solvents", *Energy and Fuels*, 1999, 13, 323.

Moschopedis, S.E. and Speight, J.G. "Oxygen Functions in Asphaltenes", *Fuel*, 55, 1976, 222.

Moschopedis, S.E., Fryer, J.F. and Speight, J.G. "Investigation of Asphaltene Molecular Weights", *Fuel*, 55, 1976, 227.

Murgich, J., Abanero, J.A. and Strausz, O.P. "Molecular Recognition in Aggregates Formed by Asphaltene and Resin Molecules from the Athabasca Oil Sands", *Energy and Fuels*, 1999, 13, 278.

Overfield, R.E., Sheu, E.Y., Sinha, S.K. and Liang, K.S. "SANS Study of Asphaltene Aggregation", *Fuel Science and Technology International*, 7(5-6), 1989, 611.

Peramanu, S., Pruden, B.B. and Rahimi, P. "Molecular Weight and Specific Gravity Distribution for Athabasca and Cold Lake Bitumens and Their Saturate, Aromatic, Resin, and Asphaltene Fractions", *Industrial and Engineering Chemistry Research*, 38(8), 1999, 3123.

Petersen, J.C. "An Infra-red Study of Hydrogen Bonding in Asphalt", Fuel, 1967, 304.

Pfeiffer, J.P. and Saal, R.N.J. "Asphaltic Bitumens as Colloid System", *Journal of Physical Chemistry*, 44, 1940, 140.

Ravey, J.C., Ducouret, G. and Espinat, D. "Asphaltene Macrostructure by Small Angle Neutron Scattering", *Fuel*, 1988, 67, 1560.

Rogel, E. "Studies on Asphaltene Aggregation via Computational Chemistry", *Colloids and Surfaces A:Physicochemical and Engineering Aspects*, 104, 1995, 85.

Rogel, E. "Simulation of Interactions in Asphaltene Aggregates", *Energy and Fuels*, 2000, 14, 567.

Rogel, E., Leon, O., Torres, G. and Espidel, J. "Aggregation of Asphaltenes in Organic Solvents using Surface Tension Measurements", *Fuel*, 79, 2000, 1393.

Schmitter, J.M., Dorbon, M., Derycke, G., Ignatiadis, I. and Arpino, P.J. "Characterization of Polyaromatic Nitrogen Compounds in Crude Oils", *30th Annual Conference on Mass Spectrometry and Allied Topics*, Honolulu, 1982.

Scott, R.L. and Magat, M. "The Thermodynamics of High-Polymer Solutions: I. The Solubility and Fraction of a Heterogeneous Distribution", *Journal of Chemical Physics*, 13(5), 1945a, 172.

Sheu, E.Y. "Physics of Asphaltene Micelles and Microemulsions – Theory and Experiment", *Journal of Physics Condensed Matter*, 8(25), 1996, 125.

Sheu, E.Y., Storm, D.A. and De Tar, M.M. "Asphaltene in Polar Solvents", *Journal of Non-Crystalline Solids*, 1991, 131-133, 341.

Speight, J.G. and Moschopedis, S.E. "Some Observations on the Molecular Nature of Petroleum Asphaltenes", *American Chemical Society, Preprint*, 24(4), 1979, 910.

Speight, J.G. "Latest Thoughts on the Molecular Nature of Petroleum Asphaltenes", *Symposium of Analytical Chemistry of Heavy Oils/Resids*, American Chemical Society, Dallas Meeting, 1989, 221.

Speight, J.G. "The Chemistry and Technology of Petroleum", Third Edition, Marcel Dekker Inc., New York, 1999.

Strausz, O.P., Mojelsky, T.W. and Lown, E.M. "The Molecular Structure of Asphaltene:An Unfolding Story", *Fuel*, 1992, 71, 1355.

Wiehe, I.A. and Liang, K.S. "Asphaltenes, Resins, and Other Petroleum Macromolecules", *Fluid Phase Equilibria*, 117 (1996) 201.

Xu, Y., Koga, Y. and Strausz, O.P. "Characterization of Athabasca Asphaltenes by Small Angle X-ray Scattering", *Fuel*, 1995, 74(7), 960.

Yarranton, H.W. and Masliyah, J.H. "Molar Mass Distribution and Solubility Modeling of Asphaltenes", *AIChE Journal*, 42(12), 1996, 3533.

Yarranton, H.W., Alboudwarej, H. and Jakher, R. "Investigation of Asphaltene Association with Vapor Pressure Osmometry and Interfacial Tension Measurements", *Industrial and Engineering Chemistry Research*, 39(8), 2000, 2916.

Yen, T.F. "Structure of Petroleum Asphaltene and its Significance", *Energy Sources*, 1(4), 1974, 447.

APPENDIX

```
/*************************************************************************
* Programmed by Mayur Agrawala as a part of M.Sc. thesis at U of C.
* This program calculates the average molar mass and molar mass
* distribution of asphaltenes as a function of temperature, solvent
* and type of asphaltenes.  A linear polymerization scheme is used to
* determine fit parameters: molar ratio of terminators to propagators,
* association constant and diminution parameter.  The model also
* requires two estimated parameters: the average monomer molar masses
* of terminators and propagators.
*************************************************************************/

//C++ header files

#include <fstream.h>
#include <iostream.h>
#include <math.h>
#include <iomanip.h>

//global variable declaration

double const rho_s = 841;
double const Ms = 92.1;
double const Mr = 800;
double const Ma = 1800;

int const MAX = 50;

//function prototypes

double func_deriv(double i, double K, double To, double Po, double m);
double func(double i, double K, double To, double Po, double m,double
            &term_frac,double prop[MAX], double term[MAX]);
double newton_raphson(double k, double K, double To, double Po, double
                      m_initial);

//main function

int main()
{

//output.txt stores the molar mass distribution for concentrations from
//0.1 kg/m3 to 110 kg/m3

//molar_mass.txt stores the average molar mass of the system at the
//various concentrations (0.1 to 110 kg/m3)

  ofstream fout("output.txt");
  ofstream fout2("molar_mass.txt");

  double K,TP,k,Co,prop_frac,tf;
  double prop[MAX],term[MAX],total[MAX],zM[MAX],w[MAX],Mmass[MAX];
  double term_frac = 0;
```

```
  double v = Ms/rho_s;

  cout << "Enter the association constant for the system" << endl;
  cin >> K;
  cout << "Association constant, K = " << K << endl;

  cout << "Enter the molar ratio of Terminators to Propagators in the
          asphaltene fraction" << endl;
  cin >> TP;
  cout << TP << endl;

  cout << "Enter the diminuation constant for the system" << endl;
  cin >> k;
  cout << "diminuation constant k = " << k << endl;

  Co = 0.1;
  while(Co<=100)
    {
        tf = TP/(1+TP);

          double Mtot = tf*Mr+(1-tf)*Ma;
          double tot_moles = Co/Mtot+(1/v);
          double Po = ((Co/Mtot)/(1+TP))/tot_moles;
          cout << "Initial mole fraction of propagators is " << Po <<
          endl;
          double To = ((Co/Mtot)*TP/(1+TP))/tot_moles;
          cout << "Initial mole fraction of terminators is " << To <<
          endl;

//initial guess for the equilibrium concentration of propagators in the
//system

          double a = K*K*(Po+To);
          double b = 1+K*(2*Po+To);
          double c = Po;
          double m_initial = (b-sqrt(b*b-4*a*c))/(2*a);
          cout << "m_initial = " << m_initial << endl;

//calculation of equilibrium concentration of propagators and
//terminators

      prop_frac = newton_raphson(k,K,To,Po,m_initial);
      cout << "The equilibrium mole fraction of propagators is "
           << prop_frac << endl;

      double templ = func(k,K,To,Po,prop_frac,term_frac,prop,term);
      cout << "The equilibrium mole fraction of terminators is " <<
              term_frac << endl;

//calculation of average molar mass of asphaltenes at the specified
//concentration

      double sum = 0;
      double suml = 0;
```

```
      for(int j=0;j<MAX;j++)
      {
        total[j] = prop[j] + term[j];
        Mmass[j] = prop[j]*(j+1)*Ma + term[j]*(j*Ma+Mr);
        sum1 += Mmass[j];
        sum += total[j];
      }

      double avg_mmass = sum1/sum;
      cout << "The average molar mass is " << avg_mmass << endl;

      fout2 << Co << "  " << avg_mmass << endl;

      if (Co < 0.9)
      Co += 0.1;
      else
      {
        if (Co < 10)
          Co += 1;
        else
          Co += 10;
      }

//calculation of molar mass distribution in wt percent asphaltenes
//versus molar mass

      double sum2 = 0;
      for(j=0;j<MAX;j++)
      {
        zM[j] = Mmass[j]/sum;
        sum2 += zM[j];
      }

      fout << Co << "   kg/m3" << endl;
      for(j=0;j<MAX;j++)
      {
        w[j] = zM[j]/sum2;
        fout << (prop[j]*(j+1)*Ma + term[j]*(j*Ma+Mr))/total[j] << "
                " << w[j] << endl;
      }
      }
  fout.close();
  fout2.close();

  return 0;
}

/*********************************************************************
* this function calculates the terminator and propagator mole fraction
* as well as the mole fraction of individual aggregates in the system,
* given the initial mole fraction of terminators and propagators and
* the association constant.
*********************************************************************/
```

```
double func(double i, double K, double To, double Po, double m, double
            &term_frac, double prop[MAX], double term[MAX])
{
  double array[MAX];
  double sum,sum1,sum2,sum3;
  sum = sum1 = sum2 = sum3 = 0;

  for(int j=0;j<MAX;j++)
    {
      prop[j] = (j+1)*pow(i,(j*(j-1)/2))*m*pow((m*K),j);
      sum1 += prop[j];
      array[j] = (j+1)*pow(i,(j*(j+1)/2))*pow((m*K),(j+1));
      sum2 += array[j];
      term[j] = pow(i,(j*(j-1)/2))*pow((m*K),j);
      sum3 += term[j];
    }

  term_frac = To/sum3;
  sum = sum1 + To*sum2/sum3 - Po;
  for(j=0;j<MAX;j++)
    {
      prop[j] /= (j+1);
      term[j] *= term_frac;
    }
  return sum;
}

/*************************************************************************
* this function returns the derivative of the above function
*************************************************************************/

double func_deriv(double i, double K, double To, double Po, double m)
{
  double array1[MAX],array2[MAX],array3[MAX],array4[MAX],array5[MAX];
  double dsum,dsum1,dsum2,dsum3,sum2,sum3;
  dsum = dsum1 = dsum2 = dsum3 = sum2 = sum3 = 0;

  for(int j=0;j<MAX;j++)
    {
      array1[j] = pow((j+1),2)*pow(i,(j*(j-1)/2))*pow((m*K),j);
      dsum1 += array1[j];
      array2[j] = pow((j+1),2)*pow(i,(j*(j+1)/2))*K*pow((m*K),j);
      dsum2 += array2[j];
      array3[j] = j*pow(i,(j*(j-1)/2))*K*pow((m*K),(j-1));
      dsum3 += array3[j];
      array4[j] = (j+1)*pow(i,(j*(j+1)/2))*pow((m*K),(j+1));
      sum2 += array4[j];
      array5[j] = pow(i,(j*(j-1)/2))*pow((m*K),j);
      sum3 += array5[j];
    }

  dsum = dsum1 + To*(dsum2*sum3-dsum3*sum2)/pow(sum3,2);
  return dsum;
}
```

```
/*************************************************************************
* This function uses the Newton-Raphson convergence technique for
* solving the function above for the equilibrium mole fration of
* propagators in the system.  The initial guess is obtained from the
* simple analytical solution while considering the two-parameter model.
*************************************************************************/

double newton_raphson(double k, double K, double To, double Po, double
                      m_initial)
{
  double m, m_new, delta, error = 1;

  double term_frac = 0.0;
  double prop[MAX],term[MAX];
  while(fabs(error) > 0.0001)
  {
  m = m_initial;
  delta=-func(k,K,To,Po,m,term_frac,prop,term)/func_deriv(k,K,To,Po,m);
  m_new = m + delta;
  error = (m-m_new)/m;
  m_initial = m_new;
  }

  cout << "The value of m is = " << m_new << endl;
  return m_new;
}
```